

Discovery of cytotoxic natural products from South African marine sponges

By

Mookho Sylvia Lerata

**A thesis submitted in partial fulfilment of the requirement
for
the degree of Master of Science in Pharmaceutical Science
in the
Faculty of Natural Sciences,
University of the Western Cape.**

The logo of the University of the Western Cape is a faint, light blue watermark in the background. It features a classical building with four columns and a pediment, with the text 'UNIVERSITY of the WESTERN CAPE' written below it in a serif font.

Supervisor: Professor Denzil Beukes
Co-supervisors: Professor Mervin Meyer
Professor Edith M. Antunes

March 2018

ABSTRACT

Cancer is a major health problem worldwide and killing millions of people each year. The use of natural products as chemotherapeutic agents is well established, however, many of the currently available drugs are associated with undesirable side effects and high toxicity. Furthermore, the development of drug resistant cancers makes the search for anticancer lead compounds a priority. In this study a library of prefractionated marine sponge extracts was established and used to prioritise samples for isolation of bioactive metabolites. From the generated library, two of the sponges of genera *Ircinia* sp. and *Latrunculid* sp. resulted in isolation of furanosesterterpenes (7E,12Z,20Z,18S-variabilin) and pyrroloiminoquinone (tsitsikammamine A and tsitsikammamine N-18 oxime) alkaloids respectively. The structures of these compounds were elucidated by analysis of 1D and 2D NMR data. These compounds displayed moderate to potent cytotoxicity against MCF-7, PC-3, U-87 and HEK-293 cells lines through apoptosis, with lack of selectivity for cancer cell lines.

Keywords: Cancer, marine sponges, *Ircinia* sp., *Latrunculid* sp. pyrroloiminoquinones alkaloids, furanosesterterpenes, cytotoxicity, marine natural product libraries.



DECLARATION

I Mookho Sylvia Lerata, declare that "Discovery of cytotoxic marine natural products" is my original work and to my knowledge has not been submitted for award of the degree or assessment at any university and that the all the sources and quotes I used have been acknowledged by means of complete references.

Mookho Sylvia Lerata

Date signed



ACKNOWLEDGEMENTS

First and foremost I thank God for giving me strength, all this would have been impossible without Him.

I would like to express my sincere gratitude to my supervisor **Professor Denzil Beukes** for accepting me as his master's student. His undying support, patience and guidance throughout this research helped me as I build a career in natural product chemistry.

A very special thanks to **Professor Edith Antunes** for always being available to help with planning of the experiments and sharing her expertise, especially with chromatography and NMR experiments, as well as analysing NMR data. She was indeed a true mentor.

I would also like to thank **Professor Mervin Meyer** from the department of biotechnology for allowing me to use his facilities and providing me with all the necessary support I needed for the biological studies.

Another person who played a crucial part in my research is **Dr. Nicole Sibuye** by training and guiding me throughout my tissue culture experience. I am honoured to have worked with such an amazing person.

I also want to acknowledge **Dr. Sarah D'Souza** for assisting me with solid lipid nanoparticles studies as well as organising the prefractionated sponge samples library. It was a great pleasure to work with her.

A very special thanks to **Mr. Yunus Kippie** for all the mass spectroscopy experiments he did for me and **Ms Audrey Ramplin** for her technical support and ensuring that all equipment in the lab was functional.

I would also like to extend my gratitude to Ada and Bertie Levenstein and The Government of Lesotho for their financial support, it would have been impossible for me to complete my studies without their support.

A big thank you to my fellow lab mates in the Marine Biodiscovery Research lab for their support and motivation. We had great laughs in and outside of the lab.

Last but not least, I am very grateful to my family and friends. Their kind and encouraging words kept me going even when I did not believe in myself.

DEDICATION

To my late mom, Mrs. M.A. Lerata and my dad, Mr. L.B. Lerata



TABLE OF CONTENTS

Abstract	i
Declaration	ii
Acknowledgements	iii
Dedication	iv
List of figures	vii
List of tables	x
List of isolation schemes	xi
List of abbreviations	xii
Chapter 1. General introduction	1
1.1 The burden of cancer.....	1
1.2 Cancer Carcinogenesis and treatment.....	2
1.3 Hypothesis.....	4
1.4 Aims and Objectives.....	4
1.5 Thesis overview.....	5
1.6 References.....	6
Chapter 2. Literature review: Nature as a source of anticancer natural products	8
2.1 Nature as a source of therapeutic agents.....	8
2.1.1 <i>Anticancer drugs from plants</i>	9
2.1.2 <i>Anticancer agents from microbial sources</i>	13
2.2 Anticancer agents from marine sources.....	15
2.2.1 <i>Marine sponges as sources of anticancer agents</i>	17
2.3 Marketed marine derived anticancer drugs.....	20
2.4 Other marine derived natural compounds in advanced clinical trials.....	24
2.5 References.....	28
Chapter 3. Development of a pre-fractionated library of marine sponge extracts..	33
3.1 Introduction.....	33
3.2 Results and discussion	37
3.3.1 <i>Extraction and prefractionation</i>	37
3.3.2 <i>Chemical profiling</i>	40
3.3.3 <i>Biological activity</i>	42
3.3 Conclusion.....	45
3.4 Experimental.....	46
3.4.1 <i>General experimental procedures</i>	46
3.4.2 <i>Invertebrate material</i>	46

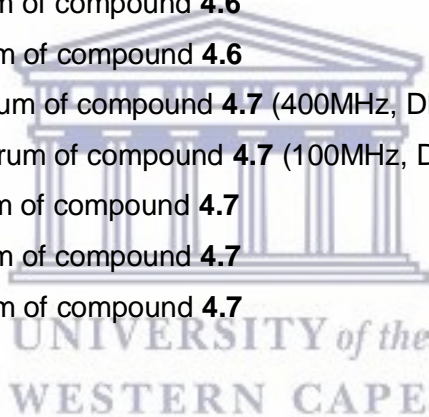
3.4.3 Extraction and fractionation of marine sponges.....	46
3.4.4 Cytotoxicity.....	47
3.5 References.....	49
Chapter 4. Cytotoxic metabolites from two South African marine sponges of the genera <i>Ircinia</i> and <i>Latrunculia</i>	51
4.1 Introduction.....	51
4.1.1 Natural products from the genus <i>Ircinia</i>	51
4.1.2 Natural products from the genus <i>Latrunculia</i>	52
4.2 Results and discussion	53
4.2.1 Extraction and isolation of sesterterpenes from <i>Ircinia</i> sp.....	53
4.2.2 Structure elucidation of sesterterpenes from <i>Ircinia</i> sp.....	55
4.2.3 Extraction and isolation of pyrroloiminoquinones from <i>Latrunculid</i> sp.	60
4.2.4 Structure elucidation of pyrroloiminoquinones from <i>Latrunculid</i> sp.....	61
4.3 Conclusion.....	66
4.4 Experimental.....	67
4.5 References.....	69
Chapter 5. Cytotoxicity of furanosesterterpenes and pyrroloiminoquinone alkaloids and improvement of activity by incorporation into solid lipid nanoparticles	71
5.1 Introduction.....	71
5.2 Results and discussion.....	72
5.2.1 Cytotoxicity assay.....	72
5.2.2 Solid lipid nanoparticles.....	77
5.2.3 Solid lipid nanoparticles: Improved cytotoxicity of compound 4.5	78
5.2.4 APOPercentage™ assay.....	79
5.3 Conclusion.....	81
5.4 Experimental procedures.....	82
5.4.1 Synthesis of solid lipid nanoparticles (SLNPs) incorporating compound 4.5	82
5.4.2 Cytotoxicity assays.....	82
5.4.3 APOPercentage™ assay.....	82
5.5 References.....	84
Chapter 6. General conclusion and recommendations	86
Supplementary data	87

LIST OF FIGURES

- Figure 1.1.** A graph showing percentage increase in neoplasm related deaths reported in South Africa from 2011 to 2015. Graph generated from data obtained from Statistics South Africa (2011-2015).
- Figure 1.2.** The process of cancer formation from a single mutation to malignancy; photograph accessed from [http://www.ndhealthfacts.org/wiki/Oncology_\(Cancer\)](http://www.ndhealthfacts.org/wiki/Oncology_(Cancer)).
- Figure 2.1.** Summary of all new drugs approved by the FDA for clinical use between year 1981 and 2014 $n=1562$.
- Figure 2.2.** Structures of vincristine (2.1), vinblastine (2.2), vinorelbine (2.3), and vindesine (2.4).
- Figure 2.3.** Chemical structures of camptothecin 2.5, topotecan 2.6 and irinotecan 2.7.
- Figure 2.4.** Podophyllotoxin 2.8 and its synthetic derivatives etoposide (2.8) and teniposide (2.10).
- Figure 2.5.** Structures of paclitaxel 2.11 and docetaxel 2.12.
- Figure 2.6.** Structures of daunorubicin 2.13, doxorubicin 2.14, idarubicin 2.15, and epirubicin 2.16.
- Figure 2.7.** Structures of bleomycin A2 2.17, bleomycin B2 2.18 and actinomycins D 2.19.
- Figure 2.8.** Structures of spongouridine (2.20) and spongothymidine (2.21).
- Figure 2.9.** New marine natural compounds isolated from year 2008 to 2015.
- Figure 2.10.** Structure of discodermolide 2.22.
- Figure 2.11.** Structure of spongiastatin-1 2.23.
- Figure 2.12.** Structures of hemiasterlin 2.24, HTI-286 2.25 and E-7974 2.26.
- Figure 2.13.** Structures of cytarabine 2.27 and vidarabine 2.28.
- Figure 2.14.** Structure of ET-743 2.29.
- Figure 2.15.** Structures of eribulin 2.30 and halichondrin B 2.31.
- Figure 2.16.** Structure of brentuximab vedotin 2.32.
- Figure 2.17.** Structure of Kahalalide F 2.33.
- Figure 2.18.** Structure of bryostatin-1 2.34.
- Figure 2.19.** Structures of didemnin B 2.35 and aplidin 2.36.
- Figure 3.1.** Summary of processes involved in lead discovery from natural products.
- Figure 3.2.** A photograph of prefractionated library samples stored at Marine Biodiscovery research lab, University of the Western Cape.
- Figure 3.3.** Histogram presentation of organic extract recovery expressed as a percentage of the total extract.

- Figure 3.4.** A bar chart presentation of mass recovery expressed as percentage of the total crude extract.
- Figure 3.5.** Chart showing percentage distribution of masses per solvent mixture.
- Figure 3.6a.** ^1H NMR spectra of TS2712, crude extract, fraction 1, fraction 2, fraction 3, fraction 4 and fraction 5.
- Figure 3.6b.** ^1H NMR spectra of TS2707, crude extract, fraction 1, fraction 2, fraction 3, fraction 4 and fraction 5.
- Figure 3.6c.** ^1H NMR spectra of TS2713, crude extract, fraction 1, fraction 2, fraction 3, fraction 4 and fraction 5.
- Figure 3.6d.** ^1H NMR spectra of TS2714, crude extract, fraction 1, fraction 2, fraction 3, fraction 4 and fraction 5.
- Figure 3.7.** Cell viability of (a) SKOV-3, (b) MCF-7 and (c) HEK-293 after treatment with 50 $\mu\text{g/mL}$ of library fractions
- Figure 4.1.** Structure of variabilin (4.1).
- Figure 4.2.** Structures of makaluvic acid (4.2), discorhabdin (4.2) and tsitsikammamines (4.4).
- Figure 4.3.** A photograph of TS2713 (*Ircinia* sp.) prior to extraction.
- Figure 4.4.** ^1H NMR spectrum of compound 4.5 (400 MHz, CDCl_3)
- Figure 4.5.** The ^{13}C NMR spectrum of compound 4.5 (100 MHz, CDCl_3). 0-48 ppm (top) and 90-180 ppm (bottom)
- Figure 4.6.** A section of the HSQC for compound 4.5.
- Figure 4.7.** COSY and HMBC correlations of compound 4.5.
- Figure 4.8.** ^1H NMR spectrum of compound 4.6 (400 MHz, $\text{DMSO}-d_6$)
- Figure 4.9.** ^{13}C DEPT 135 of compound 4.6 (400MHz, $\text{DMSO}-d_6$)
- Figure 4.10.** A section of the HSQC spectrum showing aromatic hydrogens correlations to corresponding carbons.
- Figure 4.11.** COSY and HMBC correlations of compound 4.6.
- Figure 4.12.** A section of ^1H NMR of compound 4.7.
- Figure 5.1.** Structure of a solid lipid nanoparticle.
- Figure 5.2.** Morphological changes in MCF-7 cells after treatment with compounds 4.5, 4.6 and 4.7
- Figure 5.3.** Morphological changes in PC-3 cells after treatment with compounds 4.5, 4.6 and 4.7
- Figure 5.4.** The viability of HEK-293, PC-3, U-87 and MCF-7 cells after treatment with compounds 4.5, 4.6 and 4.7
- Figure 5.5.** Changes in the ^1H NMR spectrum of compound 4.5 over time

- Figure 5.6.** ^1H NMR spectrum of compound **4.5** (blue) and compound **4.5**-SLNP (red) (400 MHz, CDCl_3).
- Figure 5.7.** Comparative analysis of toxicity of compound **4.5** and compound **4.5**-SLNP
- Figure 5.8.** Percentage of apoptotic PC-3 and MCF-7 cells induced by compounds **4.5**, **4.6** and **4.7** and ceramide after treating for 24 hours
- Figure S4.1** ^1H NMR spectrum of compound **4.5** (400MHz, CDCl_3)
- Figure S4.2** ^{13}C NMR spectrum of compound **4.5** (100MHz, CDCl_3)
- Figure S4.3** COSY spectrum of compound **4.5**
- Figure S4.4** HSQC spectrum of compound **4.5**
- Figure S4.4** HMBC spectrum of compound **4.5**
- Figure S4.5** NOESY spectrum of compound **4.5**
- Figure S4.6** ^1H NMR spectrum of compound **4.6** (400MHz, $\text{DMSO}-d_6$)
- Figure S4.6** ^{13}C DEPT 135 of compound **4.6** (400MHz, $\text{DMSO}-d_6$)
- Figure S4.7** COSY spectrum of compound **4.6**
- Figure S4.8** HSQC spectrum of compound **4.6**
- Figure S4.9** HMBC spectrum of compound **4.6**
- Figure S4.10** ^1H NMR spectrum of compound **4.7** (400MHz, $\text{DMSO}-d_6$)
- Figure S4.11** ^{13}C NMR spectrum of compound **4.7** (100MHz, $\text{DMSO}-d_6$)
- Figure S4.12** COSY spectrum of compound **4.7**
- Figure S4.12** HSQC spectrum of compound **4.7**
- Figure S4.13** HMBC spectrum of compound **4.7**



LIST OF TABLES

- Table S3.1.** Cell viability of MCF-7, SKOV-3 and HEK-293
- Table 4.1.** NMR data of compound **4.5** compared to that of variabilin available in Barrow et al. (1988)
- Table 4.2.** NMR data for compound **4.6**, (400 MHz, DMSO- d_6)
- Table 4.3.** NMR data for compound **4.7**, (400 MHz, DMSO- d_6)
- Table 5.1.** IC_{50} (μM) values for compounds **4.5**, **4.6** and **4.7** in PC-3, HEK-293, U-87 and MCF-7 cells
- Table 5.2.** IC_{50} (μM) values for compounds **4.5** and compound **4.5**-SLNP in PC-3 and MCF-7 cells.



LIST OF ISOLATION SCHEMES

Scheme 3.1. Desalting and diol fractionation of sponge extracts.

Scheme 4.1. Isolation of sesterterpenes from *Ircinia* sp.

Scheme 4.2. Isolation of pyrroloiminoquinone metabolites from *Latrunculia* sp.



ABBREVIATIONS

^{13}C NMR	Carbon Nuclear Magnetic Resonance
^1H NMR	Proton Nuclear Magnetic Resonance
COSY	Correlation Spectroscopy
DEPT-135	Distortionless Enhancement by Polarization Transfer-135
DMEM	Dulbecco's Modified Eagles Medium
DMSO	Dimethyl Sulfoxide
DNA	Deoxyribonucleic Acid
ED ₅₀	Median effective dose
EMA	European Medicines Agency
FBS	Foetal Bovine Serum
FDA	Food and Drug Authority
HEK-293	Human Embryonic Kidney-293
HMBC	Heteronuclear Multiple Bond Correlation
HSQC	Heteronuclear Single-Quantum Correlation
IARC	International Agency for Research on Cancer
IC ₅₀	Half Maximal Inhibitory Concentration
IR	Infrared Radiation
MCF-7	Michigan Cancer Foundation-7
MS	Mass Spectroscopy
NCI	National Cancer Institute
NMR	Nuclear Magnetic Resonance
NP	Natural Product
PBS	Phosphate Buffer Solution
PKC	Protein Kinase C
RPMI	Roswell Park Memorial Institute
SLNP	Solid Lipid Nanoparticle
UV	Ultra Violet
VCL	Vinblastine
VCR	Vincristine

WHO

World Health Organisation

WST-1

Water Soluble Tetrazolium salt -1



UNIVERSITY *of the*
WESTERN CAPE

Chapter 1

General introduction

1.1 The burden of cancer

“Cancer is an abnormal growth of cells caused by multiple changes in gene expression leading to dysregulated balance of cell proliferation, cell death and ultimately developing into a population of cells that can invade tissues and metastasize to distant sites, causing significant morbidity and finally, if left untreated death of the host” [Ruddon, 2007].

Cancer constitutes an enormous burden worldwide that is expected to escalate due to the increasing growth and life expectancy of the population, and because of the adoption of behaviours and lifestyle factors known to cause cancer. In the United States of America, cancer is the second leading cause of mortality, after cardiac diseases, and is expected to surpass heart disease as a leading cause of death in the next few years [Siegel et al., 2017]. The statistics report made by GLOBOCAN, a project of the International Agency for Research on Cancer (IARC), stated that there were 14.1 million new cancer cases, 8.2 million cancer deaths and 32.6 million people living with cancer (within 5 years of diagnosis) globally in the year 2012. Although the rates of many cancers in high income countries are decreasing, low- and middle-income countries are experiencing a rise in cancers commonly found in high income countries due to adaptation of western lifestyles such as smoking, lack of physical activity and excess body weight [Torre et al., 2016]. It is estimated that the overall cancer burden will rise by 70% in 2030 [Antoni et al., 2016]. In South Africa, cancer related mortalities increased from 7.3 percent in 2011 to 9.1 percent in 2015 (Figure 1.1) which is an increase of 1.8 percent in a period of 4 years

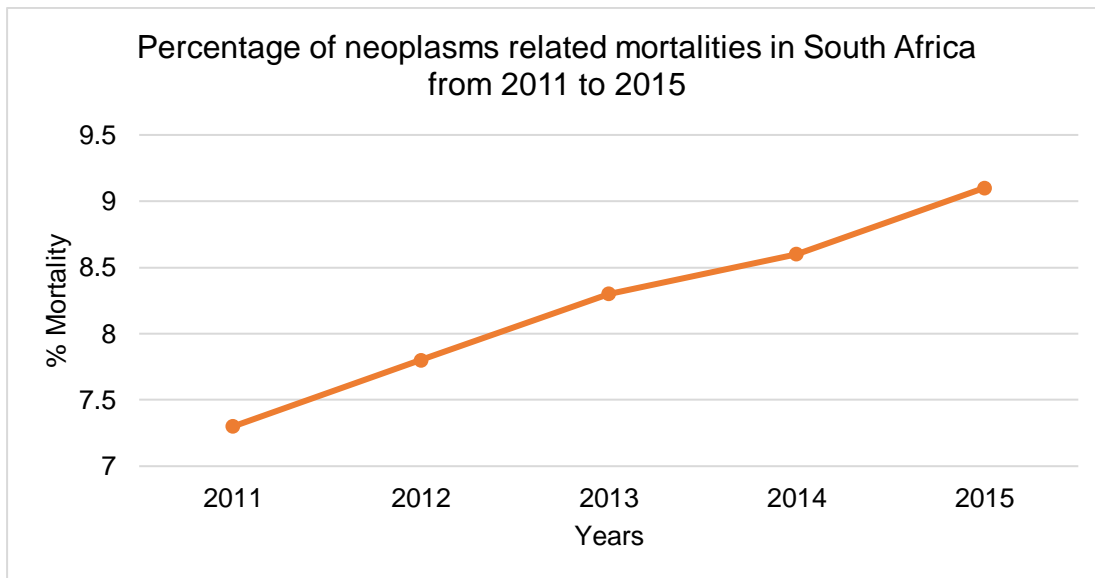


Figure 1.1. A graph showing percentage increase in neoplasm related deaths reported in South Africa from 2011 to 2015. Graph generated from data obtained from Statistics South Africa (2011-2015).

1.2 Cancer carcinogenesis and treatment

The development of cancer, known as carcinogenesis, is a multistep process arising from one cell or a small number of cells which undergo metabolic and behavioural changes leading them to proliferate in a manner that is excessive. It is a result of the damage to DNA which occurs in normal cells which leads them towards growth and survival advantages [Pardee and Stein, 2011]. These changes (mutations) may occur when:

- i. There are genetic changes which modify the DNA sequence, or
- ii. Chromatin conformation is modified.

As a result, the mechanisms that control cell proliferation and life spans, the relationship with neighbouring cells and the capacity to escape the immune system are modified, leading to an accumulation of mutations that develop into tumours. Once tumours are able to escape from their site of initiation and infiltrate other parts of the body, a process known as metastasis, they are termed malignant tumours. Figure 1.2 shows the process of how a single cell can develop into a tumour and ultimately migrate to other parts of the body.

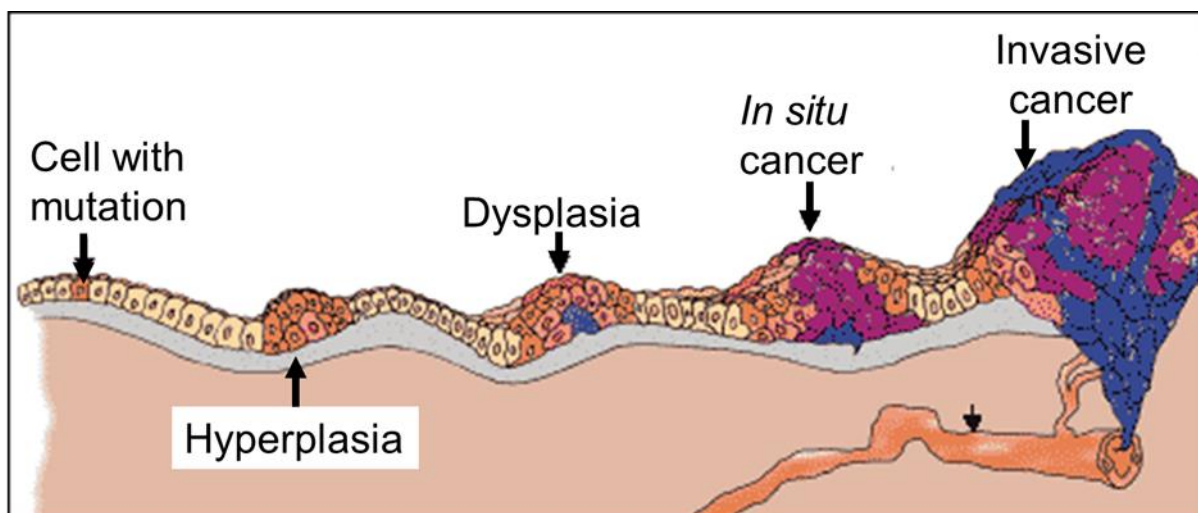


Figure 1.2. The process of cancer formation from a single mutation to malignancy; photograph accessed from [http://www.ndhealthfacts.org/wiki/Oncology_\(Cancer\)](http://www.ndhealthfacts.org/wiki/Oncology_(Cancer)).

Cancer initiation and progression depends on both external factors in the environment, such as tobacco, chemicals, radiation and infectious organisms, and factors within the cell, such as inherited mutations, hormones, immune conditions and mutations which may occur from metabolism. Together, these factors can result in abnormal cell behaviour and excessive proliferation, which in turn results in cell mass growth and expansion with the potential of spreading to other parts of the body [Hejmadi, 2010].

The ideal treatment aims to completely remove the cancer without damaging normal body cells. Different treatment modalities exist and include surgery, radiation, chemotherapy, immunotherapy, targeted therapy, hormone therapy and stem cell transplant among others. The choice of treatment used depends on the location, grade of tumour and stage of the disease and different modalities are often used in conjunction with each other to avoid remission. Surgery is one of the oldest, primary methods used by surgeons to remove tumours, however, it may be impractical to surgically remove some cancers because of their location, the type of cancer or the stage at which it is diagnosed and for such cancers, chemotherapy remains the mainstay of treatment [Sudhakar, 2009].

Use of chemotherapy to treat cancer began in the 1940s with the introduction of nitrogen mustards to a patient with non-Hodgkin's lymphoma by Yale and colleagues [Devita and Chu, 2008]. The outcome triggered support for the synthesis of other alkylated compounds including derivatives such as chlorambucil and cyclophosphamide [Devita and Chu, 2008]. Later, anticancer agents derived from natural sources made a breakthrough in the 1950s with the introduction of actinomycin D which gained popularity for use in paediatric tumours in the 1950s and 1960s [Devita and Chu, 2008]. Other natural product derived anticancer agents

that became popular were the vinca alkaloids and cytarabine which were approved for clinical use in 1963 and 1969, respectively [Devita and Chu, 2008; Mayer et al., 2010].

Although use of chemotherapy has resulted in the successful treatment of many cancer types over the years, this method of treatment is limited by toxicity and undesirable side effects caused by lack of selectivity of anticancer drugs [Sudhakar, 2009]. Some of the most common side effects include vomiting, diarrhoea, mucositis, myelosuppression and alopecia.

In addition to the above mentioned adverse effects associated with use of chemotherapy, resistance to anticancer drugs is another factor that limits the effectiveness of cancer chemotherapy. Resistance constitutes a lack of response to drug-induced tumour growth inhibition and it may be inherent or acquired as a response to drug exposure [Luqmani, 2005]. Acquired resistance is a particular problem, as tumours not only become resistant to the drugs originally used to treat them but could also become cross-resistant to other drugs with different mechanisms of action. Resistance to chemotherapy is believed to cause treatment failure in over 90% of patients with metastatic cancer, and resistant micrometastatic tumour cells may also reduce the effectiveness of chemotherapy in the adjuvant setting [Longley and Johnston, 2005].

It is these problems associated with use of chemotherapy in cancer treatment that necessitates the search for more lead compounds to address the challenge faced with currently available drugs.

1.3 Hypothesis

Marine sponges live in a strenuous environment where they have to compete for space and nutrients. Therefore, to survive, they produce toxins and other compounds known as secondary metabolites to repel and deter predators, as well as for protection against infections. Some of these compounds have the potential for killing and/or inhibiting cancer cells proliferation.

1.4 Aims and objectives

The aim of the current study is to discover anticancer lead compounds from South African marine sponges.

The main objectives are:

- To prepare a small library of fractionated marine sponge extracts.
- To perform *in vitro* bio-assays of sponge extracts for anticancer activity on several different tumour cells.
- To isolate compounds from active marine sponge extracts.

- To determine the structures of active sponge metabolites via spectroscopic methods.

1.5 Thesis overview

Chapter one provides a general introduction to cancer and contextualizes the study while anticancer natural products are briefly reviewed in *chapter two*. The preparation and screening of a small fractionated marine extract library is described in *chapter three*. *Chapter four* describes the isolation and characterization of cytotoxic metabolites from two marine sponges from the genera *Ircinia* and *Latrunculia*. The use of solid lipid nanoparticles to improve the activity of nonpolar marine natural products is described in *chapter five*. *Chapter six* provides a brief summary of the study and outlines future work.



1.6 References

Antoni, S.; Soerjomataram, I.; Moller, B.; Bray, F.; Ferlay, J. An assessment of GLOBOCAN methods for deriving national estimates of cancer incidence. *Bulletin of the World Health Organisation* **2016**, *94*, 174–184.

DeVita, V.T.Jr.; Chu, E. A history of cancer chemotherapy. *Cancer Research* 2008, *68*(21), 8645-8653.

Hejmadi, M. Introduction to cancer biology; BookBoons.com: Frederiksberg, Denmark, 2010.

[http://www.ndhealthfacts.org/wiki/Oncology_\(Cancer\)](http://www.ndhealthfacts.org/wiki/Oncology_(Cancer))

Longley, D.; Johnston, P. Molecular mechanisms of drug resistance. *Journal of pathology*. **2005**, *205*, 275-292.

Luqmani, Y.A. Mechanisms of Drug Resistance in Cancer Chemotherapy. *Medical Principles and Practice* **2005**, *14*, 35-48.

Mayer, A.M.S.; Glaser, K.B.; Cuevas, C.; Jacobs, R.S.; Kem, W.; Little, R.D.; McIntosh, J.M.; Newman, D.J.; Potts, B.C.; Shuste, D.E. The odyssey of marine pharmaceuticals; a current pipeline perspective. *Trends in Pharmacological Sciences* **2010**, *31*(6), 255-265.

Pardee, A.B.; Stein, G.S. The biology and treatment of cancer; John Wiley & Sons: New York, NY, 2011.

Ruddon, R.W. Cancer biology; Oxford University Press: Oxford, 2007.

Siegel, R.L.; Miller, K.D.; Fedewa, S.A.; Ahnen, D.J.; Meester R.G.S.; Barzi, A.; Jemal, A. *CA: A Cancer Journal for Clinicians* **2017**, *67*, 7-30.

Statistics South Africa. Statistical Release P0309.3: Mortality and Causes of Death in South Africa, 2012. Findings from Death Notification. Pretoria: Statistics South Africa; 2014. [Retrieved October 20, 2017] from <http://www.statssa.gov.za> .

Statistics South Africa. Statistical Release P0309.3: Mortality and Causes of Death in South Africa, 2011. Findings from Death Notification. Pretoria: Statistics South Africa; 2014. [Retrieved October 20, 2017] from <http://www.statssa.gov.za> .

Statistics South Africa. Statistical Release P0309.3: Mortality and Causes of Death in South Africa, 2015. Findings from Death Notification. Pretoria: Statistics South Africa; 2017. [Retrieved October 20, 2017] from <http://www.statssa.gov.za> .

Statistics South Africa. Statistical Release P0309.3: Mortality and Causes of Death in South Africa, 2013. Findings from Death Notification. Pretoria: Statistics South Africa; 2014. [Retrieved October 20, 2017] from <http://www.statssa.gov.za> .

Statistics South Africa. Statistical Release P0309.3: Mortality and Causes of Death in South Africa, 2014. Findings from Death Notification. Pretoria: Statistics South Africa; 2015. [Retrieved October 20, 2017] from <http://www.statssa.gov.za> .

Sudhakar, A. History of Cancer, Ancient and Modern Treatment Methods. *Journal of Cancer Science and Therapy* **2009**, 1(2), 1-4.

Torre, L.A.; Siegel, R.L.; Ward, E.M.; Jemal, A. Global cancer incidence and mortality rates and trends- An update. *Cancer Epidemiology, Biomarkers and Prevention* **2016**, 25(2), 16-27.



Literature review: Nature as a source of anticancer natural products

2.1 Nature as a source of therapeutic agents

Natural products (NPs) are typically secondary metabolites, produced by living organisms such as plants, microorganisms and marine organisms in response to external stimuli. Throughout the ages humans have relied on nature to cater for their basic needs, not the least of which are medicines for the treatment of a wide range of diseases [Cragg and Newman, 2013]. Historically, pharmaceutical companies used relatively crude plant extracts for therapeutic formulations; it was only in the mid-twentieth century when purified compounds became common [Mishra and Tiwari, 2011]. Through evolution, living organisms have equipped themselves for survival in competitive environments by producing toxic chemicals to deter predators. It is these chemicals that scientists have used or manipulated for drug discovery and development. A review by David Newman and Gordon Cragg in 2016 showed that out of 1562 new drugs approved for use between the years 1981 and 2014, only 27% (figure 2.1) were totally synthetic, while development of other drugs were in one way or another related to natural products [Newman and Cragg, 2016].

Natural products often possess complex structures with multiple chiral centres, hydrogen bond donors and/or acceptors, and may not comply with Lipinski's rule of five. However, these chemical compounds have evolved to interact efficiently with their biological targets, therefore, they occupy a biologically relevant chemical space and represent validated starting points for drug discovery [Mishra and Tiwari, 2011]. Therapeutic areas of infectious diseases and oncology have indeed benefited from these types of compounds for drug discovery and development [Montaser and Luesch, 2011].

It is therefore not surprising that at least one third of the top selling drugs are either natural products or natural product derivatives with about 60% of drugs used in haematology and oncology being derived from natural products [Dyshlove and Honecker, 2003], many of which were discovered through the screening of natural products from plants, microorganisms, animals and marine organisms. This chapter gives a brief review of natural products in clinical use from various sources and the contribution of marine natural products in drug discovery, particularly for anticancer applications.

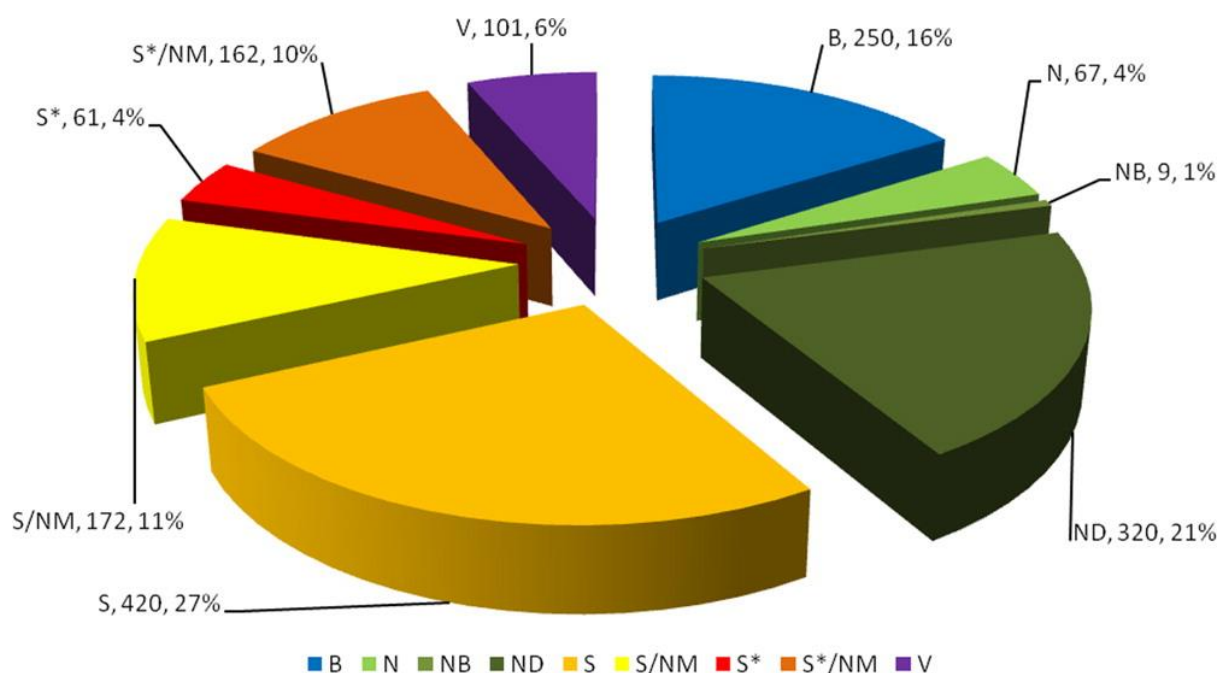


Figure 2.1. Summary of all new drugs approved by the FDA for clinical use between year 1981 and 2014 $n = 1562$. [Newman and Cragg, 2016]

Where *B* = Biological macromolecule, *N* = Unaltered natural product, *NB* = Botanical drug (defined mixture), *ND* = Natural product derivative, *S* = synthetic drug, *S** = Synthetic drug (NP pharmacophore), *V* = Vaccine and *NM* = Mimic of natural product

2.1.1 Anticancer drugs from plants

Plant products played a dominant role in development of sophisticated traditional medicine systems. World Health Organisation (WHO) estimates that at least 80% the population in Asian and African countries depend on traditional medicine for primary health care while 70-80% of population in developed countries use plant products as some form of alternative or complementary medicine [Khazir et al., 2014]. Starting in the early 1800s, advances in scientific knowledge led to the discovery of pure bioactive compounds, commonly referred to as natural products (NPs) [Newman and Cragg, 2014]. Several plant-derived compounds are currently successfully employed in cancer treatment; some of the most significant examples include the vinca alkaloids, the podophyllotoxins, camptothecins and the taxanes. In this section a review of commonly used plant derived anticancer drugs will be discussed.

Vinca alkaloids

The first vinca alkaloids, vincristine (**2.1**) and vinblastine (**2.2**) were discovered by Canadian scientists Robert Noble and Charles Beer in the 1950s from the Madagascar periwinkle plant *Catharanthus roseus* as potential antidiabetic agents [Moudi et al., 2013]. While investigating the plant's source of potential oral hypoglycaemic agents, the team noted that its extracts reduced white blood cell count and caused bone marrow depression in rats and were subsequently shown to be active against lymphocytic leukaemia in mice. The discovery of

vincristine (VCR) and vinblastine (VBL) was indirectly attributed to the observation unrelated to medical use of the source plant [Donadio et al., 2002]. VCR and VBL, and their synthetic analogues vinorelbine (**2.3**) and vindesine (**2.4**), exert their cytotoxicity effects through the inhibition of tubulin polymerization and are applied clinically in combination with other anticancer agents for the treatment of several cancers including leukaemia, lymphoma, breast, lung and advanced testicular cancers [Cragg and Newman, 2009]. Regardless of their benefits in the treatment of cancer, use of vinca alkaloids is associated with untoward side effects manifesting as peripheral neuropathy, neutropenia, severe myelosuppression, gastrointestinal toxicities and hepatic insufficiency [Moudi et al., 2013]

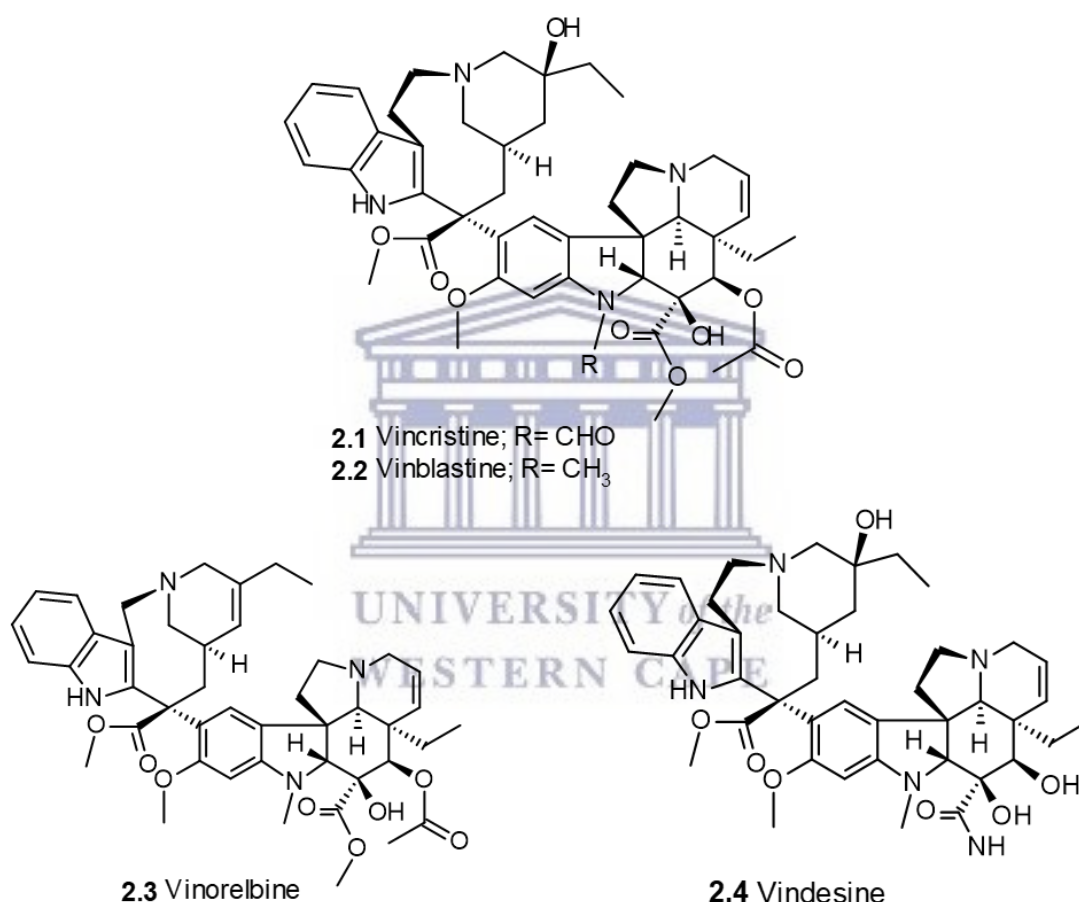


Figure 2.2. Structures of vincristine (**2.1**), vinblastine (**2.2**), vinorelbine (**2.3**), and vindesine (**2.4**).

Camptothecins

Camptothecin (**2.5**) is a member of the quinolinoalkaloid group consisting of a pentacyclic ring structure that includes a pyrrole (3,4 β)-quinoline moiety and one asymmetric centre within the α -hydroxy lactone ring with 20(S) configuration (ring E) [Srivastava et al., 2005]. Camptothecin was first discovered in 1958 from *Camptotheca acuminata*, (Nyssaceae) a Chinese native tree by M.E Wall and M.C Wani while searching for possible sources of steroidal precursors for production of cortisone. They discovered that the leave extract of the plant exhibited good

antitumour activity when tested against L1210 mouse leukaemia prolongation assay [Wall and Wani, 1995], and its mechanism of cell death was later revealed to involve the inhibition of topoisomerase I (T-I), an enzyme implicated in replication, transcription and recombination [Wall and Wani, 1995, Lorence Nessler, 2004]. Despite its potent activity, camptothecin had very poor water solubility and as a result, its clinical trials were initiated with the sodium salt of its lactone hydrolysis product. Unfortunately, the salt had reduced efficacy and severe toxicity resulting in suspension of the clinical trials [Lorence and Nessler, 2004]. However, scientists were later able to synthesise its analogues topotecan (**2.6**) and irinotecan (**2.7**), which are currently marketed as Hycamtin® and Camptosar®, respectively.

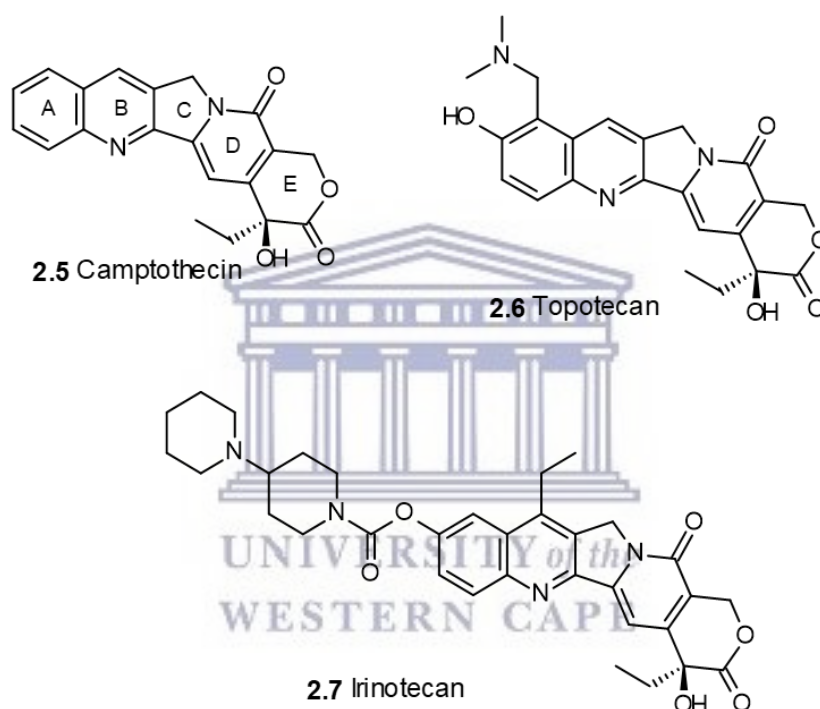


Figure 2.3. Chemical structures of camptothecin **2.5**, topotecan **2.6** and irinotecan **2.7**.

Podophyllotoxins

Podophyllotoxins are naturally occurring lignans found in plants, predominantly in the genus *Podophyllum* and they have been used for over a 1000 years as medicines [Hande, 1998]. Podophyllin, an extract of *Podophyllum peltatum* has been used for the treatment of medical conditions such as syphilis, gonorrhoea, liver and kidney diseases [Damayanthi and Lown, 1998]. Effectiveness of podophyllin against genital warts in 1942 inspired studies for its activity on tumour tissue but it was only in 1958 that isolation, structural characterizations and synthetic approaches to the active constituents were reviewed [Damayanthi and Lown, 1998]. Podophyllotoxin (**2.8**) is a major component of podophyllin and exhibits a wide range of pharmacological applications such as treatment of rheumatoid arthritis, genital and perianal

warts, herpes simplex and *Condyloma acuminatum* viral infections and measles [Gordaliza, 2007]. In addition to these, podophyllotoxin is a potent antitumour agent and is used in the treatment of genital tumours, Wilm's tumours, non-Hodgkin's lymphomas and lung cancers. Despite its potency, podophyllotoxin's clinical use declined rapidly because of unwanted side effects and lack of selectivity leading to damage of normal tissue cells. Nonetheless, its remarkable biological activity has made it an important lead compound for the discovery of more effective antitumour agents [Liu et al., 2015]. The two active derivatives etoposide (**2.9**) and teniposide (**2.10**) were a result of a chemical synthetic programme initiated to produce compounds with reduced toxicity but potent activity [Nobili et al., 2009]. Both etoposide and teniposide exhibit their antitumour activity through formation of a complex with topoisomerase II and DNA, thus preventing DNA reseat and ultimately cell death [Nobili et al., 2009]. These analogues displayed activity against several cancers including acute myeloid leukaemia, Hodgkin's disease, non-Hodgkin's lymphoma, lung cancer (both small cell and non-small cell), gastric cancer, breast cancer and ovarian cancer and etoposide was approved for use by the FDA in 1983, while teniposide obtained approval 10 years later [Hande, 1998] .

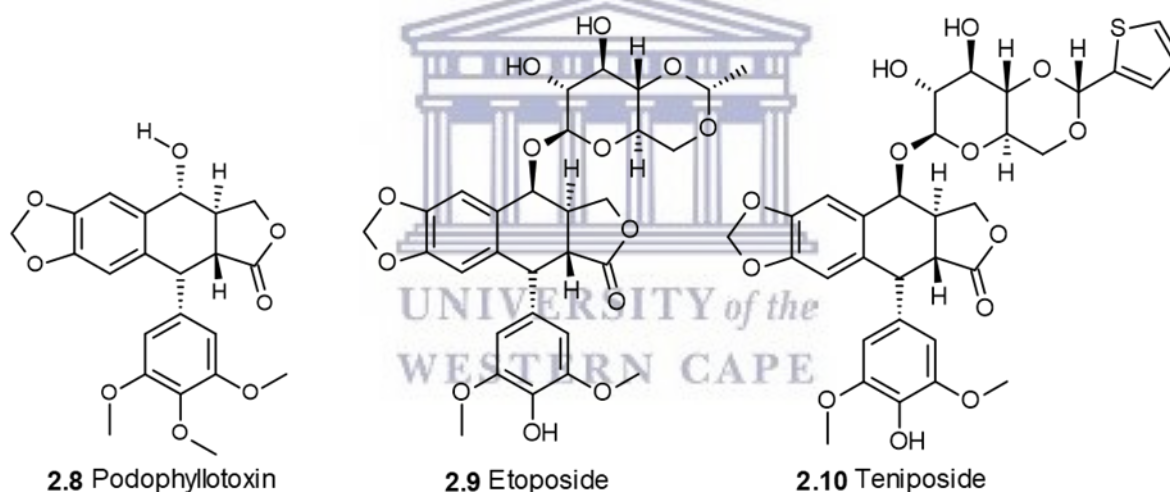


Figure 2.4. Podophyllotoxin **2.8** and its synthetic derivatives etoposide (**2.8**) and teniposide (**2.10**)

Taxanes

Taxanes are anticancer cytotoxic agents classified under tubulin binding agents. The two examples in clinical use are paclitaxel (**2.11**) and docetaxel (**2.12**). Their mechanism of action was discovered in 1979 and involves arrest of cell cycle by stabilizing microtubule formation at G2/M phase and S phase for paclitaxel and docetaxel, respectively [Crown and O'Leary, 2000; Howat et al., 2014]. Paclitaxel was originally isolated from the bark of *Taxus brevifolia* in 1962 and is currently approved for the treatment of breast, lung and non-small cell cancers and its uses are predicted to expand to other types of cancers [Howat et al., 2014]. Docetaxel is a second generation semi-synthetic derivative obtained by esterification of a side chain to

10-deacetylbaccatin III (the inactive taxane precursor). Both paclitaxel and docetaxel consist of a complex taxane ring linked to an ester at the C-13 position. The moieties at the C-2' and C-3' positions on the C-13 side chain are essential for their antimicrotubule activity [Rowinsky, 1997]. The use of docetaxel has been reported to improve survival in metastatic breast cancer and decreased mortality in breast cancer, however, like the vinca alkaloids, the use of taxanes is associated with peripheral neuropathy and myelosuppression [Cella et al., 2003]. In addition, the taxanes are also known to cause arthralgias, myalgias and skin reactions [Cella et al., 2003; Ho and Mackey, 2014].

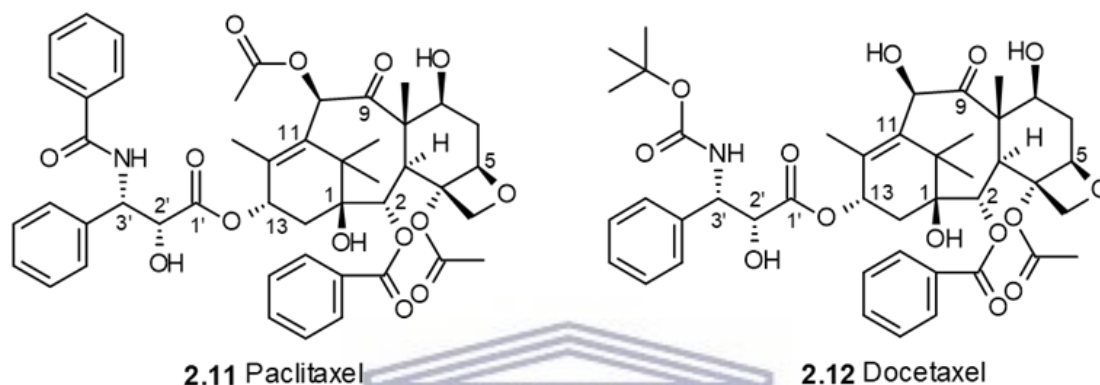


Figure 2.5. Structures of paclitaxel **2.11** and docetaxel **2.12**.

2.1.2 Anticancer agents from microbial sources

Microbial secondary metabolites represent a large source of compounds endowed with novel structures and potent biological activities and are widely used therapeutically as antibacterial, immunosuppressive, cholesterol lowering and anticancer agents [Donadio et al., 2002]. This section discusses a few of the common microbial derived natural products used in cancer treatment and includes the anthracyclines, bleomycins and actinomycins.

Anthracyclines

Anthracyclines are anticancer antibiotics consisting of a tetracyclic ring structure containing an anthraquinone chromophore and an aminoglycoside. The first anthracycline, daunorubicin (**2.13**) and doxorubicin (**2.14**) were isolated from the pigment-producing bacterium *Streptomyces peucetius* in early in 1966 and 1967, respectively, and they rank among the most effective anticancer drugs ever developed [Minotti et al., 2004]. These drugs have since been used widely for the treatment of a wide range of cancers which include among others: breast, lung, gastric, ovarian, thyroid, non-Hodgkin's and Hodgkin's lymphoma, multiple myeloma, sarcoma, and paediatric cancers. Their proposed mechanism of action is believed to be through (i) intercalation into DNA and disruption of topoisomerase-II-mediated DNA repair and (ii) generation of free radicals and their damage to cellular membranes, DNA and proteins [Thorn et al., 2011]. Use of these drugs, however pose challenges in the form of

development of resistance by tumour cells and general toxicity, mainly in the form of chronic cardiomyopathy and congestive heart failure. To overcome these challenges, several analogues of these drugs have been synthesised and idarubicin (**2.15**) and epirubicin (**2.16**) were successful in reaching clinical trials and were approved for use as alternatives to doxorubicin and daunorubicin, respectively [Nobili et al., 2009]. The structures of doxorubicin, daunorubicin, idarubicin and epirubicin are shown in figure 2.6.

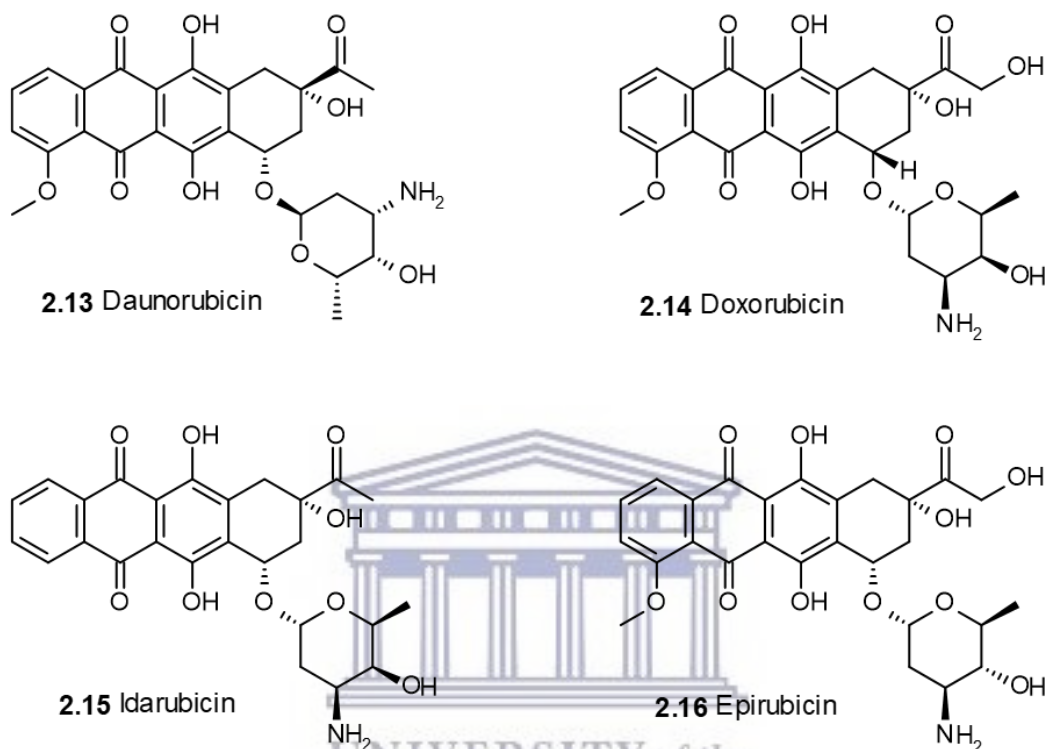


Figure 2.6. Structures of daunorubicin **2.13**, doxorubicin **2.14**, idarubicin **2.15**, and epirubicin **2.16**.

Other antitumour antibiotics include the bleomycins, actinomycins, mitomycins geldanamycin, sirolimus, etc. Bleomycins are a group of glycopeptides discovered by Umezawa and colleagues from *Streptomyces* sp. [Muller et al., 1972]. They are currently used in combination with other anticancer agents for the treatment of several types of tumours, particularly squamous cell carcinomas and malignant lymphomas [Hecht, 2000]. They are therapeutically available as a mixture of several congeners known as blexanone containing predominantly bleomycin A2 (**2.17**) and B2 (**2.18**) [Hecht, 2000]. Actinomycins are a well-known class of chromopeptides containing the same actinoyl chromophore (2-amino-4,6-dimethylphenoxazine-3-one-1,9-dicarboxylic acid [Bitzer et al., 2006]. Actinomycin D (**2.19**), the most common compound of this group has found its use in the treatment of highly malignant and high-risk tumours such as Wilms' tumour, gestational choriocarcinoma, Ewing's sarcoma and rhabdomyosarcoma [Bitzer et al., 2006, Wang et al., 2008]. Its mechanism of

action involves DNA intercalation with subsequent inhibition of DNA transcription [Bitzer et al., 2006; Wang et al., 2008; Veal et al., 2003].

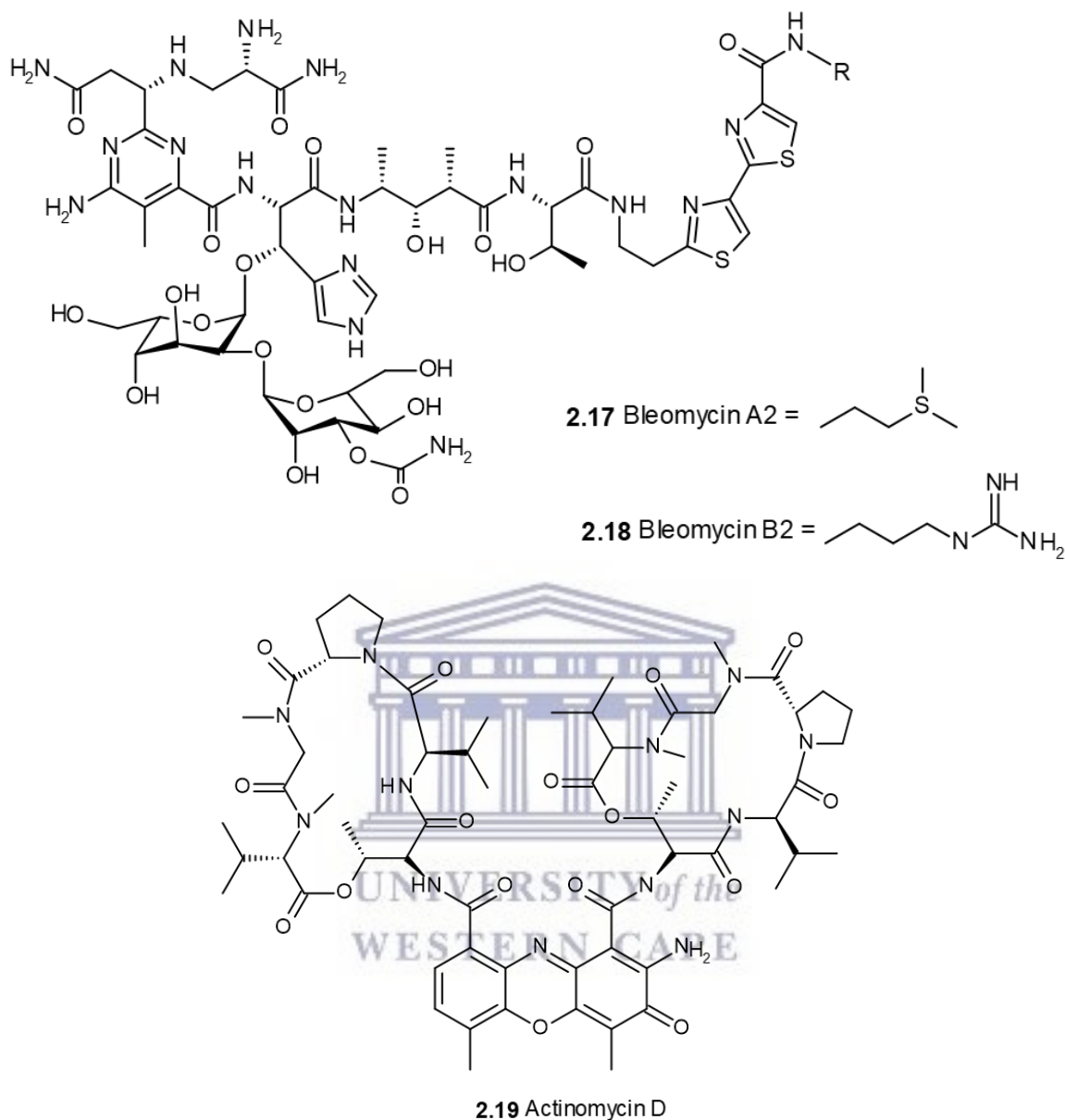


Figure 2.7. Structures of bleomycin A2 **2.17**, bleomycin B2 **2.18** and actinomycins D **2.19**.

2.2 Anticancer agents from marine sources

Unlike terrestrial plants and microbial metabolites which have been used as sources of drugs for many years, the discovery of marine derived natural products is a promising, but relatively new field [Mehbub et al., 2014]. Compared to terrestrial compounds, marine natural products show a higher incidence of chemical novelty making them a significant source of diverse chemical and bioactive secondary metabolites which can be widely applied in pharmaceutical and cosmeceutical industries [Zhang et al., 2016]. With the oceans covering 70% of the earth's surface and consisting of up to 36 phyla, marine organisms represent an unrivalled source of

biodiversity [Zhang et al., 2016; Ruiz-Torres et al., 2017]. Use of marine natural products as therapeutic agents started in 1950s with the discovery of uncommon nucleosides, spongouridine (**2.20**) and spongothymidine (**2.21**) from the marine sponge *Cryptotethya crypta* by Bergmann and Feeny [Mehbub et al., 2014; Zhang et al., 2016; Ruiz-Torres et al., 2017].

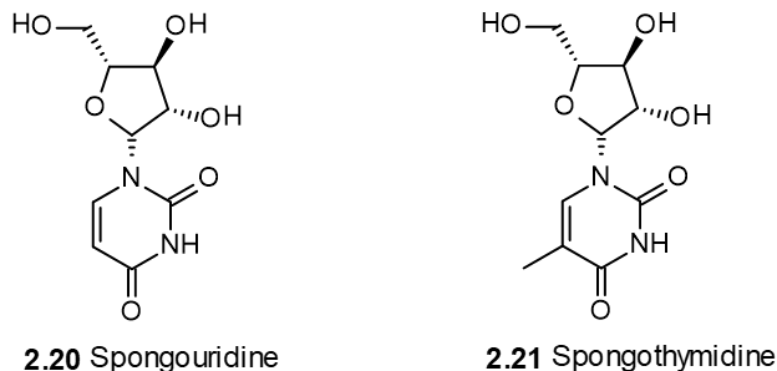


Figure 2.8. Structures of spongouridine (**2.20**) and spongothymidine (**2.21**).

The annual review of marine natural products by Blunt and collaborators has revealed that over 1000 new compounds isolated from marine organisms were reported each year in the past decade (figure 2.9). To date eight marine natural product derived compounds namely: cytarabine, vidarabine, ziconotide, trabectedin, eribulin mesylate, brentuximab vedotin, omega-3 acid ethyl esters and iota carrageenan, have been approved by the Food and Drug Authority (FDA) and/or European Medicines Evaluation Agency (EMA) for different medical conditions and four of these compounds are approved for use in cancer treatment.

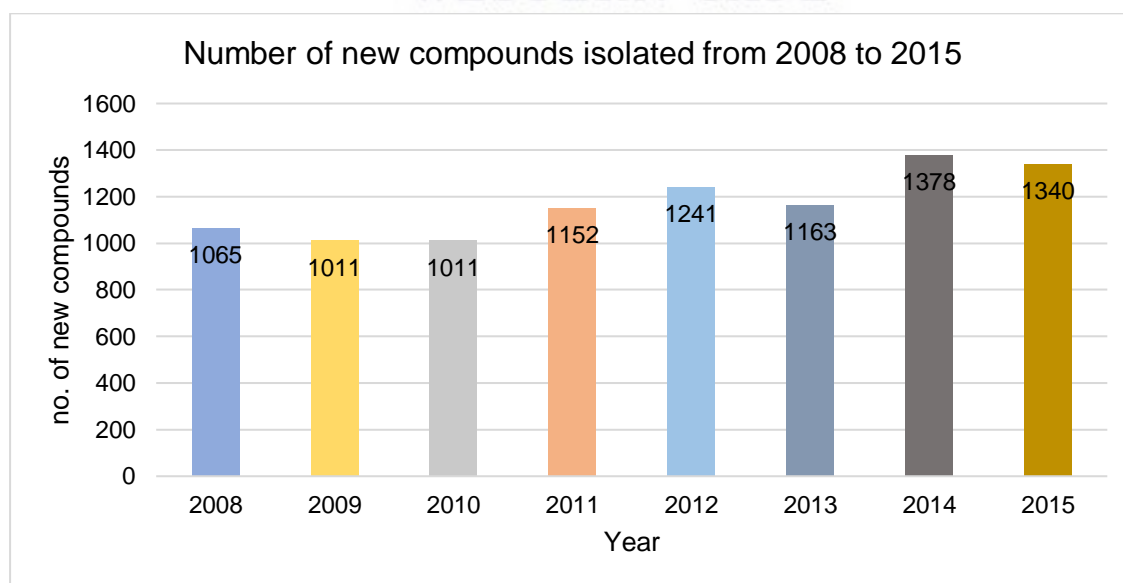


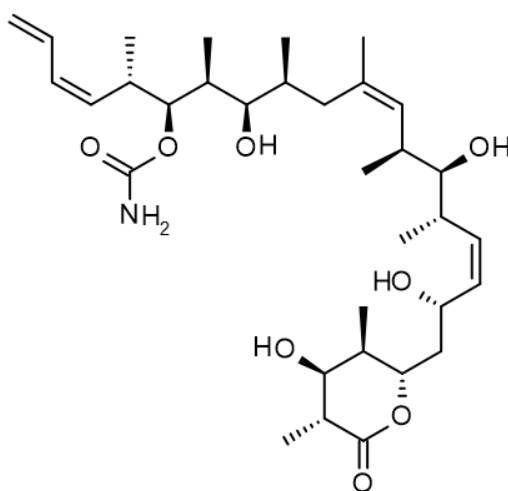
Figure 2.9. New marine natural compounds isolated from year 2008 to 2015.

2.2.1 Marine sponges as sources of anticancer agents

Sponges (Phylum: Porifera) are sessile invertebrates lacking an innate immune system, mechanical defence structures like shells or spines, and living in an environment with so much diversity, it would be surprising if they were not prey to other animals. However, through evolution sponges have developed, or acquired microorganisms with, complex biochemical pathways to produce metabolites that act as a self-defence to deter predators and survive the harsh environment [Calcabrini et al., 2017]. Among all marine organisms, sponges are the most dominating source of marine secondary metabolites, contributing 30% of all marine natural products so far, with at least more than 200 new compounds reported each year for the last decade [Mehbub et al., 2014; Calcabrini et al., 2017]. These compounds have been revealed to have a wide spectrum of biological activities, including: anticancer, antibacterial, antiviral, anti-inflammatory, antifungal, antifouling, antihelmintic, immunosuppressive, neurosuppressive, neuroprotective, antiprotozoal and many other activities [Mehbub et al., 2014]. This section of the chapter discusses some of marine sponge derived anticancer compounds which reached clinical trials.

Discodermolide

(+)-Discodermolide (**2.22**) is a polyketide natural product originally isolated from a Caribbean deep sea sponge *Discodermia dissolute* [Gunasekera et al., 2002]. The compound was reported to elicit its anticancer activity through polymerisation and stabilisation of microtubules in a manner similar to that of paclitaxel [Gunasekera et al., 2002; Schwarzenberg and Vollmar, 2013]. *In vitro* studies showed its ability to inhibit several cancer cell lines including paclitaxel resistant ovarian and colon cancer cells [Gunasekera et al., 2002]. Like many other natural products, discodermolide was isolated in minute quantities from its natural source, however, inspired by the total synthesis of the drug by the Paterson and Smith groups, Novartis Pharma AG were able to develop synthetic steps and enter it into clinical trials [Gomes et al., 2016; Kingston, 2009]. Sadly, due to its high toxicity, it had to be pulled out of clinical trials [Schwarzenberg and Vollmar, 2013; Kingston, 2009].

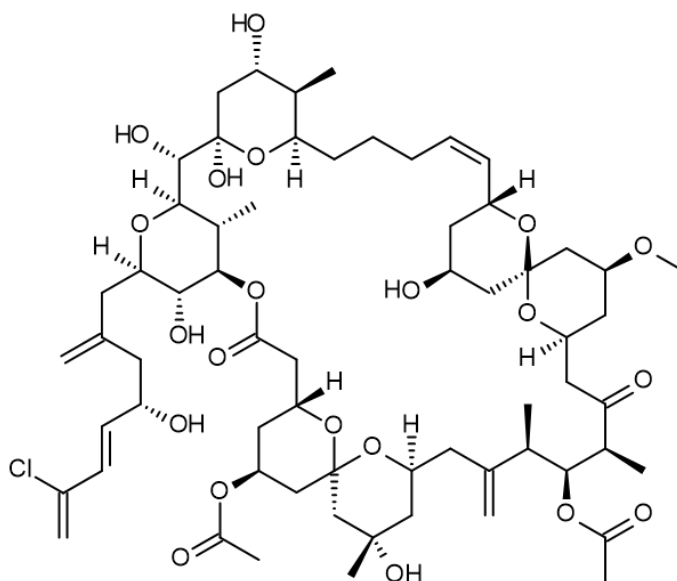


2.22 Discodermolide

Figure 2.10. Structure of discodermolide **2.22**.

Spongiastatin-1

Another noteworthy discovery was that of spongiastatin-1 (**2.23**), a macrocyclic ring with six pyran rings. With its selective, potent activity at a picomolar concentration against the NCI 60 panel of cancer cell lines, the spongiastatin-1 profile proved to be one of the best in the NCI's evaluation program with IC_{50} of 10^{-10} M against small cell lung cancer, colon cancer, renal cancer, ovarian cancer and breast cancer sets [Pettit, 1996]. Spongiastatin-1 is believed to induce cell death through inhibition of tubulin polymerisation, antimetastatic effects and caspase-independent pro-apoptotic activity [Gomes et al., 2016]. Spongiastatin-1 was reported by the Pettit group from a black Maldives sponge *Hyrtios* sp [Pettit, 1996]. Although the group had been working on the similar compounds from a South African sponge since 1973, it was only in 1988 that they could solve the first structure of the spongiastatins series due to the challenge presented by the small quantities isolated at that time. Currently, the Smith group has successfully managed to develop a 27 step synthetic method of spongiastatin-1 [Gomes et al., 2016]. Spongiastatin-1 has entered phase I of clinical trials.

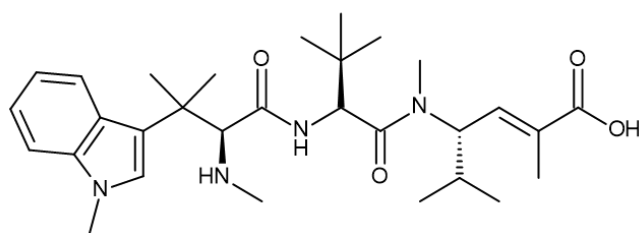


2.23 Spongiastatin-1

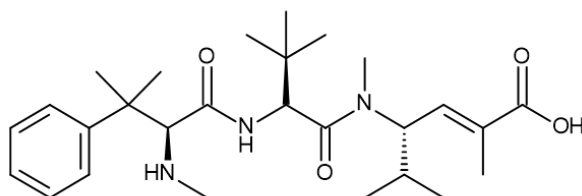
Figure 2.11. Structure of spongiastatin-1 **2.23**.

Hemiasterlin

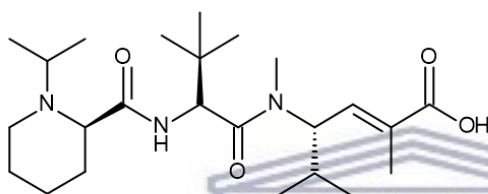
Another sponge derived compound of interest is HTI-286 (**2.25**), a synthetic analogue of Hemiasterlin (**2.24**). Hemiasterlin is a naturally occurring tripeptide originally isolated from a South African marine sponge *Hemiasterella minor*, but also found in sponges of the species *Aymbastela*, *Siphonochalina* and *Auletta* [Tran et al., 2014]. Both hemiasterlin and its analogue HTI-286, attracted clinical interest due to their potent cytotoxicity at nanomolar concentrations; HTI-286 was reported to have activity against 18 human cancer cell lines at a mean IC_{50} of 2.5 nM, including cells that are VCR and paclitaxel resistant [Barlocco et al., 2003]. In 2003, HTI-286 entered phase I clinical trials but could not proceed with phase II due to lack of objective response and toxicity. Nonetheless, another analogue of hemiasterlin E7974 (**2.26**), made its way into clinical trials showing great potency *in vivo* against many human xenograft models [Tran et al., 2014].



2.24 Hemiasterlin



2.25 HTI-286



2.26 E7974

Figure 2.12. Structures of hemiasterlin **2.24**, HTI-286 **2.25** and E-7974 **2.26**.

2.3 Marketed marine derived anticancer drugs

Cytarabine (Cytosar U®) FDA 1969)

Cytarabine is a synthetic pyrimidine nucleoside derived from a nucleoside, spongouridine, originally isolated from a Caribbean sponge *Cryptotethya crypta* [Mayer et al., 2010]. Inspired by the presence of an arabinose unit instead of ribose in the nucleosides spongouridine and spongothymidine, several ara-nucleosides were synthesised, which lead to the development of cytarabine (**2.27**) and vidarabine (**2.28**). The FDA approved these compounds in 1969 and 1976 as anticancer and antiviral drugs, respectively, and they are available as conventional cytarabine (Cytosar-U®) and as a liposomal formulation (Depocyt®) [Zhang et al., 2017; Mayer et al. 2010]. Intracellularly, cytarabine is converted to its active metabolite cytarabine triphosphate, which in turn inhibits DNA polymerase by competing with physiological deoxycytidine triphosphate, resulting in inhibition of DNA synthesis and cell death [Zhang et al., 2017]. Cytarabine continues to be the preferred drug for the treatment of myeloid leukaemia, non-Hodgkin's lymphoma and meningeal leukaemia and it is used alone or in combination with other anticancer agents [Zhang et al., 2017].

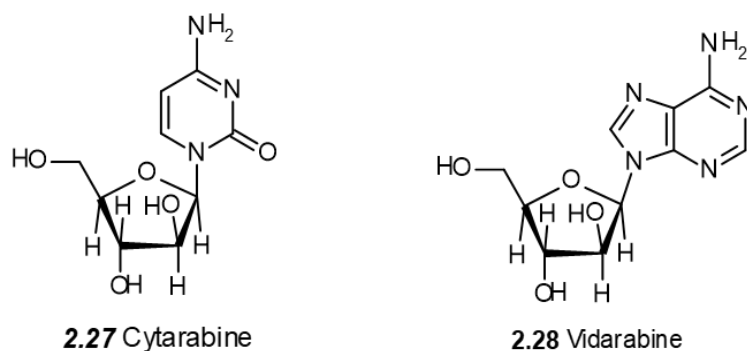


Figure 2.13. Structures of cytarabine **2.27** and vidarabine **2.28**.

Ecteinascidin (Yondelis®) EMEA 2007, FDA 2015

Ecteinascidin-743 (ET-743) (**2.29**) commercialised as Yondelis® by PharmaMar is a naturally occurring tetrahydroisoquinolone alkaloid originally isolated from a Caribbean tunicate *Ecteinascidia turbinata* [Gerwick and Moore, 2012]. ET-743 was isolated in extremely small quantities, which resulted in its structure taking 30 years to elucidate. The compound is now made available by semi-synthesis from a microbial natural product, cyanosafracin B, a fermentation product of *Pseudomonas fluorescens* [Martins et al., 2014; Gerwick and Moore, 2012]. At nanomolar concentrations, ET-743 showed potent activity against a variety of solid tumour cell lines including melanoma, non-small lung carcinoma, ovarian and colon cell lines [Erba et al., 2001]. Its mechanism of action involves interaction with DNA and subsequent blockade of G2/M and p53-independent apoptosis [Gerwick and Moore, 2012]. Yondelis is approved for treatment of soft tissue sarcomas and relapsed ovarian cancer and metastatic liposarcoma or leiomyosarcoma patients previously treated with anthracycline containing regimen [Gordon et al., 2016].

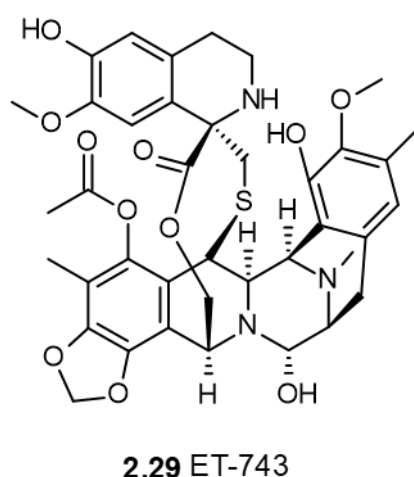


Figure 2.14. Structure of ET-743 **2.29**.

Eribulin mesylate (Halaven®) FDA 2010, EMEA 2011

Eribulin (**2.30**) is a synthetic analogue of halichondrin B (**2.31**), a polyether macrolide originally isolated by Hirata and Uemura in 1985 from a rare Japanese sponge *Halichondria okadai* [Swami et al., 2012]. Upon discovery, halichondrin B was shown to possess potent anticancer activity in a variety of animal cancer models and its mechanism of action was found to be through binding to the vinca sites of tubulin and causing mitotic arrest due to inhibition of tubulin polymerization and microtubule assembly dependent on microtubule-associated proteins [Cortes et al., 2012]. Despite its remarkable anticancer activity, use of halichondrin B as a therapeutic agent was limited by its low yields when isolated from natural sources, with only about 300 mg biomass yield from a one ton of *Lyssodendoryx* sp. which was another promising source of halichondrin B [Yeung, 2011]. It is clear from this information that it would have been unfeasible to depend solely on nature for supply of this drug, hence synthesis of its analogues was the most realistic approach for a reliable supply. This synthesis-cytotoxicity coupled evaluation, revealed that the entire western portion of halichondrin B could be stripped away whilst retaining a positive therapeutic effect [Radjasa et al., 2011] resulting in the discovery of eribulin. Eribulin obtained US FDA and EMEA approval in 2010 and 2011, respectively, for use in metastatic breast cancer patients who have previously received at least two chemotherapeutic regimens for the treatment of metastatic disease [Cortes et al., 2012; Radjasa et al., 2011].



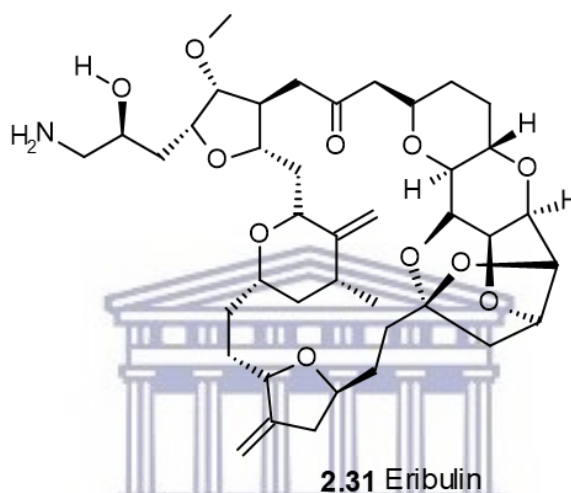
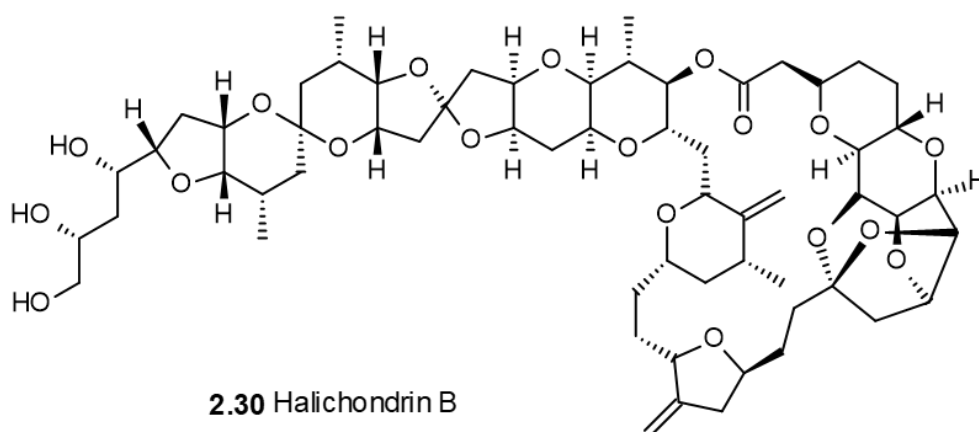
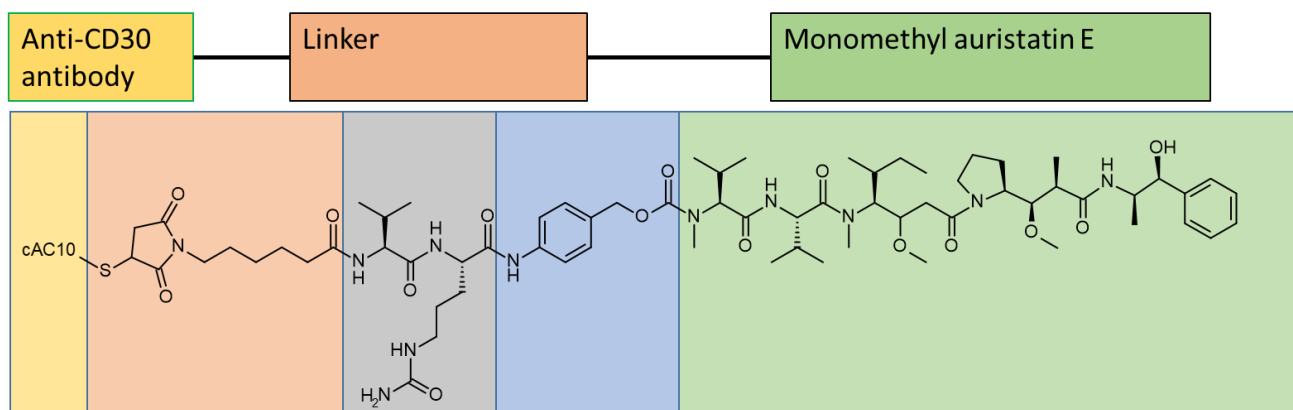


Figure 2.15. Structures of eribulin **2.30** and halichondrin B **2.31**.

Brentuximab vedotin 63 (Adcetris®) FDA 2011

Brentuximab vedotin 63 (Adcetris®) (**2.32**) is the most recent addition to the marine derived drugs, entering the market after approval by the FDA in 2011. Adcetris® is a synthetic analogue of dolastatin 10, which was originally isolated from the Indian Ocean sea hare, *Dolabella auricularia* by Pettit's group in 1987 [Gerwick and Moore, 2012]. At the time of its isolation, dolastatin 10 proved to be one of the most potent antineoplastic substances with an effective dose that produces therapeutic response in 50% of the subjects (ED₅₀) in the picomolar range against a number of cancer cell lines [Martins et al., 2014]. Nonetheless, its phase I and II clinical trials were unsuccessful due to lack of efficiency and its toxicity. Development of Adcetris® was achieved by linking a semisynthetic monomethyl auristatin E (dolastatin analogue) to a CD30 targeting antibody cAC10 by a protease cleavable linker resulting in a highly effective and well tolerated agent for treatment of Hodgkin's lymphoma and anaplastic large lymphoma [Gerwick and Moore, 2012; Martins et al., 2014]. Other analogues of dolastatin 10 such as soblidotin and tasidotin have also made it to clinical trials but were later discontinued for various reasons.



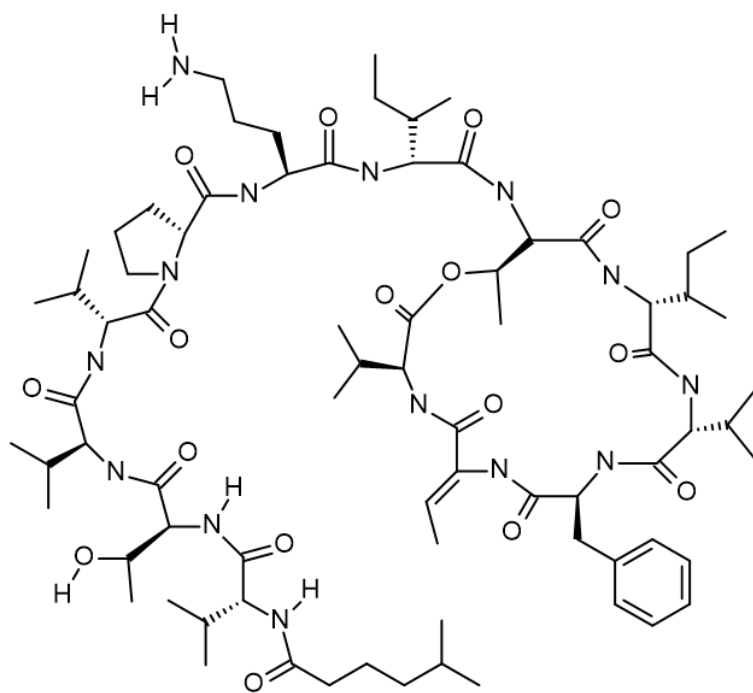
2.32 Brentuximab vedotin 63

Figure 2.16. Structure of brentuximab vedotin **2.32**.

2.4 Other marine derived natural compounds in advanced clinical trials

Kahalalide F

Kahalalide F (**2.33**), a depsipeptide, was originally isolated from a mollusc *Elysia rufescens* and subsequently from *Bryopsis pennata*, an alga that *E. rufescens* feeds on. It was also found in different species of the Indian Ocean *Elysia* [Newman and Cragg, 2014]. Kahalalide showed activity against a variety of tumour cells derived from breast, non-small cell lung and hepatic cancer cell lines and, most importantly, showing up to 40 times less activity against non-cancer cells like Human umbilical vein endothelial cells [Schwarzenberg and Vollmar, 2013]. The compound was licensed to PharmaMar who developed synthetic methods to produce the compounds in bulk using peptide chemistry techniques. Kahalalide F is currently in phase II clinical trials for the treatment of non-small cell lung cancer in Spain under the EudraCT number 2004-001253-39 [Newman and Cragg, 2014].

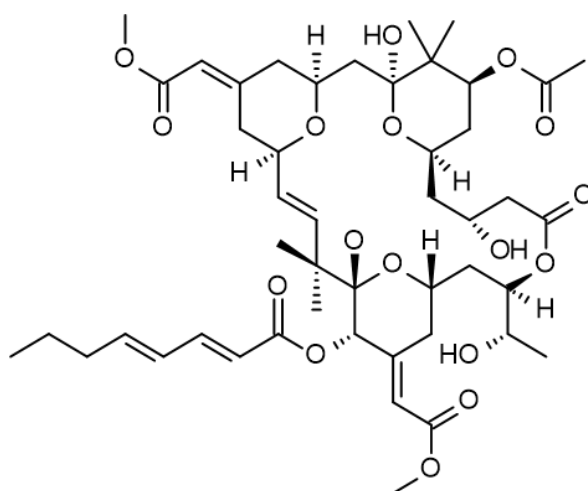


2.33 Kahalalide F

Figure 2.17. Structure of Kahalalide F **2.33**.

Bryostatin-1

Bryostatin-1 (**2.34**), a member of a group of compounds known as bryostatins, is an antineoplastic complex macrolide originally isolated by Pettit and his collaborators from a bryozoan *Bugula neritina* [Cragg and Newman, 2013]. Bryostatin-1 was isolated in sufficient quantities to permit more than 80 clinical trials to date and has displayed positive responses. Acting as a single agent with effects ranging from complete to partial remission, its mechanism of action is believed to be due to its ability to interact with protein kinase C (PKC) isoenzymes [Dias et al., 2012]. Bryostatins have been a target for many synthetic chemists, undergoing extensive studies to produce simpler analogues possessing comparable or better activity, particularly when related to binding to some of the molecular targets PKC isoenzymes [Gragg et al., 2013]. Using pharmacophoric and docking hypotheses, Wender and Baryza were able to synthesise structurally simplified bryostatin-1 analogues possessing bryostatin-like activity, but with greater potency *in vitro* and limited *in vivo* activity in comparison with the natural product [Wender et al., 2011]. Bryostatin-1 is currently in phase I clinical trials for treatment of cancer and Alzheimer's disease [Ruiz-Torres et al., 2017].

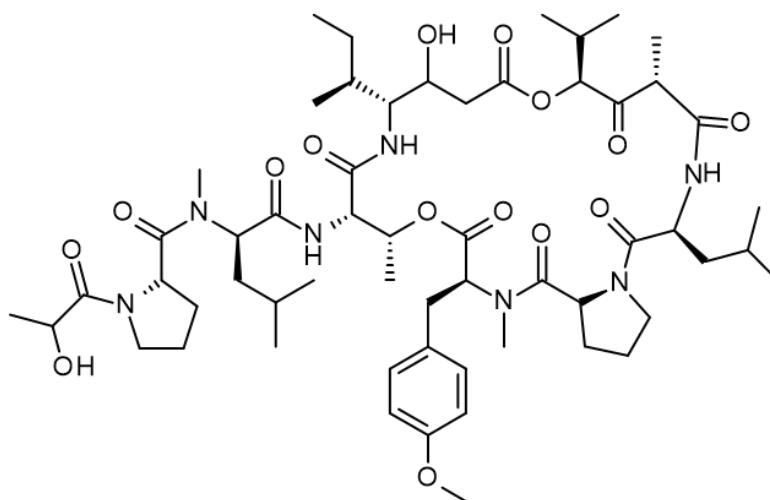


2.34 Bryostatin-1

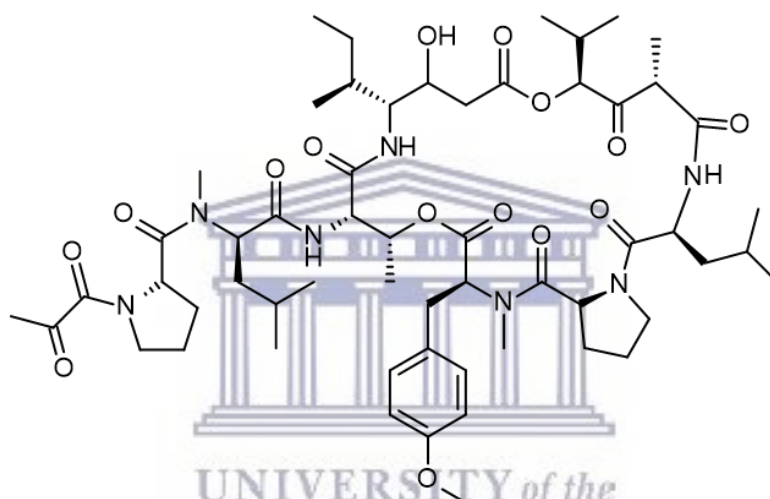
Figure 2.18. Structure of bryostatin-1 **2.34**.

Didemnin B and Pliditepsin (aplidin)

A cyclic antiproliferative depsipeptide didemnin B (**2.35**) was isolated from the Caribbean tunicate *Trididemnum solidum* by Riheart *et al.*, and it became the first marine natural product to enter clinical trials as an antitumour agent [Simmons *et al.*, 2005]. The compound demonstrated potent antitumour activity, however, due to its significant toxicity, studies were discontinued after phase II clinical trials [Tsukimoto *et al.*, 2011]. Another compound structurally similar to didemnin B, aplidin (**2.36**), formerly known as dehydroididemnin B was isolated from the Mediterranean tunicate *Aplidin albicans*. Its preclinical trials suggested potential high anticancer activity against various rapidly proliferating tumours due interference to cell cycle progression at G1 [Schwartzmann *et al.*, 2001].



2.35 Didemnin B



2.36 Aplidin

Figure 2.19. Structures of didemnin B **2.35** and aplidin **2.36**.

This short review not only shows the potential of natural products in general, and marine natural products specifically, but also some of their shortcomings such as adverse effects and the development of resistance to available drugs, which makes the continued search for new and more selective antitumour agents an important area of research.

2.5 References

- Barlocco, D.; Barrett, D.; Edwards P.; Lanston, S.; Perez-Perez, M.J.; Walker M.; Weidner, J.; Westwell, A. Monitor: Molecules and profiles. *Drug Discovery Today* **2003**, 8(20), 955-957.
- Bitzer, J.; Gesheva, V.; Zeech, A. Actinomycins with altered threonine units in the β -peptidolactone. *Journal of Natural Products* **2006**, 69, 1153-1157.
- Calcabrini, C.; Catanzaro, E.; Bishayee, A.; Turrini, E.; Fimognari, C. Marine sponge natural products with anticancer potential: An updated review. *Marine Drugs* **2017**, 15, 310.
- Cella, D.; Peterman, A.; Hudgen, S.; Webster, K.; Socinski, M.A. Measuring the side effects of taxane therapy in oncology. *Cancer* **2003**, 94(4), 822-837.
- Cortes, J.; Montero, A.J.; Gluck, S. Eribulin mesylate, a novel microtubule inhibitor in the treatment of breast cancer. *Cancer Treatment Reviews* **2012**, 38, 141-151.
- Cragg, G. M.; Newman, D. J. Natural Products: A Continuing Source of Novel Drug Leads. *Biochimica et Biophysica Acta* **2013**, 1830(6), 3670-3695.
- Cragg, G. M.; Newman, D. J. Nature: a Vital Source of Leads for Anticancer Drug Development. *Phytochemistry Reviews* **2009**, 8(2), 313—331.
- Crown, J.; O'Leary, M. The taxanes: an Update. *Lancet*. **2000**, 355(9210), 1176-1178.
- Damayanthi, Y.; Lown, J.W.; Podophyllotoxins: Current status and recent developments. *Current Medicinal Chemistry* **1998**, 5, 205-252.
- Dias, D.A.; Urban, S.; Roessener, U. A historical overview of natural products in drug discovery. *Metabolites* **2012**, 2, 303-331.
- Donadio, S.; Monciardini, P.; Alduina, R.; Mazza, P.; Chiocchini, C; Cavaletti, L.; Sosio, M.; Puglia, M.A. Microbial technologies for the discovery of novel bioactive metabolites, *Journal of Biotechnology* **2002**, 99(3), 187-198.
- Dyshlove, S.A.; Honecker, F. Marine Compounds and Cancer: Where do we Stand? *Marine Drugs* **2003**, 13, 5657-5665.
- Erba, E.; Bergamaschi, D.; Bassano, L.; Damia, G.; Ronzoni, S.; Faircloth, G.T.; D'Incalci, M. Ecteinascidin-743 (ET-743), a natural marine compound with unique mechanism of action. *European Journal of Cancer* **2001**, 37(1), 97-105.
- Gerwick, W.H.; Moore, B.S. Lessons from the past and charting the future of marine natural products drug discovery and chemical biology. *Chemistry and Biology* **2012**, 19, 85-98.

Gomes, N.G.M.; Dasari, R.; Chandra, S.; Kiss, R.; Kornienko, A. Marine invertebrate metabolites with anticancer activities: Solutions to the "Supply Problem". *Marine Drugs* **2016**, *14*, 98.

Gordaliza, M. Natural products as leads to anticancer drugs. *Clinical and Translational Oncology* **2007**, *9*, 767-776.

Gordon, E.M.; Sankhala, K.K.; Chawla, N.; Chawla, S.P. Trabectedin for Soft Tissue Sarcoma: Current Status and Future Perspectives. *Advances in Therapy* **2016**, *33*, 1055-1071.

Gragg, G.M.; Grothaus, P.G.; Newman, D.J. New horizons for old drugs and drug leads. *Journal of Natural Products* **2014**, *77*(3), 703-723.

Gunasekera, S.P.; Paul, G.K.; Longley, R. E.; Isbrucker, R.A.; Pomponi, S.A. Five new discodermolide analogues from the marine sponge *Discodermia* species. *Journal of Natural Products* **2002**, *65*, 1643-1648.

Hande, K.R. Etoposide: Four Decades of Development of a Topoisomerase II Inhibitor. *European Journal of Cancer* **1998**, *34*(10), 1514-1521.

Hecht, S.M. Bleomycin: New perspectives on the mechanism of action. *Journal of Natural Products* **2000**, *63*, 158-168.

Ho, M.Y.; Mackey, J.R. Presentation and management of docetaxel-related adverse effects in patients with breast cancer. *Cancer Management Research* **2014**, *6*, 253-259.

Howat, S.; Park, B.; Suk, O.I.; Jin, Y.W.; Lee, E.K.; Loake, G.J. Paclitaxel: Biosynthesis, Production and Future Prospects. *New Biotechnology* **2014**, *31*(3), 242-245.

Khazir, J.; Mir, B.A.; Pilcher, L.; Riley, L.D. Role of plants in anticancer drug discovery. *Phytochemistry Letters* **2014**, *7*, 193-181.

Kingston, D.G.I. Tubulin-interactive natural products as anticancer agents. *Journal of Natural Products* **2009**, *72*(3), 507-515.

Liu, Y-Q.; Tian, J.; Qian, K.; Zhao, X-B.; Morris-Natschke S.L.; Yang, L.; Nan, X.; Tian, X.; Lee, K-H. Recent progress on C-4 modified podophyllotoxin analogues as potent antitumour agents. *Medicinal Research Reviews* **2015**, *35*(1), 1-62.

Lorence, A.; Nessler, C.L. Camptothecin, over four decades of surprising findings. *Phytochemistry* **2004**, *65*, 2735-2749.

Martins, A.; Vieira, H.; Gaspar, H.; Santos, S. Marketed marine natural products in the pharmaceutical and cosmeceutical Industries: Tips for success. *Marine Drugs* **2014**, *12*(2), 1066-1101.

Mayer, A.M.S.; Glaser, K.B.; Cuevas, C.; Jacobs, R.S.; Kem, W.; Little, R.D.; McIntosh, J.M.; Newman, D.J.; Potts, B.C.; Shuste, D.E. The odyssey of marine pharmaceuticals; a current pipeline perspective. *Trends Pharmacological Sciences* **2010**, *31*(6), 255-265.

Mehbub, M.F.; Lei, J.; Franco, C.; Zhang, W. Marine sponge derived natural products between 2001 and 2010: Trends and opportunities for the discovery of bioactives. *Marine Drugs* **2014**, *12*, 4539-4577.

Minotti, G.; Menna, P.; Salvatorelli, E.; Cairo, G.; Gianni, L. Anthracyclines: Molecular Advances and Pharmacologic Developments in Antitumor Activity and Cardiotoxicity. *Pharmacological Reviews* **2004**, *56*(2), 185-229.

Mishra, B.B.; Tiwari, V.K. Natural products: An evolving role in future drug discovery. *European Journal of Medicinal Chemistry* **2011**, *46*, 4769-4807.

Montaser, R.; Luesch, H. Marine natural products: a new wave of drugs? *Future Medicinal Chemistry* **2011**, *3*(12), 1475-1489.

Moudi, M.; Go, R.; Yien, C.Y.S.; Nazre, M. Vinca alkaloids. *International Journal of Preventative Medicine* **2013**, *4*, 1231-5.

Muller, W.E.G.; Yamazaki, Z-I.; Breter, H-J.; Zahn, R.K. Action of bleomycin on DNA and RNA. *European Journal of Biochemistry* **1972**, *31*, 518-525.

Newman, D. J.; Cragg, G. M., Natural Products as Sources of New Drugs from 1981 to 2014. *Journal of Natural Products* **2016**, *79*(3), 629-661.

Newman, D.J.; Cragg, G.M. Marine-sourced anticancer and cancer pain control agents in clinical and late preclinical development. *Marine Drugs* **2014**, *12*, 255-278.

Nobili, S.; Lippi, D.; Witort, E.; Donnini, M.; Bausi, L.; Mini, E.; Capaccioli S. Natural compounds for cancer treatment and prevention. *Pharmacological Research* **2009**, *59*, 365-78.

Pettit, G.R. Progress in the discovery of biosynthetic anticancer drugs. *Journal of Natural Products* **1996**, *59*, 812-821.

Radjasa, O.K.; Vaske, Y.M.; Navarro, G.; Vervoort, H.C.; Tenney, K.; Linington, R.G.; Crews, P.; Highlights of marine invertebrate-derived biosynthetic products: their biomedical potential and possible production by microbial associants. *Bioorganic and Medicinal Chemistry* **2011**, *19*, 6658-6674.

Rowinsky, E. K. The Development and Clinical Utility of Taxane Class of Antimicrotubule Chemotherapy Agents. *Annual Review of Medicine* **1997**, *48*, 353-374.

Ruiz-Torres, V.; Encinar, J.A.; Herranz-Lopez, M.; Perez-Sanchez, A.; Galiano, V.; Barrajon-Catalan, E.; Micol, V. An updated review on marine anticancer compounds: The use of virtual screening for the discovery of small-molecule cancer drugs. *Molecules* **2017**, *22*, 1037.

Schwartzmann, G.; Brondani da Rocha, A.; Berlinck, R.G.S.; Jimeno, J. Marine organisms as a source of new anticancer agents. *Lancet Oncology* **2001**, *2*, 221-225.

Schwarzenberg, K-V.; Vollmar, A.M. Targeting apoptosis pathways by natural compounds in cancer: Marine compounds as lead structures and chemical tools for cancer therapy. *Cancer Letters* **2013**, *333(2)*, 295-303.

Simmons, T.L.; Andrianasolo, E.; McPhail, K.; Flatt, P.; Gerwick, W.H. Marine natural products as anticancer drugs. *Molecular Cancer Therapeutics* **2005**, *4(2)*, 333-342.

Srivastava, V.; Negi, A.S.; Kumar, J.K.; Gupta M.M.; Khanuja, S.P.S. Plant-based anticancer molecules: a chemical and biological profile on some important leads. *Bioorganic and Medicinal Chemistry* **2005**, *13*, 5892-5908.

Swami, U.; Chaudhary, I.; Ghalib, M.H.; Goel, S. Eribulin- A review of preclinical and clinical studies. *Critical Reviews in Oncology/ Hematology* **2012**, *81(2)*, 163-184.

Thorn, C.F.; Oshiro, C.; Marsh, S. Doxorubicin pathways: Pharmacodynamics and Adverse Effects, *Pharmacogenetics and Genomics* **2011**, *21 (7)*, 440-446.

Tran, T.D.; Pham, N.B.; Fechner, G.A.; Hooper, J.N.A.; Quinn, R.J. Potent cytotoxic peptides from Australian marine sponge *Pipestela candelabra*. *Marine Drugs* **2014**, *12*, 3399-3415.

Tsukimoto, M.; Nagaoka, M.; Shishido, Y.; Fujimoto, J.; Nishisaka, F.; Matsomoto, S.; Harunari, E.; Iada, C.; Matsuzaki, T. Bacterial production of the tunicate-derived antitumor cyclic depsipeptide didemnim B. *Journal of Natural Products* **2011**, *74(11)*, 2329-2331.

Veal, G.J.; Errington, J.; Sludden, J.; Griffin, M.J.; Price, L.; Parry, A.; Hale, J.; Pearson, A.D.J.; Boddy, A.V.; Determination of anti-cancer drug actinomycin D in human plasma by liquid chromatography–mass spectrometry. *Journal of Chromatography B* **2003**, *795(2)*, 237-243.

Wall, M.E.; Wani, M. C. Camptothecin and Taxol: Discovery to Clinic – Thirteenth Bruce F. Cain Memorial Award Lecture. *Cancer Research* **1995**; *55*, 753-760.

Wang K-r.; Zhang, B-Z.; Zhang, W.; Yan, J-X.; Li, X.; Wang R. Potent antitumour effects of novel actinomycin D analogues Leu5 actinomycin D. *Cancer Letters* **2008**, *268(1)*, 38-45.

Wender, P.A.; Baryza, J.L.; Brenner, S.E.; DeChristopher, B.A.; Loy, B.A.; Schrier, A.J.; Verma V.A. Design, synthesis, and evaluation of potent bryostatin analogs that modulate PKC translocation selectivity. *Proceedings of the National Academy of Science of the United States of America* **2011**, *108*(17), 6721-6726.

Yeung, B. K.S. Natural product drug discovery: the successful optimization of ISP-1 and halichondrin B. *Current Opinion in Chemical Biology* **2011**, *15*, 523-528.

Zhang, G.; Li, J.; Zhu, T.; Gu, Q.; Li, D. Advanced tools in marine natural drug discovery. *Current Opinion in Biotechnology* **2016**, *43*, 13-23.

Zhang, L.; Guo, J-R.; Chen, Q-Q.; Wang, C-Y.; Zhang, W-Y.; Yao, M-C; Zhang, W. Exploring the antitumor mechanism of high-dose cytarabine through the metabolic perturbations of ribonucleotide and deoxyribonucleotide in human promyelocytic leukaemia HI-60 cells. *Molecules* **2017**, *22*, 499.



Development of a pre-fractionated library of marine sponge extracts

3.1 Introduction

Natural products exhibit a wide range of biological activities which may be exploited in the discovery of leads for the development of drugs for the treatment of human diseases [Hu et al., 2015]. For millions of years, living organisms have evolved to survive harsh living conditions and predation by other organisms by producing secondary metabolites as a means of defence. Hence, it's not surprising that many natural products exhibit potent biological activity [David et al., 2015]. Studies carried out on bioactivity and molecular interactions of natural products revealed unique pathways, targets and mechanisms of action [Bauer and Bronstrup, 2014]. Natural products played an important role as the starting point for the discovery and development of anticancer and antimicrobial agents i.e. 60% and 75%, respectively, of drugs used in these disease areas are derived from natural sources [Lam, 2007] and marine natural products in particular have proved to exhibit potent activity as anticancer lead compounds [Bugni et al., 2008]. To date, at least eight marine-derived drugs are registered for clinical use by the FDA and four of those are approved for the treatment of different types of cancers, with many others in different phases of clinical trials [Gomes et al., 2016; Martins et al., 2014].

Of all marine natural products derived drugs in development, invertebrates are the biggest contributors, with sponges in particular being the most dominant, contributing at least 30% of all reported marine natural products to date [Gomes et al., 2016; Calcabrini et al., 2017]. The preclinical antitumour screening done by the NCI revealed that marine sponge extracts exhibited greater cytotoxicity in comparison with plants and other marine invertebrates. However, only a small percentage of the total estimated species is believed to have been investigated [Bugni et al., 2008].

The process of lead discovery from natural sources involves several steps and may be labour intensive, time consuming and also require specialized equipment. Figure 3.1 gives a summary of the steps involved in lead discovery. Natural product extracts often present with several challenges. Firstly, crude extracts of animals, plants and microorganisms are often complex mixtures, potentially containing hundreds of compounds of differing structures, physicochemical properties and bioactivity at different concentrations, and, because of their complexity, these compounds may not be suitable for high throughput screening (HTS) programs. The second problem associated with natural products extracts is the presence of nuisance compounds such as the highly polar compounds like polysaccharides or very non-polar compounds such as the fatty acids which may affect certain assay types negatively and

produce false positive or false negative results [Atanosov et al., 2015]. Thirdly, minor compounds may be present in crude extracts at concentrations below the detection margin and their activity may be masked by major compounds [Bugni et al., 2008]. Fourthly, crude extracts may contain compounds with antagonising or synergistic effects [Bugni et al., 2008] and affect the overall results of biological assays. Lastly, there is also a possibility of rediscovery of known compounds after a significant investment in time and resources.

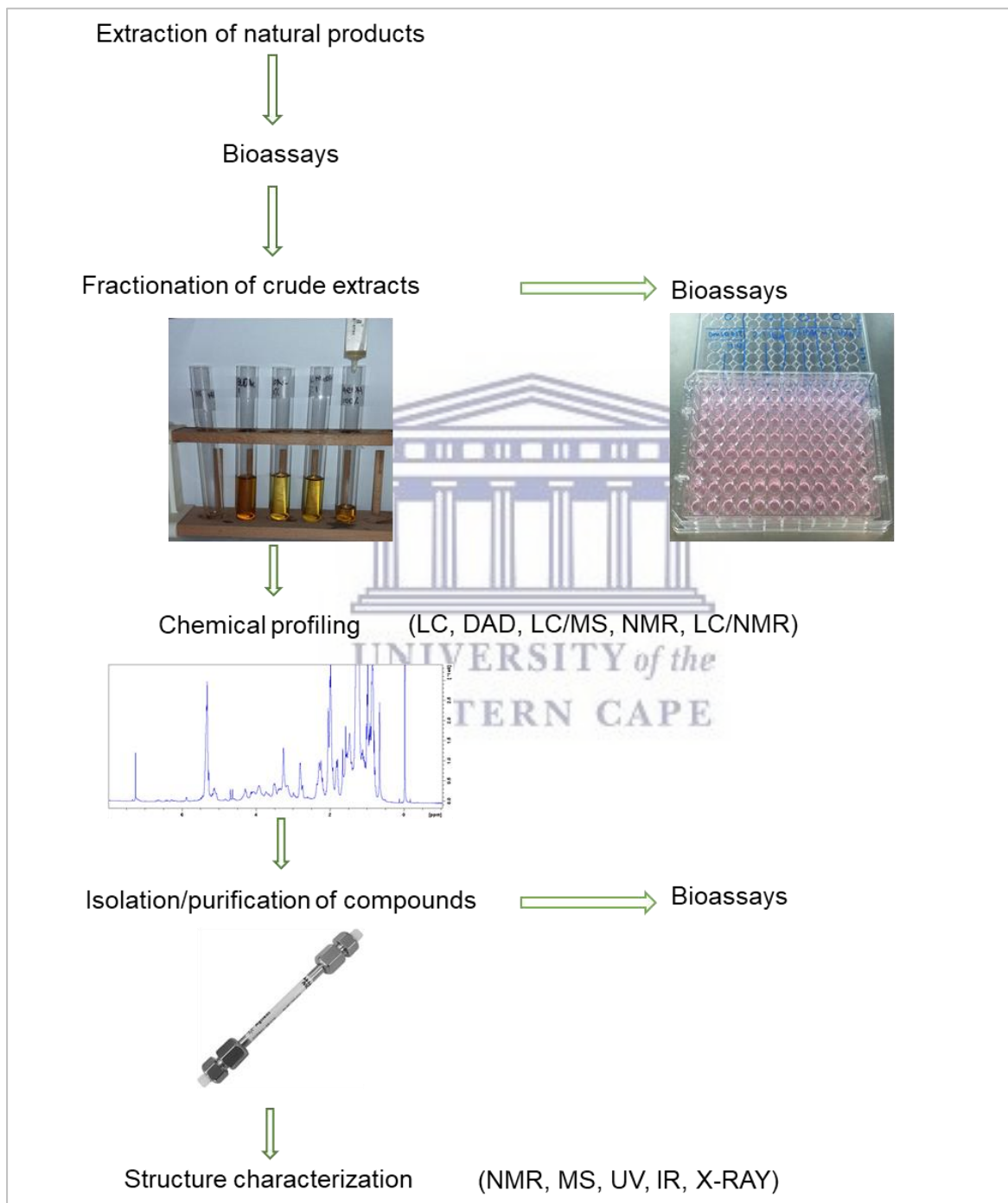


Figure 3.1. Summary of processes involved in lead discovery from natural products.

With the afore-mentioned challenges associated with the discovery of new lead compounds, it is of great importance to establish suitable methods that will enhance screening of natural products and speed up the process of lead discovery. One of the most effective ways to do this is by generating a library of natural products. Natural product libraries provide a pool of chemically diverse substances than can be used in screening programmes for therapeutic agents. These can consist of pure natural products, synthetic or semi-synthetic compounds, semi-purified fractions, fractionated natural product libraries, etc.

Pure natural product libraries comprise purified compounds derived from nature and the advantage of these libraries in drug discovery is that once a 'hit' is identified in the first screening, its evaluation in regard to its potential viability and accessibility via synthetic route can be done immediately. However, the challenge with this type of library is that they are expensive and time consuming to generate [Ulrich et al., 2002]. Semi-synthetic or synthetic natural products libraries on the other hand involves identifying natural product scaffolds with specified target and synthesising analogues of such to establish structure activity relationships. The disadvantage of these libraries is that natural products structures are often complex and their syntheses may require several steps, not to mention the low percentage yields obtained at the end of long and strenuous synthetic procedures.

Prefractionated libraries are generated by separating crude extracts into several fractions, usually by chromatographic methods. These types of libraries have been used by several laboratories to address the challenges faced with the screening of crude extracts and the fast-paced identification of lead compounds for therapeutic purposes. A variety of fractionation methods are available and, depending on the method used, these may produce fractions containing a mixture of compounds and/or semi-pure compounds. The choice of the method used will therefore depend on the type of desired library, that is, semi-pure or simplified extracts, the type of assays intended and the type of crude extracts to be fractionated. The cost and time required to build the libraries are also important features to consider when making a choice of fractionation method to use. The advantages associated with prefractionated natural product libraries is that they provide sufficient information regarding active fractions, and the process of lead compound discovery can be significantly shortened. Also, prefractionation can be used to eliminate compounds that are less "drug-like", too hydrophilic/hydrophobic, and increase the titre of minor components in fractions [Martins et al., 2014]. Prefractionated natural product libraries are relatively cheaper and take less time to generate. An example of the prefractionated samples obtained for the marine sponge extracts stored in the UWC Marine BioDiscovery laboratory is shown in figure 3.2.

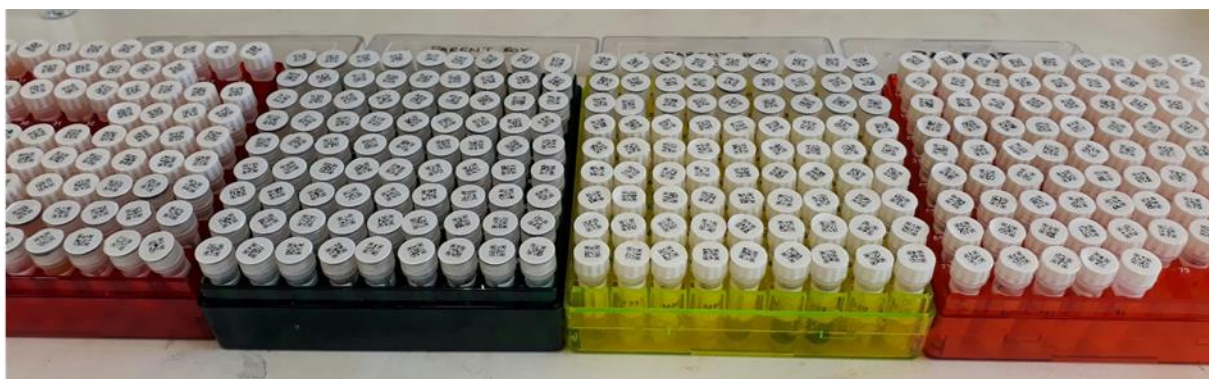


Figure 3.2. A photograph of prefractionated library samples stored at Marine Biodiscovery research lab, University of the Western Cape.

Chromatographic or spectroscopic profiling of each fraction of a library ensures the reproducibility of results and allows for the rapid identification and dereplication of individual compounds in each fraction. Ultra violet (UV) and infrared (IR) spectroscopies provide the least informative data, hence can only be used in combination with other spectroscopic methods [Zani and Carrol, 2017]. Comparatively, mass spectrometry (MS) is a very sensitive and rapid tool to use in dereplication techniques, requiring small quantities of samples for analysis; however, there are several limitations associated with this method. Firstly, the raw data sets obtained from different mass analysers may vary and, secondly, the fragmentation data of many compounds with identical molecular weights may be ambiguous. Lastly, analysing MS data based only on the fragmentation pattern and elemental composition can be tiresome and become a limitation to the efficient use of MS-based dereplication [Bakiri et al., 2017; Hubert et al. 2017]. Use of computerised approaches to organise MS data sets (molecular networking) may be the answer to many of the shortcomings associated with use of MS as a dereplication tool.

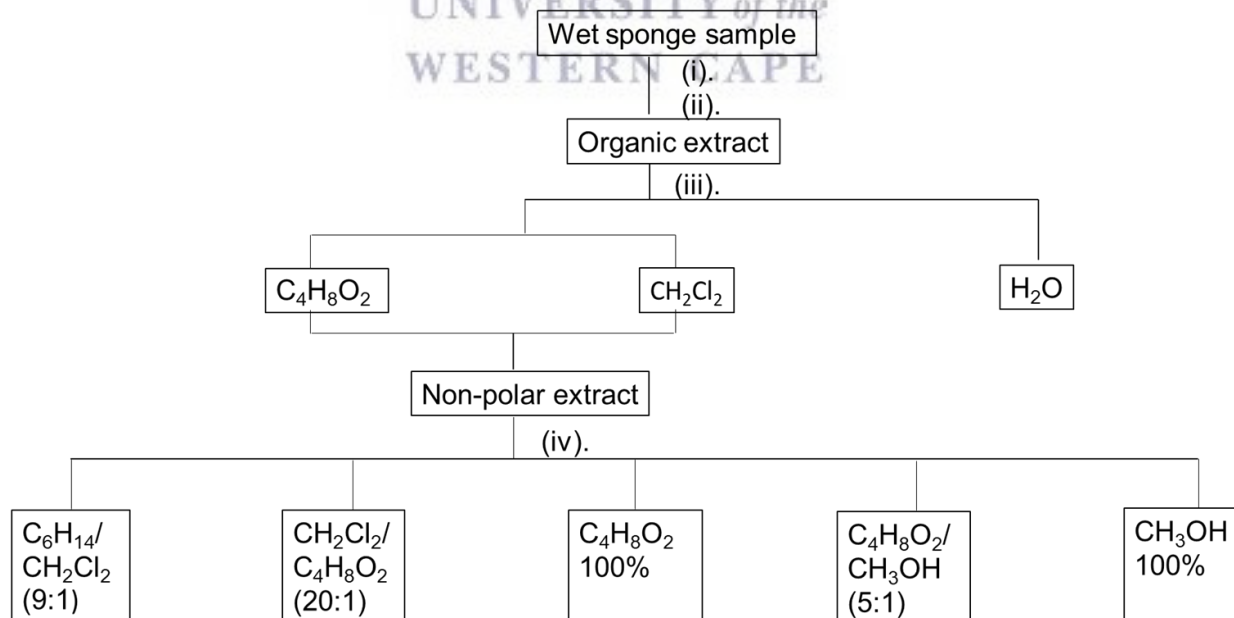
Alternatively, nuclear magnetic resonance (NMR) has been described as the universal chemical detector with its ability to provide sufficient information to derive structural features in molecules with same molecular weight, but different constitutions or configurations [Zani and Carrol, 2017]. NMR thus remains by far the most efficient technique to unambiguously elucidate complex structures of individual molecules [Bakiri et al., 2017; Hubert et al. 2017]. “With the advent of high field magnets, capillary and cryogenic probes, the lower sensitivity of NMR as compared to MS-based analytical methods has been progressively counterbalanced, and even the structure elucidation of minor compounds within mixtures becomes possible” [Hubert et al. 2017].

In this chapter we discuss the prefractionation of marine sponge extracts, coupled with NMR profiling and cytotoxicity screening as a method to identify potential anticancer compounds from marine invertebrates.

3.2 Results and discussion

3.3.1 Extraction and prefractionation

In this chapter, the main goal was to generate a library of fractionated sponge extracts of decreased complexity and increased titre of potentially biological active minor metabolites, suitable for cytotoxicity assays. To achieve this, a two-step method was used to generate a collection of prefractionated sponge extracts: (i) desalting of sponge extracts and (ii) separation of metabolites by a chromatographic method (scheme 3.1). Fourteen marine sponge samples (TS2707, TS2710, TS2712, TS2713, TS2714, TS2715, TS2716, SAF96-003, SAF96-026, SAF96-053, SAF96-069, SAF96-082, SAF96-108 and SAF96-114) previously collected from the South African coastline were thawed and sequentially extracted with MeOH and CH₃OH/CH₂Cl₂. The desalting process was achieved by liquid-liquid partitioning between C₄H₈O₂-H₂O and CH₂Cl₂-H₂O to obtain three fractions (H₂O, C₄H₈O₂ and CH₂Cl₂). The C₄H₈O₂ and CH₂Cl₂ fractions were later combined, dried under reduced pressure and subjected to diol functionalised silica gel column chromatography. The column was developed by adsorbing the extracts to 10% of the diol stationary phase, while the rest was packed in a polypropylene cartridge. The column was eluted with five solvent mixtures of increasing polarity (C₆H₁₄-CH₂Cl₂, CH₂Cl₂-C₄H₈O₂, C₄H₈O₂, C₄H₈O₂-CH₃OH and CH₃OH) to give a total of seventy fractions from fourteen sponges. This protocol has been successfully used to generate a library of natural products before at the NCI by the Gustafson group [Datta et al., 2013], and it has also been employed in other natural products isolation studies at NCI, thus it was adopted for this study.



Scheme 3.1. Desalting and diol fractionation of sponge extracts.

(i) Extraction with CH₃OH, (ii) Extraction with CH₂Cl₂/CH₃OH 1:1, (iii) Desalting; (iv) Fractionation using diol functionalised silica gel (40-75μm).

The first step in generating a small library of fractionated sponge metabolites was removal of the inorganic salts from the crude extract by separating water soluble components of the extract from intermediate and non-polar compounds. For a better evaluation of how much inorganic salts were removed from the crude extracts, all samples were weighed prior to and after the desalting process. In most samples, 70 percent of the extract was retained in the aqueous layer, with samples such as TS2713, TS2710, TS2716, SAF96-082 and SAF96-108 recovering less than 10% of the total extract, figure 3.3, confirming that marine sponges contain large quantities of water soluble inorganic salts as stated by Bugni et al. (2008). Although, most of the biomass was retained in the aqueous phase, this may not necessarily mean that the entire mass in the aqueous layer was inorganic salts, but rather some highly polar components such as amino acids and saccharides could have been trapped in the water fraction as was the case in a study by Cutignano and collaborators (2015). As a result, other techniques to extract such compounds from the water fraction would be necessary.

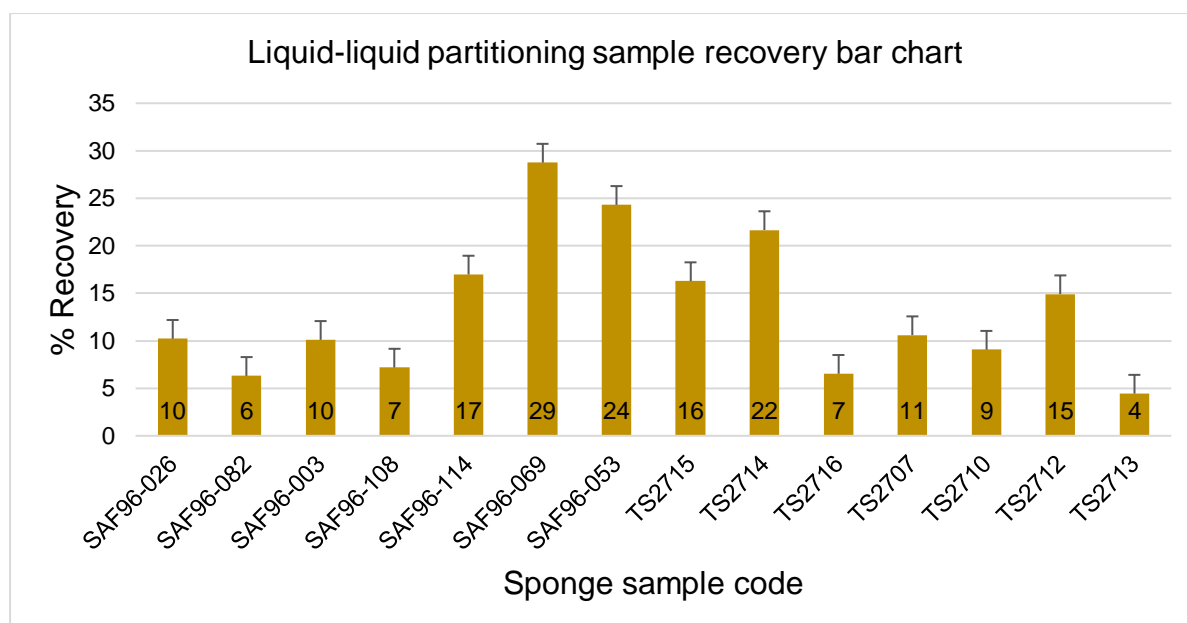


Figure 3.3. Histogram presentation of organic extract recovery expressed as a percentage of the total extract.

The second step was to fractionate the crude sponge extracts to generate a collection of prefractionated samples for biological and chemical profiling. Solid phase extraction with bonded silica (diol functionalised silica gel) was used for separation. An advantage of diol bonded silica was that it allowed use of a wide range of solvent polarities i.e. from the non-polar hexane to the polar solvent methanol. In addition, diol-bonded-phase silica is less chemically reactive and can be used as a substitute for silica gel based normal phase separations where silica gel-like elution properties are desired [Datta et al., 2013]. In this study, an evaluation of the sample recovery was determined by comparing the total sample

recovered from the column to the total extract loaded and calculated as a percentage (figure 3.4). In most samples, there was relatively good recoveries, ranging from 54% to 95% with an average recovery of 81%. More than 70% of the extracts were recovered in most cases except for one sample, TS2715, which only had 54% of the total extract recovered. The difference in behaviour as observed for this sample could mean that the sample contains compounds with a high affinity for the bonded silica gel and it may require a different type of stationary phase to separate its metabolites. Although diol-bonded Si gel showed a relatively good recovery for most samples, it should be noted that the choice of stationary phase for separation of natural products may be highly influenced by the type of metabolites extracted, since none of the chromatographic media currently available can work as a blanket stationary phase for all kinds of metabolites.

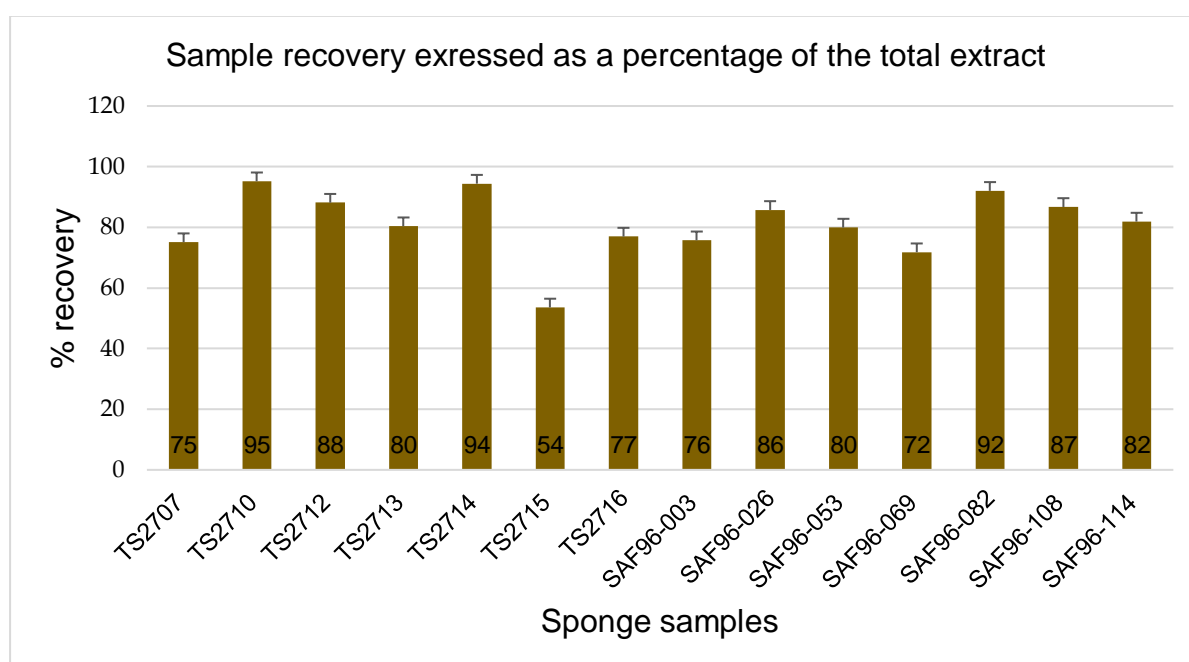


Figure 3.4. A bar chart presentation of mass recovery expressed as percentage of the total crude extract.

Another comparison was made to determine which of the five solvent combinations extracted more biomass from the column. Individual percentage yields for each fraction were calculated for each sample and an average was charted, as percentage of all the five fractions (figure 3.6). A mixture of CH_2Cl_2 and $\text{C}_4\text{H}_8\text{O}_2$ at a ratio of 20:1 dominated, pulling out most of the metabolites from the extract with CH_3OH extracting the least of the metabolites at 9%. This was not unexpected since the desalting process with water might have pulled out most of the polar compounds from the extract. A pie chart below (figure 3.5) shows the percentage distribution of masses obtained from the five solvent combinations used.

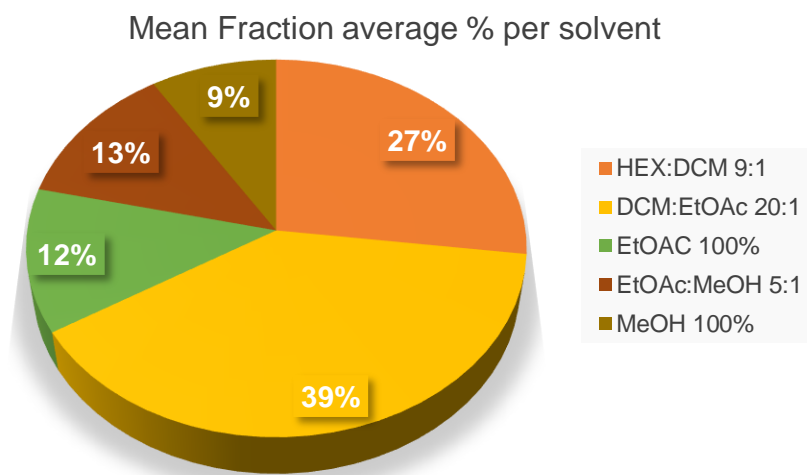


Figure 3.5. Chart showing percentage distribution of masses per solvent mixture.

3.3.2 Chemical profiling

In the current study ^1H NMR spectroscopy was used to provide insight into the “types” of metabolites (chemical profiling) present in the extracts. Chemical shifts in ^1H NMR spectra provide information about the type of protons the molecules are likely to have and this is used to exclude known structures where discovery of novel compounds is the target of the research. “Nuisance compounds” such as fats and sugars can also be readily identified in the crude extracts. Chemical profiling of all seventy fractions obtained from prefractionation of fourteen sponges with diol functionalised silica gel was done by ^1H NMR spectroscopy. ^1H NMR spectra of all fractions were analysed using TopSpin 3.2 and compared with that of the crude extract. ^1H NMR spectra displayed similarities in most of the fractions 1 (C_6H_{14} - CH_2Cl_2 9:1) and fractions 2 (CH_2Cl_2 - $\text{C}_4\text{H}_8\text{O}_2$ 20:1), displaying a cluster of peaks between 0 and 2.5 ppm commonly associated with fatty acids and sterols. This is more likely because these two fractions are highly non-polar compounds and it is known that marine sponges produce a wide variety of metabolites including, among others, steroids and fatty acids which are also non-polar in nature. Another general observation was that the first two fractions, and to some extent fraction 3 ($\text{C}_4\text{H}_8\text{O}_2$ 100%), seemed to contain most of the components of the crude extract; again this may be due to the fact that fraction 4 (EtOAc-MeOH 5:1) and fraction 5 (MeOH 100%) are relatively polar and most of the polar compounds were most likely retained in the aqueous fraction during the desalting process. A considerable variation in the spectra of TS2712 (figure 3.6a) was seen between 3.35 ppm and 5.50 ppm, whereby fraction 1 displayed the two multiplets at 4.14 and 4.39 ppm, while fraction 2 showed a multiplet at 3.57 ppm and a doublet at 4.68 ppm. Fractions 1 and 2 of TS2707 (figure 3.6b) displayed a similar NMR profile with fraction 1, however, the peaks in fraction 1 was suggestive of lower concentrations for the responsible compound(s) based on the intensity of the peaks seen. A similar pattern

was observed with sample TS2713 (figure 3.6c), while TS2714 (figure 3.6d) showed an opposite behaviour, with the less polar fraction (fraction 3) showing more intense peaks than the non-polar fraction 2. With these observations, it is evident that the fractionation of these crude extracts coupled with chemical profiling provide enough information as required for the prioritisation of samples for the discovery of lead compounds.

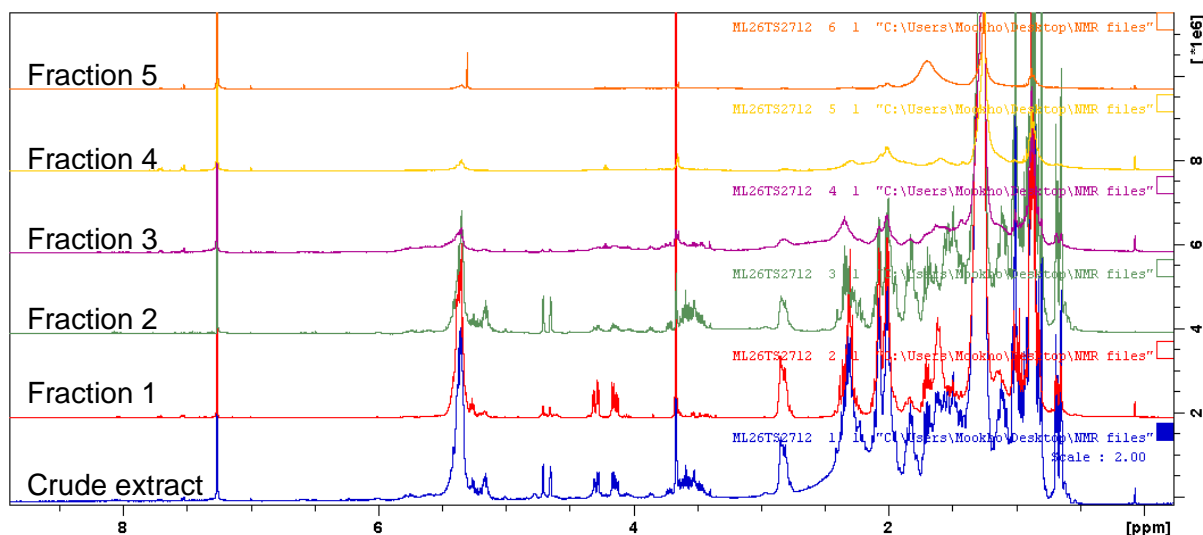


Figure 3.6a. ^1H NMR spectra of TS2712, crude extract, fraction 1, fraction 2, fraction 3, fraction 4 and fraction 5.

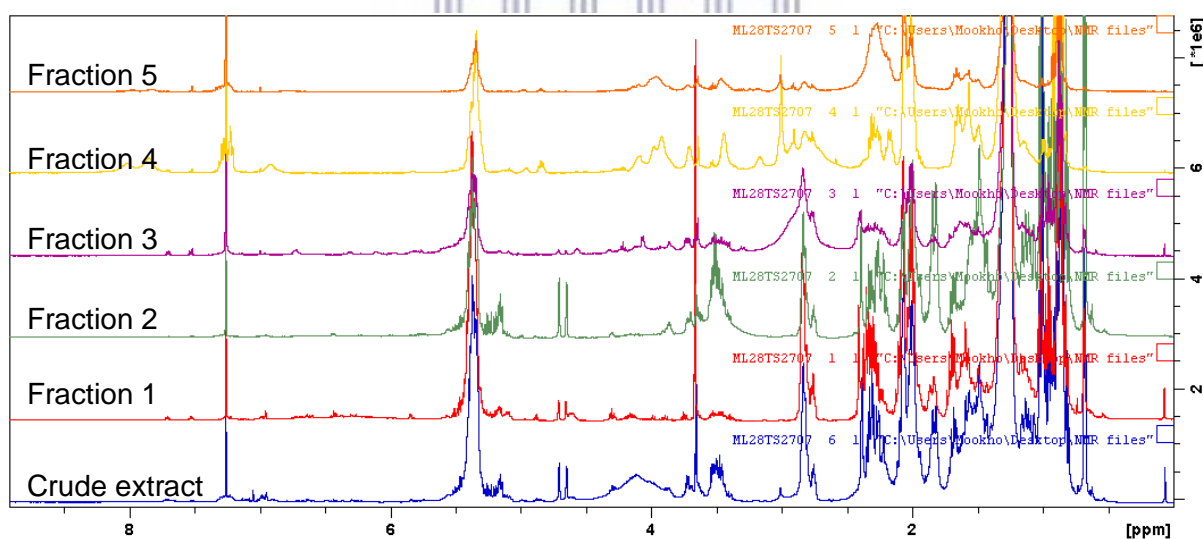


Figure 3.6b. ^1H NMR spectra of TS2707, crude extract, fraction 1, fraction 2, fraction 3, fraction 4 and fraction 5.

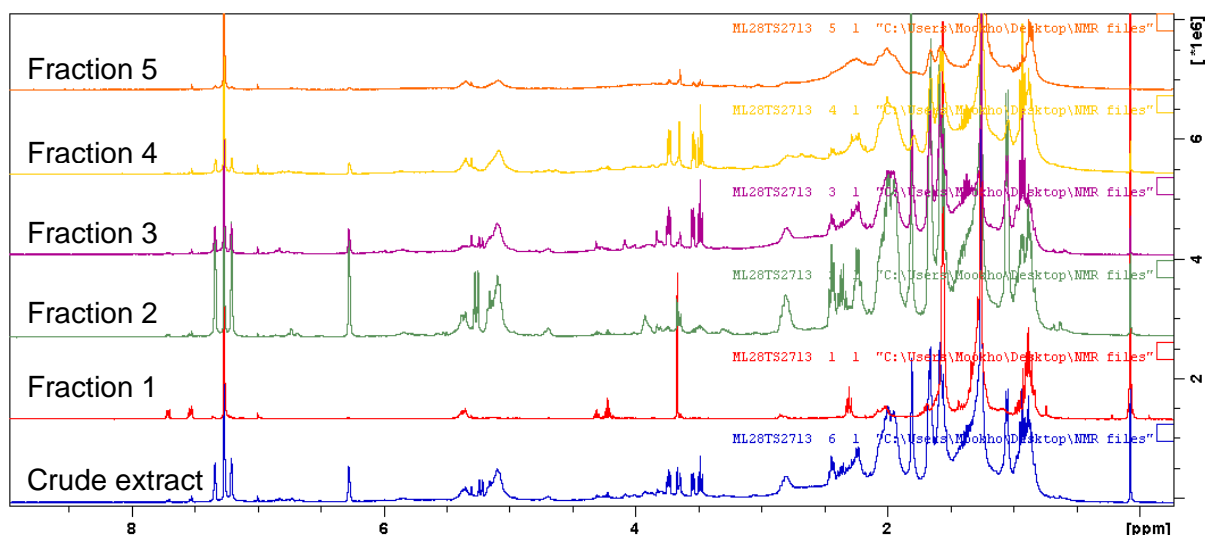


Figure 3.6c. ^1H NMR spectra of TS2713, crude extract, fraction 1, fraction 2, fraction 3, fraction 4 and fraction 5.

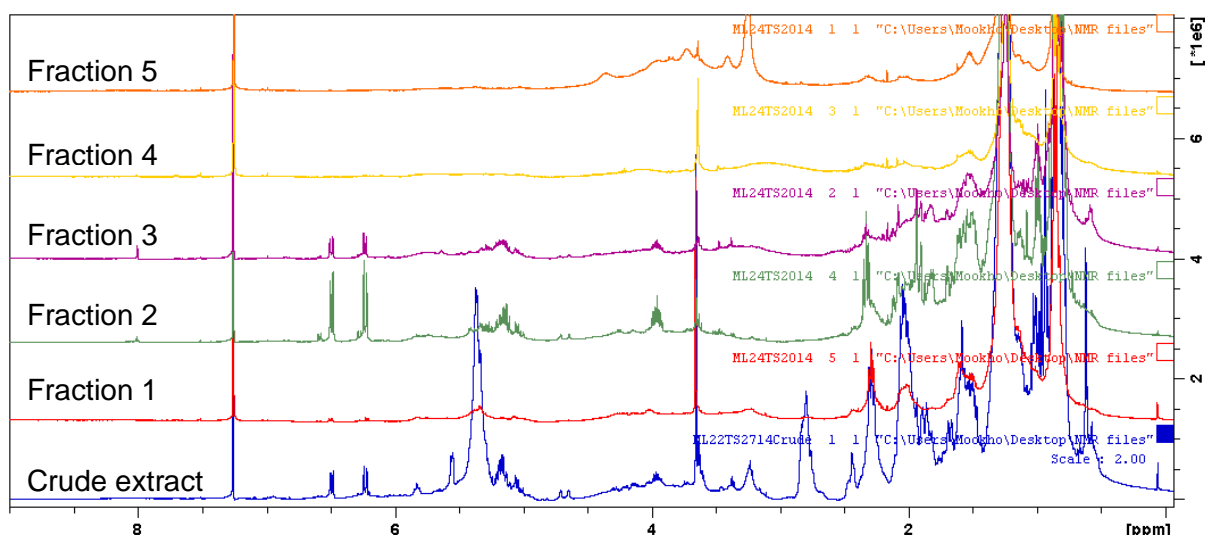


Figure 3.6d. ^1H NMR spectra of TS2714, crude extract, fraction 1, fraction 2, fraction 3, fraction 4 and fraction.

3.3.3 Biological activity

The aim of this study was to discover marine natural products with anticancer activity hence evaluation of the library for cytotoxicity was performed on three cell lines, i.e. human breast cancer cells (MCF-7), human ovarian cancer cells (SKOV-3) and human embryonic kidney 293 cells (HEK-293). MCF-7 has been widely used in several cytotoxicity studies involving the screening of natural products such as diterpenoids, steroids and peptides isolated from marine organisms and therefore it was a good model for screening the library samples. To increase the panel of screening, another cancer cell line SKOV-3 was selected. Both breast cancer and ovarian cancer are commonly diagnosed among women in South Africa [Smith and Guidozi, 2009; South African Health Review, 2017]. HEK-293 cells are non-cancerous and are used in this study to evaluate the selectivity of the library samples to cancer cells.

The three human cell lines (HEK-293, MCF-7 and SKOV-3) were treated with 50 µg/ml of each of the 70 fractions over 24 hours after which cell viability was determined by a WST-1 (water soluble tetrazolium dye) antiproliferation assay. The bar charts below (figure 3.7a, 3.7b and 3.7c) show the response of cells after 24 hours of treatment with prefractionated samples.

In both MCF-7 and SKOV-3 cells, TS2715 was the most active followed by TS2714 while SAF96-053, TS2707 and SAF96-026 were generally found to be the least active. Fractions 2, 3, 4 and 5 of TS2715 were the most active, inhibiting cell proliferation of SKOV-3 by 89%, 99%, 79% and 98%, respectively. A similar response with these fractions was observed with the MCF-7 cells, with cell inhibitions ranging from 62% to 92%. TS2714 also showed great potency and the most active fractions were fractions 2, 3 and 4 with inhibition of cell growth at 86%, 100%, and 48% for SKOV-3 cells and 73%, 72% and 66% for MCF-7 cells, respectively. Fraction 3 of TS2714 was found to be the most active among all fractions, inhibiting proliferation of SKOV-3 cells by 100%. Another interesting observation was that of SAF96-114 which displayed increasing activity against MCF-7 cells as the polarity of the fractions increased but had very low activity for the non-polar fractions 4 and 5 with 4% and 0% respectively. With a few exceptions, fraction 2 showed greatest potency followed by fractions 3 and 4 and the least activity was seen with fractions 1 and 5.

To assess the selectivity of the samples for cancer cells, a non-cancerous cell line (HEK-293) was treated in a same manner as MCF-7 and SKOV-3. As seen with MCF-7 and SKOV-3 cells, HEK-293 cells were highly susceptible to TS2715 and fractions 2, 3 and 5 displayed 100% inhibition of cell growth, proving to be non-selective. While the activity of TS2714 was almost comparable to that of TS2715 against MCF-7 and SKOV-3 cells, it showed a moderate inhibition for HEK-293, with an average cell inhibition of 35%, whereas sponges such as TS2710, TS2712 and SAF96-108 showed greater activity against non-cancerous cells (HEK-293) than the cancerous cells MCF-7 and SKOV-3. Although most sponges showed moderate activity against HEK-293 cells, it would still be interesting to assess the activity of purified samples from the library, especially those fractions that exhibited potent activity when tested against cancer cells for potential optimisation into less toxic compounds.

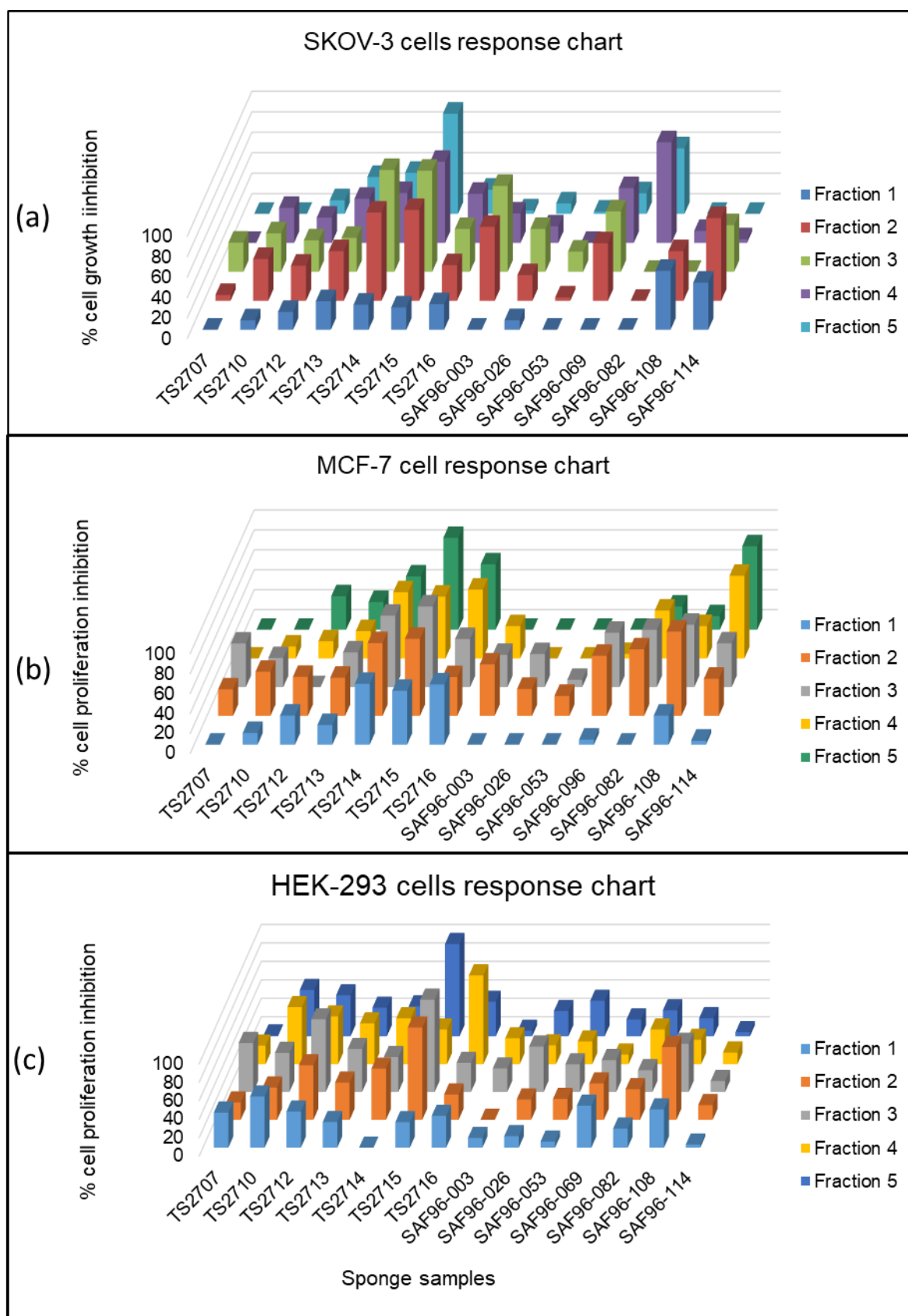


Figure 3.7. Cell viability of (a) SKOV-3, (b) MCF-7 and (c) HEK-293 after treatment with 50 $\mu\text{g/mL}$ of library fractions.

3.3 Conclusion

In conclusion, a library of prefractionated marine sponge samples was successfully generated. Solvent partitioning of the extracts between water, ethyl acetate and dichloromethane prior to solid phase extraction effectively removed most of highly polar compounds and inorganic salts commonly found in marine sponge extracts. Fractionation with diol functionalised silica gel was effective in separating metabolites, generating a library of 70 fractions. Chemical profiling, coupled with biological screening provides sufficient information that can be used to prioritize samples for further studies, whether it's discovery of new compounds whereby unique chemical profile can easily be identified, or bioactive compounds with proven activity for evaluation of desired targets. The cytotoxicity data obtained for the library samples is summarised as supporting data in table S3.1

From the data presented in this chapter it was now possible to select sponges with interesting chemical profiles and good cytotoxicity for further study. These follow up studies are presented in chapters 4 and 5.



3.4 Experimental

3.4.1 General experimental procedures

All extractions were performed using redistilled solvents. NMR data were recorded on a Bruker Avance spectrometer at 400 MHz in deuterated chloroform. Chemical shifts are referenced to undeuterated solvent signals at δ_H 7.26 and reported in ppm. Cell growth medium Dulbecco's modified Eagle's medium (DMEM) and Roswell Park Memorial Institute (RPMI) 1640 were purchased from Gibco and supplemented with 10% foetal bovine serum (FBS) and 1% penicillin-streptomycin 10000iu. All cells used in this study were provided by Professor Mervin Meyer (Department of Biotechnology, University of the Western Cape). Cell culture flasks and plates were purchased from ThermoFisher Scientific. Cell counting was done using Countess automated cell counter (Invitrogen) and absorbance was measured using POLARstar Omega microplate reader (BMG Labtech).

3.4.2 Invertebrate material

All sponge samples were collected by Dr Toufiek Samaai (Department of Environmental Affairs) from the coast of South Africa, given codes and stored at -20°C until further processed. Samples of the codes: TS2707, TS2710, TS2712, TS2713, TS2714, TS2715, TS2715, TS2716, SAF96-003, SAF96-026, SAF96-053, SAF96-069, SAF96-082, SAF96-108 and SAF96-114 were extracted and prefractionated to generate a library of marine sponge metabolites. Voucher specimens are stored at Marine Biodiscovery Research Laboratory at the University of the Western Cape.

3.4.3 Extraction and fractionation of marine sponges

Fresh or freeze dried sponge samples were cut into small pieces and extracted with MeOH, followed by DCM: MeOH (1:1) overnight each, at room temperature. The extracts were combined and dried under reduced pressure. Crude extracts were then partitioned between water and EtOAc and DCM, and organic fractions were combined, dried under reduced pressure and weighed.

Fractionation of all the organic extracts was performed using diol functionalized spherical silica gel 40-75 μ m (Sigma Aldrich, USA) as part of the larger study in which different stationary phases were assessed for development of fractionated marine natural product libraries and the protocol used in this part of the study was used to generate the library of natural products at NCI by Dr. Gustafson's group [Datta et al., 2013]. Briefly, crude extracts (75-150 mg) were weighed and dissolved in 1.8 ml of MeOH/DCM (1:1). 100 mg of Diol functionalised spherical silica gel was added to the solution and the mixture was dried under reduced pressure. The dry extract/silica complex was transferred to a 5 g capacity column packed with 900 mg of diol silica gel and eluted with 6 ml of Hexane/DCM 9:1, DCM/EtOAc 20:1, EtOAc 100%, EtOAc

/MeOH 5:1 and MeOH 100 to obtain 5 fractions. The solvents were removed from the samples using rotatory evaporator. The aqueous layer from liquid-liquid partitioning was not fractionated because it contained mainly inorganic salts.

3.4.4 Cytotoxicity

All cytotoxicity work were done under the supervision of Professor Mervin Meyer and Dr Nicole Sibuyi in the Department of Biotechnology, University of the Western Cape.

Cell seeding

Cells were collected from -150°C, thawed and harvested by centrifugation in a 15 ml centrifuge tube containing 2 ml of complete growth medium. The resulting supernatant was discarded while the pellet was resuspended in 5 ml of suitable complete growth medium, transferred to a T25 cell culture flask and incubated at 37 °C in a humidified 5% CO₂ incubator. Cells were monitored daily for growth and possible contamination and growth medium was changed every alternate day until 90% confluency was attained.

Cell counting

Cell count was done using the Countess™ automated cell counter (Invitrogen). The Countess™ automated cell counter is a benchtop automated cell counter that performs cell count and viability measurements using trypan blue stain. 10 µl of cells in growth medium was homogenised with 10 µl of trypan blue. The homogenous mixture was loaded onto the Countess™ cell counting chamber slide and inserted into the machine for cell counting and cell viability percentage calculations. Live cells were visualized on the countess™ screen as round bodies with clear centres while dead cells appear as blue bodies.

Cell trypsinizing

Trypsinisation was done when cells had reached 70-90% confluency. The growth medium was removed and cells were washed with 2 ml of DPBS and then incubated in 2 ml of trypsin for 3-5 minutes to allow cells to detach. Trypsin is a serine protease enzyme that cleaves the peptide bonds, breaking the bonds between the cells and the protein coating at base of the culture flask. Once cells have detached, fresh growth medium was added to the flask to deactivate trypsin and the contents of the flask were transferred into the centrifuge tube by aspiration and cells were recovered by centrifuging at 3000 rpm for 3 minutes. Cells were then resuspended in either growth medium or growth medium containing 10% DMSO depending on whether they were to be used for continuing experiments or stored at -150 °C respectively. For storage purposes, 1 ml aliquots of cells in 10% DMSO were transferred to labelled cryo vials and stored at -150°C.

WST-1 assay

Cytotoxicity assay was done using tetrazolium salt WST-1 which is converted to formazan in the presence of live cells. MCF-7, SKOV3 and HEK-293 cell lines were seeded in 96 well plated at a density of 100 µl of 1×10^5 cells per well and incubated for 24 hours at 37° C in a 5% CO₂ humidified incubator. After 24 hours of incubation, the growth medium was replaced with a fresh medium containing 50 µg/ml of each fraction for treated cells and fresh medium for negative control cells all in triplicates and incubated for another 24 hours. At the end of 24 hours incubation, 50 µl of WST-1 dye was added to the cells and incubated for another three hours after which absorbance was measured at a wavelength of 440 nm using a microplate reader. Cell percentage viability was calculated using the formula below.

$$\% \text{ Cell proliferation inhibition} = 100 - \frac{\text{Absorbance of treated cells}}{\text{Absorbance of negative control}} \times 100\%$$



3.5 References

Atanosov, A.G.; Waltenberger, B.; Pferschy-Wenzig, E-M.; Linder, T.; Wawrosch, C.; Uhrin, P.; Temml, V.; Wang, L.; Schwaiger, S.; Heiss, E.H.; Rollinger J.M.; Schuster, D.; Breuss, J.M.; Bochkov, V.; Mihovilovic, M.D.; Kopp, B.; Bauer, R.; Dirsch, V.M.; Stuppner, H. Discovery and resupply of pharmacologically active plant-derived natural products: A review. *Biotechnnnology Advances* **2015**, 33(8), 1582-1614.

Bakiri, A.; Hubert, J.; Reynaud, R.; Lanthony, S.; Dominique Harakat, D.; Renault, J-H.; Nuzillard, J-M. Computer-Aided ¹³C NMR chemical profiling of crude natural extracts without fractionation. *Journal of Natural Products* **2017**, 80, 1387-1396.

Bauer, A.; Bronstrup, M. Industrial natural product chemistry for drug discovery and development. *Natural Product Reports* **2014**, 31, 35-60.

Bugni T.S.; Harper M.K.; McCulloch M.W.; Reppart, J.; Ireland C.M. Fractionated Marine Invertebrate Extract Libraries for Drug Discovery. *Molecules* **2008**, 13(6):1372-1383

Bugni, T.S.; Richards, B.; Bhoite, L.; Cimbor, D.; Harper, M.K.; Ireland C.M. Marine natural products for high throughput screening and rapid drug discovery. *Journal of Natural Products* **2008**, 71, 1095-1098.

Calcabrini, C.; Catanzaro, E.; Bishayee, A.; Turrini, E.; Fimognari, C. Marine sponge natural products with anticancer potential: An updated review. *Marine Drugs* **2017**, 15, 310. Cutignano, A.; Nuzzo, G.; Ianora, A.; Luongo, E.; Romano, G.; Gallo, C.; Sansone, C.; Aprea, S.; Mancini, F.; D'Oro, U.; Fontana, A. Development and Application of a Novel SPE-Method for Bioassay-Guided Fractionation of Marine Extracts. *Marine Drugs* **2015**, 13, 5736-5749.

Datta, S.; Zhou, Y-D.; Nagle, D.G. Comparative study of chromatographic medium-associated mass and potential antitumor activity loss with bioactive extracts. *Journal of Natural Products* **2013**, 76, 642-647.

David, B.; Wolfender, J-L.; Dias, D.A. The pharmaceutical industry and natural products: historical status and new trends. *Phytochemistry Reviews* **2015**, 14, 299-315.

Gomes, N.G.M.; Dasari, R.; Chandra, S.; Kiss, R.; Kornienko, A. Marine invertebrate metabolites with anticancer activities: Solutions to the "Supply Problem". *Marine Drugs* **2016**, 14, 98.

Hu, Y.; Chen, J.; Hu, G.; Yu, J.; Zhu, X.; Lin, Y.; Chen, S.; Yuan, J. Statistical Research on the Bioactivity of New Marine Natural Products Discovered during the 28 Years from 1985 to 2012. *Marine Drugs* **2015**, 13(1), 202-221.

Hubert, H.; Nuzillard, J-M.; Renault, J-H. Dereplication strategies in natural product research: How many tools and methodologies behind the same concept? *Phytochemistry Reveiws* **2017**, 16(1), 55-95.

Lam, K.S. New aspects of natural products in drug discovery. *Trends in microbiology* **2007**, 15(6), 279-289.

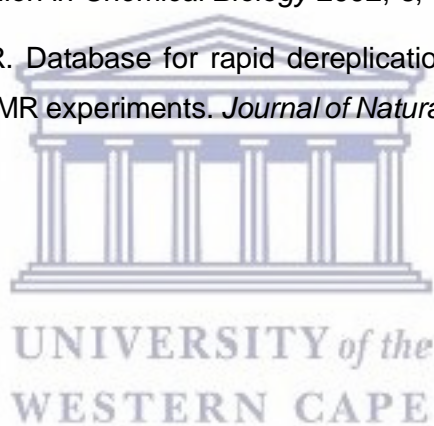
Martins, A.; Vieira, H.; Gaspar, H.; Santos, S. Marketed marine natural products in the pharmaceutical and cosmeceutical Industries: Tips for success. *Marine Drugs* **2014**, 12(2), 1066-1101.

Smith, T.; Guidozzi, F. Epithelial ovarian cancer in Southern Africa. *South African Journal of Gynaecological Oncology* **2009**, 1, 23-27.

South Africa Health Review 2017, 20th Ed.

Ulrich, A.; Koch, C.; Speitling, M.; Hansske, F. Modern methods to produce natural-product libraries. *Current Opinion in Chemical Biology* **2002**, 6, 453-458.

Zani, R.L.; Carrol, A.R. Database for rapid dereplication of known natural products using data from MS and fast NMR experiments. *Journal of Natural Products* **2017**, 80(6), 1758-1766.



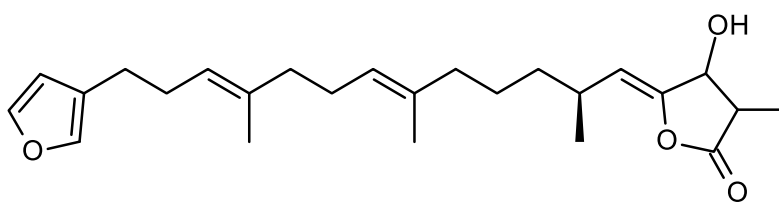
Cytotoxic metabolites from two South African marine sponges of the genera *Ircinia* and *Latrunculia*

4.1 Introduction

Following the preparation of the fractionated library, screening for biological activity and ^1H NMR-based chemical profiling two sponges were selected i.e., TS2713 (*Ircinia* sp.) and TS3392 (*Latrunculia* sp.). both of which showed good cytotoxic activity and interesting chemical profiles. In the following section, a brief of the natural products previously reported from these two genera, followed by a discussion of the isolation and structural characterization of the natural products from the two South African sponges will be given.

4.1.1 Natural products from the genus Ircinia

Ircinia sponges belong to the family Irciniidae Gray, 1867, and is one of the five families of the order Dictyoceratida (class; Desmospongiae, phylum; Porifera) [Boury-Esnault et al., 2011]. Sponges belonging to this family are mostly distributed in tropical to temperate regions, occupying the epipelagic layer at the depths of zero to 60 m [Hardoim et al., 2014]. The family of Irciniidae has three genera, namely: *Ircinia*, *Psammocinia* and *Sarcotragus*. Sponges belonging to this family have a rich chemical profile, wide geographical distribution, an unusual life strategy, high microbial abundance and metabolic activity, hence they can be widely used in scientific research [Hardoim et al., 2014], particularly in drug discovery and development fields. *Ircinia* and its family members, *Psammocinia* and *Sarcotragus* frequently produce a wide range of furanosesterterpenes characterised by furan and tetronic acid moieties at the terminal ends and they are a good model for chemotaxonomy [Holler et al., 1997; Choi et al. 2004]. The most common furanosesterterpenes, variabilin (**4.1**), was first isolated from the sponge *Ircinia variabilis* and reported by Faulkner in 1973 as an antimicrobial agent [Holler et al., 1997; Barrow et al., 1988]. In addition to the furanosesterterpenes, which are considered the major constituent, other compounds such as steroid, sphingolipid, hydroquinone and cyclic hexapeptide derivatives have been reported from *Ircinia* spp. [Mehbub et al., 2016]. Studies have shown that these compounds possess a wide range of activity including: antiviral, antibacterial, anti-inflammatory, antitumor, and protein phosphatase inhibitory activities [Choi et al., 2004; Mehbub et al., 2016].



Compound **4.1**

Figure 4.1. Structure of variabelin (**4.1**).

4.1.2 Natural products from the genus *Latrunculia*

Sponges belonging to the family Latrunculiidae are largely distributed along the temperate and sub-tropical coasts of South Africa, New Zealand, southwestern Australia, Tasmania and the cold waters of Antarctica [Antunes et al., 2004; Keyzers et al., 2004]. They are commonly found in abundance on sheltered rocky reefs down to a depth of 50 m [Keyzers et al., 2004]. These sponges are known for their production of alkaloid secondary metabolites containing a basic pyrroloiminoquinone structure [Antunes et al., 2004]. More than 60 metabolites featuring a pyrroloiminoquinone moiety have been reported from geographically disperse (tropical, temperate, and Antarctic) sponges of the genera *Latrunculia*, *Batzella*, *Prianos*, *Zyzzya*, and *Histodermella* [Ford et al., 2000] and include discorhabdins, epinadrins, batzellines, isobatzellines, makaluvamines, veiutamines and wakayins. Wakayins have been reported not only from the sponges but from the ascidian *Clavelina* sp. as well [Utkina et al., 2004]. Several studies done on these compounds revealed that these alkaloids possess a variety of biological activities such as cytotoxicity against cancer cell lines, antiviral, antimalarial, immunomodulatory, caspase inhibitory, inhibition of topoisomerase I and II, antifungal and antibacterial activities [Hu et al., 2011].

Studies carried out on the Latrunculid sponges of South Africa have reported several potent antibacterial and cytotoxic pyrroloiminoquinones produced by these compounds [Antunes et al., 2004; Davis-Coleman et al., 2004; Hooper et al., 1996]. Some of the pyrroloiminoquinone alkaloids reported from South African Latrunculid sponges include makaluvic acid (**4.2**) discorhabdins (**4.3**) and tsitsikammamines (**4.4**) [Davis-Coleman et al., 2004]. Hence this information together with the data obtained from preliminary screening (discussed in chapter 3) were used to prioritise this sponge TS3392 for this study.

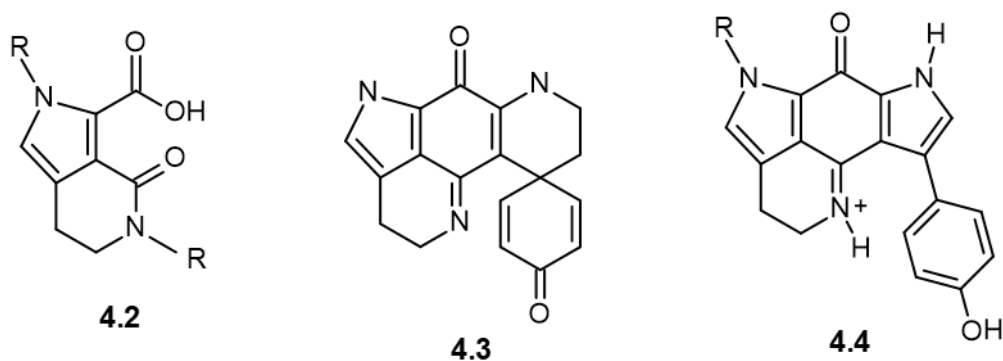


Figure 4.2. Structures of makaluvic acid (4.2), discorhabdin (4.2) and tsitsikammamines (4.4).

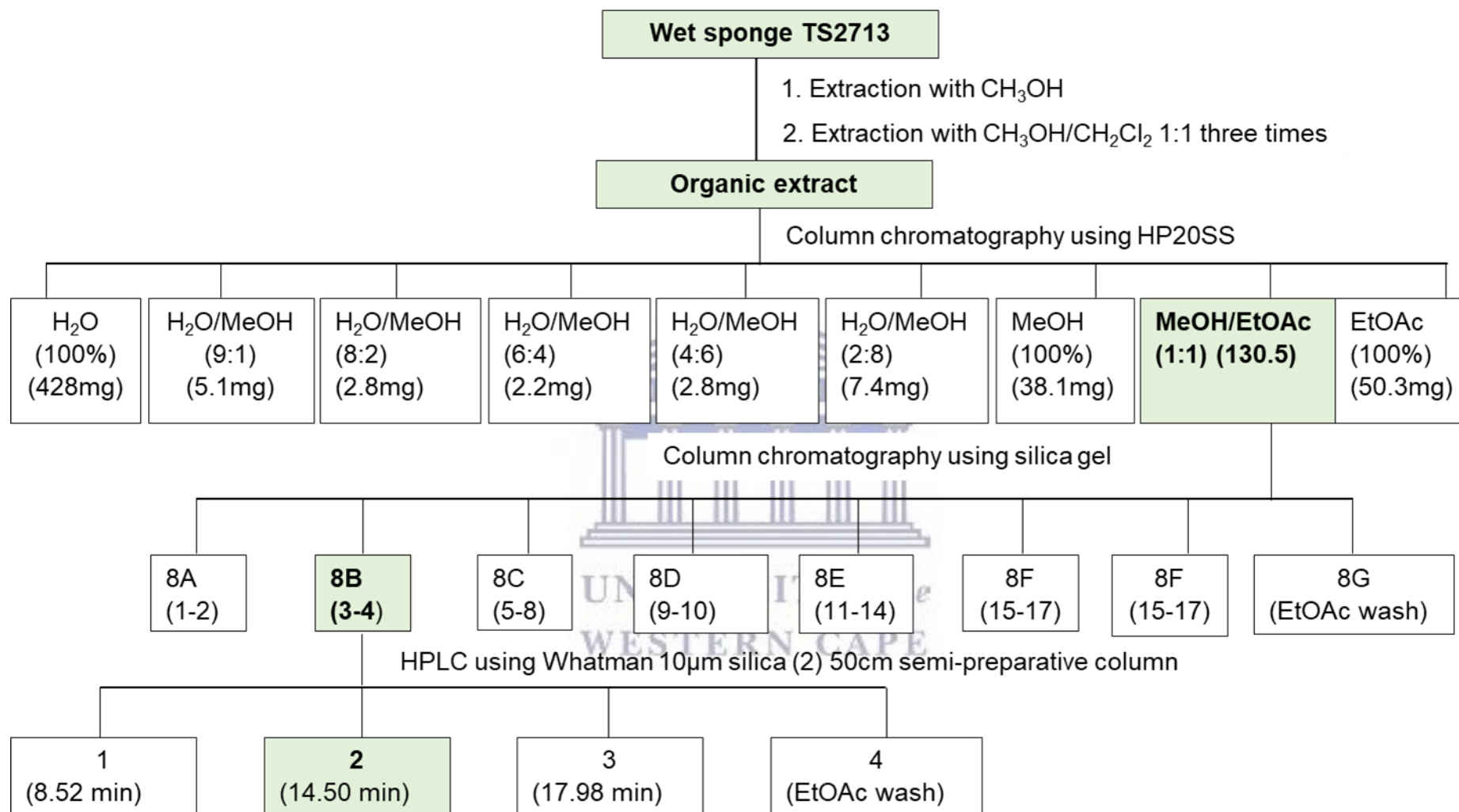
5.2 Results and discussion



Figure 4.3. A photograph of TS2713 (*Ircinia* sp.) prior to extraction.

4.2.1 Extraction and isolation of sesterterpenes from *Ircinia* sp.

A frozen sample of *Ircinia* sp. (179 g) was thawed at room temperature for approximately 1-2 hours prior to exhaustive extraction with CH_3OH followed by $\text{CH}_3\text{OH} - \text{CH}_2\text{Cl}_2$ (1:1). Organic extracts were combined and dried under reduced pressure to give 10.61 g crude extract. A portion of the extract was chromatographed on an HP20SS column using variable mixtures of water, methanol and ethyl acetate. The $\text{CH}_3\text{OH} - \text{C}_4\text{H}_8\text{O}_2$ (1:1) fraction was further subjected to silica gel column chromatography and eluted with hexane- $\text{C}_4\text{H}_8\text{O}_2$ (7:3) to give 17 fractions which were later grouped, based on TLC analyses, to four fractions (8A-8E). Fraction 8B was further purified using semi-preparative HPLC to afford compound **4.5**. The extraction scheme below (scheme 4.1) summarises the isolation of compound **4.5**, with the structure of compound **4.5** elucidated after detailed analysis of 1D and 2D NMR spectroscopy and comparison with literature data.



Scheme 4.1. Isolation of sesterterpenes from *Ircinia* sp.

4.2.2 Structure elucidation of sesterterpenes from *Ircinia* sp.

High resolution electrospray ionization mass spectrometry (HR-ESIMS) of **4.5** revealed a molecular ion peak at m/z 399.2532, corresponding to a molecular formula of $C_{25}H_{34}O_4$. The 1H NMR spectrum displayed three signals for three aromatic protons at δ 7.33 (m), 7.20 (brs) and 6.27 (m). A further three olefinic proton signals were observed at δ 5.36 (d, $J=10.1$), 5.15 (t, $J=7.0$) and 5.09 (m), as well as four methyl signals at δ 1.55 (m), 1.56 (m), 1.05 (d, $J=6.7$) and 1.81 (s) and overlapping methylene proton signals at δ 1.35, 1.94 and 2.04 (figure 4.4).

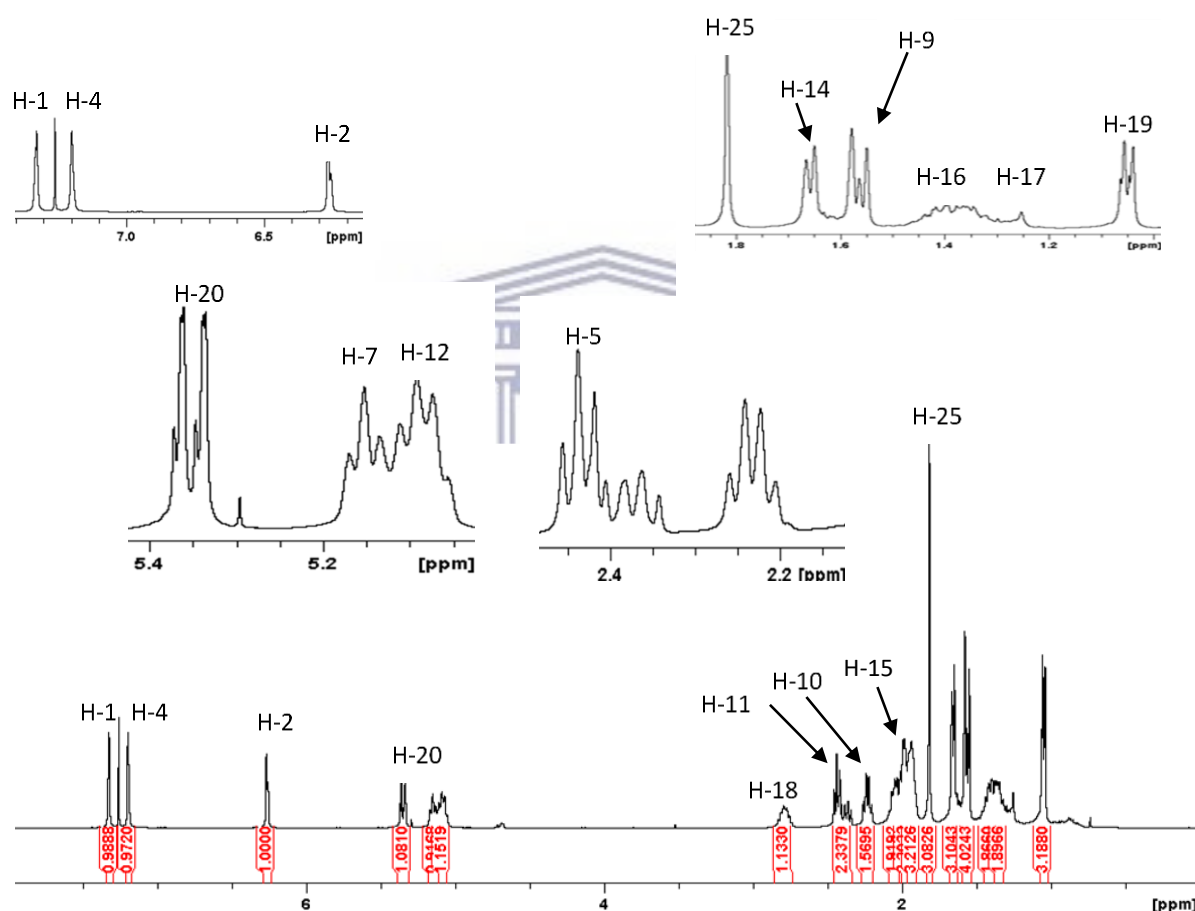


Figure 4.4. 1H NMR spectrum of compound **4.5** (400 MHz, $CDCl_3$).

The ^{13}C NMR spectrum displayed resonances for 13 sp^2 hybridised carbons observed between δ 99.5 and 172.4 and 12 sp^3 hybridised carbons between δ 6.0 and 39.9 (figure 4.5).

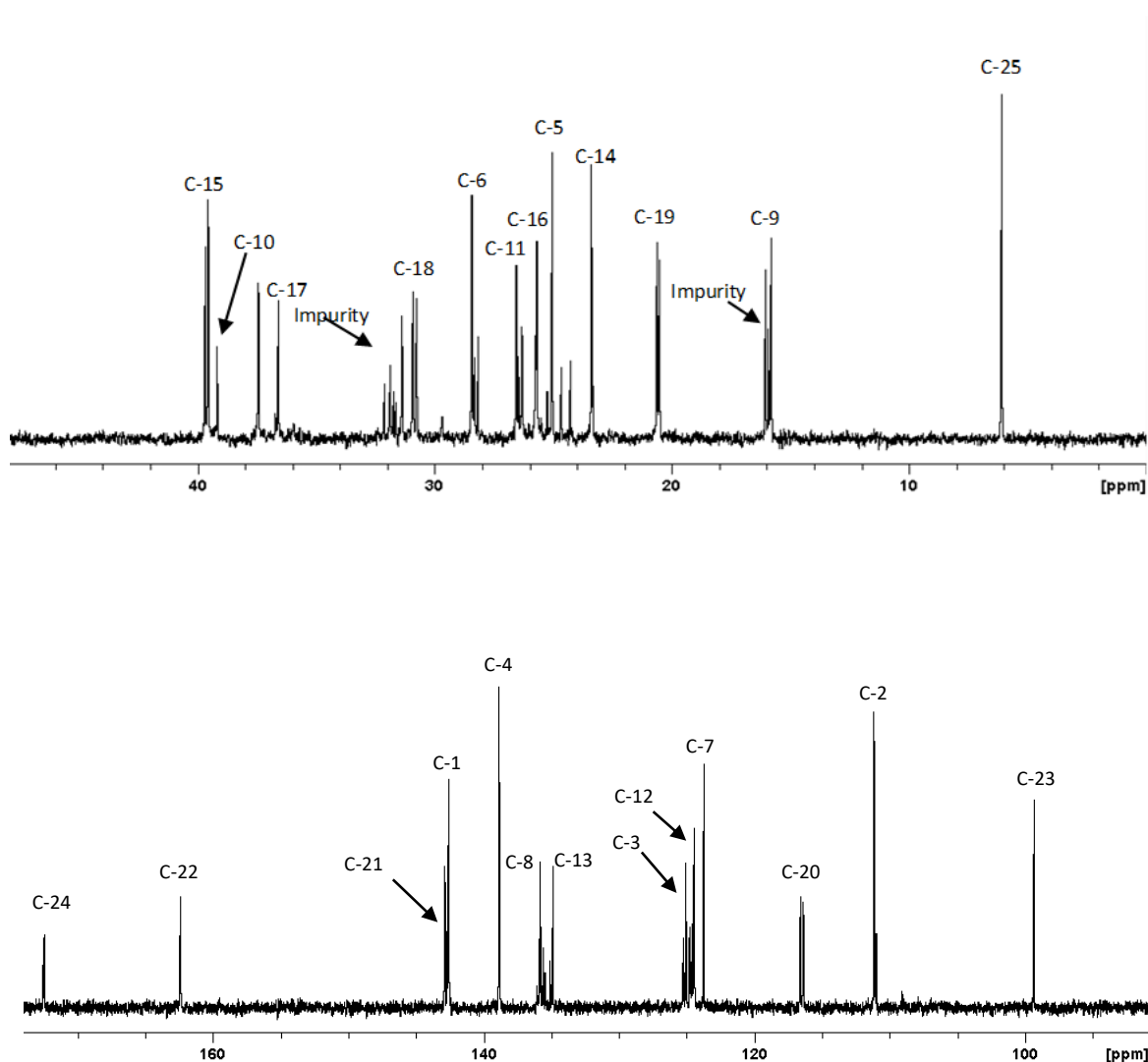


Figure 4.5. The ^{13}C NMR spectrum of compound **4.5** (100 MHz, CDCl_3). 0-48 ppm (top) and 90-180 ppm (bottom).

The aromatic protons were revealed by HSQC to be attached to carbons at δ 143.6, 111.2 and 125.1, while the olefinic protons at positions 7, 12, and 20 were found to reside on the carbons at δ 124.1, 124.7 and 115.6, respectively (figure 4.6). Methyl protons at positions 9, 14, 19 and 25 were assigned to methyl carbons at δ 15.9, 15.7, 20.4 and 6.03, respectively.

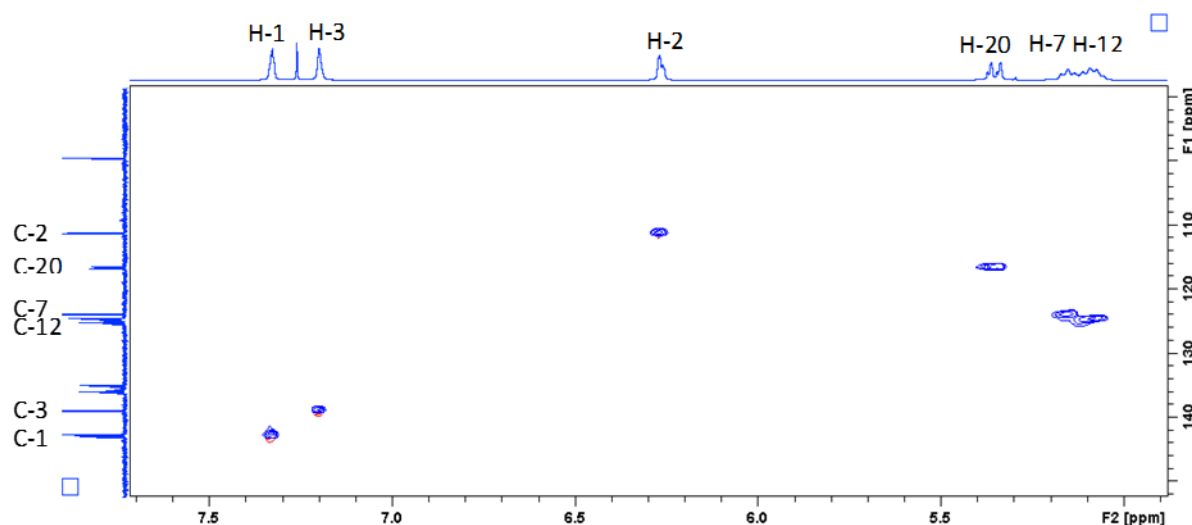


Figure 4.6. A section of the HSQC for compound **4.5**.

The geometry of the double bonds in compound **4.5** was determined by comparison with data published by Burrow et al (1988). Literature indicates that ^1H NMR characteristics of methyl groups attached to the double bonds on sesterterpene tetronic acids resonate at $\delta_{\text{H}} > 1.6$ for Z isomer and < 1.6 for E isomer, while their corresponding ^{13}C NMR signals resonate at $\delta_{\text{C}} > 20$ and < 20 for Z and E isomers, respectively [Holler et al., 1997]. The paper also goes on to say that the C-5 and C-6 methylene groups of variabilin derivatives show characteristic chemical shifts in the ^1H NMR spectra at δ 2.2 and 2.4. Therefore, the ^1H NMR of δ 1.56 (H-9) and 1.65 (H-14) as well as δ 2.43 (H-5) and 2.24 (H-6) established compound **4.5** to be 7E,12Z,20Z-variabilin. Long range ^1H - ^{13}C 2D NMR (HMBC) revealed correlations of H-1 to C-2, C-3 and C-4 and H-2 to C-3 and C-4. H-5 showed correlations to C-6 and C-7, and H-6 to C-8 and C-9, H-7 to C-10 and C-9, H-9 to C-8 and C-10, H-10 to C-11 and C-12, and finally H-11 to C-12 and C-13. Long range ^1H - ^{13}C couplings from H-1 to C-19 allowed us to build a straight chain fragment in the molecule delineating an aliphatic chain at positions 8, 13 and 18. H-25 was displayed correlations to C-22, C-23 and C-24.

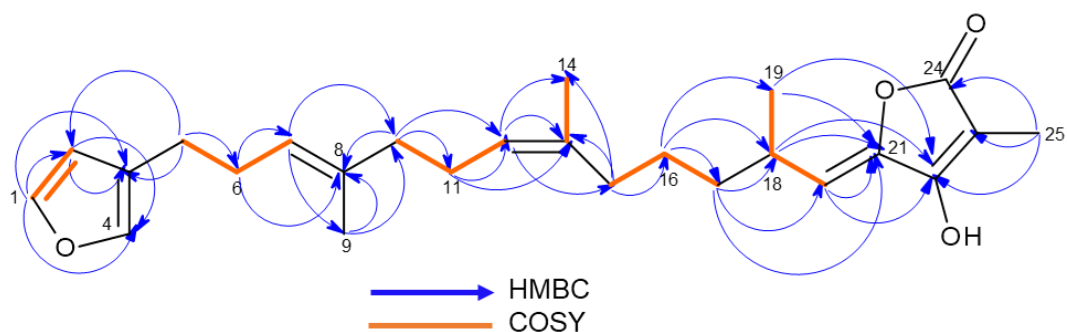


Figure 4.7. COSY and HMBC correlations of compound **4.5**.

Comparing of the NMR spectra of compound **4.5** with that of the published literature, it was evident that there was a possibility of contamination or coexistence of small amounts of its geometric isomer, strobilin. In summary, compound **4.5** was isolated as an unstable yellow oil, HR-ESIMS m/z of 399.2532, calculated for $C_{25}H_{34}O_4$. The structure of **4.5** was identified as 7E,12Z,20Z,18S-variabilin after detailed analysis of 1D and 2D NMR data and through comparison with published data. 1H and ^{13}C NMR data (400/100 MHz, $CDCl_3$), see table 4.1.

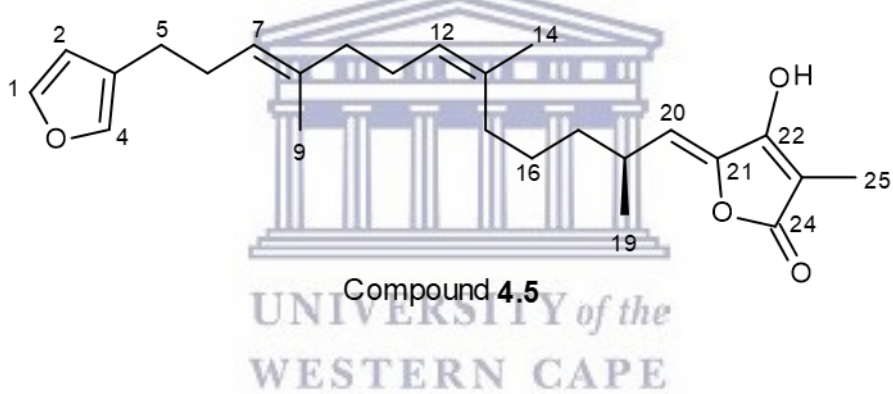
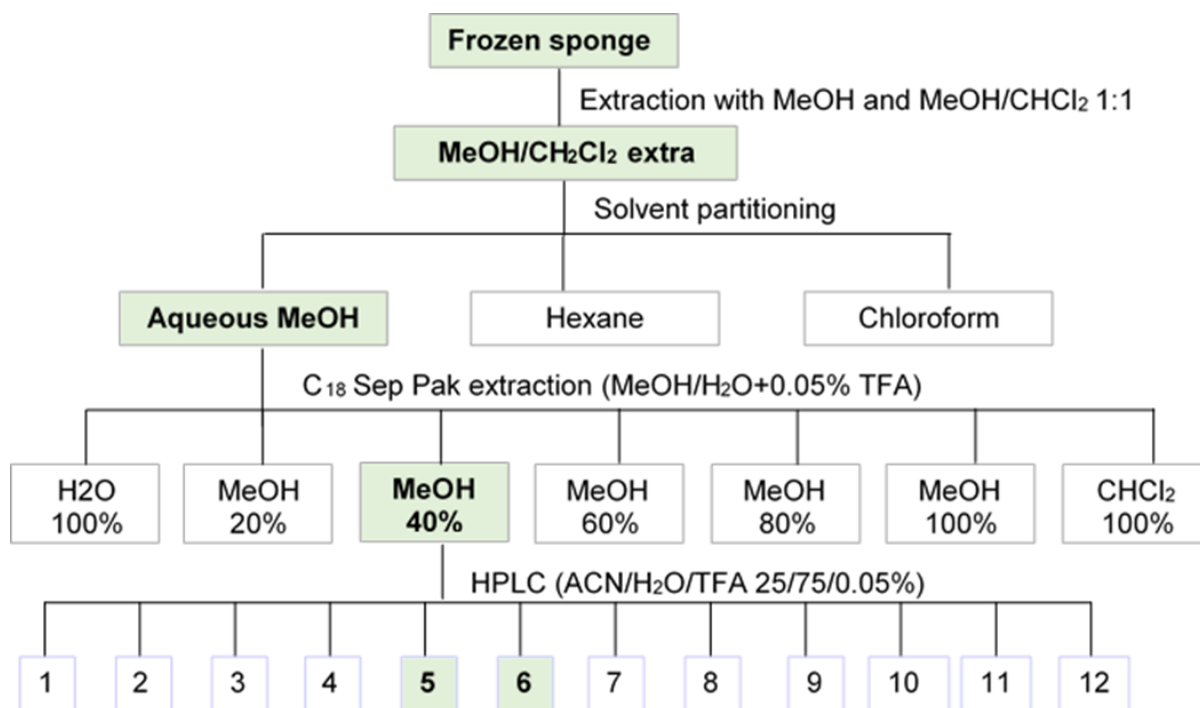


Table 4.1. NMR data of compound **4.5** compared to that of variabilin available in Barrow et al. (1988)

Position	δ_c	δ_c (literature)	δ_H (multiplicity, J, Hz)	δ_H (multiplicity, J, Hz) literature	COSY	HMBC
1	143.6	142.47	7.33 (m)	7.33 (t, J=1.8)	H-2	C-2, C-3, C-4
2	111.2	111.09	6.27 (m)	6.27 (m)	H-4	C-1, C-3, C-4
3	125.1	124.98	---			
4	139.0	138.78	7.20 (brs)	7.20 (m)	H-5	C-1, C-2,
5	25.5	25.04	2.43 (m)	2.44 (t, J=7.5)	H-6	C-2, C-3, C-4, C-6
6	28.4	28.44	2.24 (q, J=7.4)	2.25 (q, J=7.3)	H-7	C-5, C-7, C-8
7	124.1	123.72	5.15 (t, J=7.1)	5.16 (tg, J=6.9, 0.7)	H-6, H-9	C-6, C-9, C-10
8	135.6	135.71	---			
9	15.9	16.04	1.56 (m)	1.58 (d, J=0.7)	H-7	C-7, C-8, C-10
10	39.9	39.55	1.94 (m)	1.95 (m)	H-7/H-12	C-7, C-8, C-9, C-11
11	26.7	26.57	2.05 (m)	2.05 (m)	H-11	C-10, C-12, C-13
12	124.7	124.41	5.09 (m)	5.08 (tq, J=6.2, 0.7)		C-11, C-14, C-15
13	134.9	134.76	---			
14	23.3	15.80	1.65 (m)	1.55 (d, J=0.7)		C-12, C-13, C-15
15	39.7	39.68	1.94 (m)	1.95 (m)	H-16	C-12, C-13, C-14, C-16
16	25.9	25.68	1.35 (m)	1.35 (m)	H-15/H-17	C-17, C-18, C-19
17	36.6	36.57	1.35 (m)	1.35 (m)	H-16	C-16, C-18, C-19, C-20
18	30.9	30.95	2.80 (m)	2.80 (bm)	H-19	C-20, C-21
19	20.5	20.60	1.05 (d, J=6.7)	1.05 (d, J=6.4)	H-18	C-17, C-18, C-20
20	116.6	117.17	5.35 (d, J=10.0)	5.44 (d, J=10.3)		C-19, C-17, C-21, C-22
21	142.7	142.96	---			
22	162.6	162.47	---			
23	99.5	99.04	---			
24	172.4	172.54	---			
25	6.0	6.06	1.81 (s)	1.82 (s)		C-22, C-23, C-24

4.2.3 Extraction and isolation of pyrroloiminoquinones from a *Latrunculid* sp.

The frozen sponge previously collected from St Francis Bay in the Eastern Cape Province of South Africa coast was extracted by soaking in MeOH and CH₂Cl₂ overnight. The resultant extract was concentrated under reduced pressure and the remaining moisture was removed by freeze drying, giving a dark green powder. This powder was then separated using a modified Kupchan procedure to obtain three fractions: chloroform, hexane and methanol. The MeOH fraction was further subjected to a C₁₈ column chromatography and eluted using a gradient solvent system of H₂O and MeOH. Inspection of the ¹H NMR spectrum revealed the presence of characteristic pyrroloiminoquinone resonances [δ H 2.8 – 4.0 (H16 and (H-17) methylenes); 7.2-7.4 (H-14); 7.8-8.5 (NH-18); 9.5-10.5 (NH-9); and 13-14 (NH-13)] as was reported by Antunes et al. (2004) in the 40% MeOH fraction, hence this fraction was pursued further. The isolation and purification of the compounds in this fraction was particularly challenging due to their intense UV chromophores and poor behaviour on chromatographic stationary phases. The first trial of separating metabolites with C₁₈ reversed phase HPLC using UV detection did not allow for decent separation: the chromatogram showed overlapping peaks which were difficult to collect separately. After failed trials with UV detection guided fractionation, a preparative reversed phase TLC method was used but unfortunately it was also not able to afford effective separation. Ultimately, C₁₈ reversed phase HPLC was used but rather than using UV detection, the collection of fractions was time dependent. Repeated injections into the HPLC was done and fractions were collected every 30 seconds, with similar fractions later combined according to their TLC profiles to give 12 fractions (scheme 4.2). Two bispyrroloiminoquinones alkaloids, tsitsikammamine A and tsitsikammamine A N-18 Oxime were isolated from the 40% MeOH fraction as fractions 6 and 5, respectively (see extraction scheme below), and are referred to as compounds **4.6** and **4.7**, respectively, in this study.



Scheme 4.2. Isolation of pyrroloiminoquinone metabolites from *Latrunculia* sp.

4.2.4 Structure elucidation of bispyrroloiminoquinones from *Latrunculid* sp.

Tsitsikammamine A (compound **4.6**)

Low resolution electrospray ionization mass spectroscopy (LR-ESIMS) of **4.6** revealed a molecular ion peak at m/z 304.02 consistent with the molecular formula $C_{18}H_{14}N_3O_2$. Inspection of the 1H NMR data (in $DMSO-d_6$) for compound **4.6** and comparison with literature values allowed the allocation of all the signals. The 1H NMR spectrum displayed methylene protons at δ 2.93 (H-16, t, $J = 7.8$ Hz) and 3.85 (H-17, t, $J = 7.8$ Hz), and the aromatic protons for positions 1 and 5 at δ 6.87 (d, $J = 8.4$ Hz) and 2 and 4 at 7.38 (d, $J = 8.4$ Hz). Three broad singlets for N-H protons at positions 9, 13 and 18 and the OH at position 3 were also observed at δ 13.29, 13.02, 9.76 and 10.44, respectively, figure 4.8. The ^{13}C DEPT-135 NMR spectrum (figure 4.9) confirmed the presence of two methylene signals at δ 18.2 (C-16) and 45.5 (C-17) and four methine signals at δ (123.7 (C-14), 125.4 (C-8) together with the overlapping signals at δ 116.5 and 129.8 resolving into four carbons (C-1/5 and C-2/4), respectively. The COSY spectrum revealed close correlations of H-1/5 and H-2/4, H-8 and H-9, H-14 displayed close correlations to both H-13 and H16. The methylene protons at positions 16 and 17 were also shown to be connected to each to other.

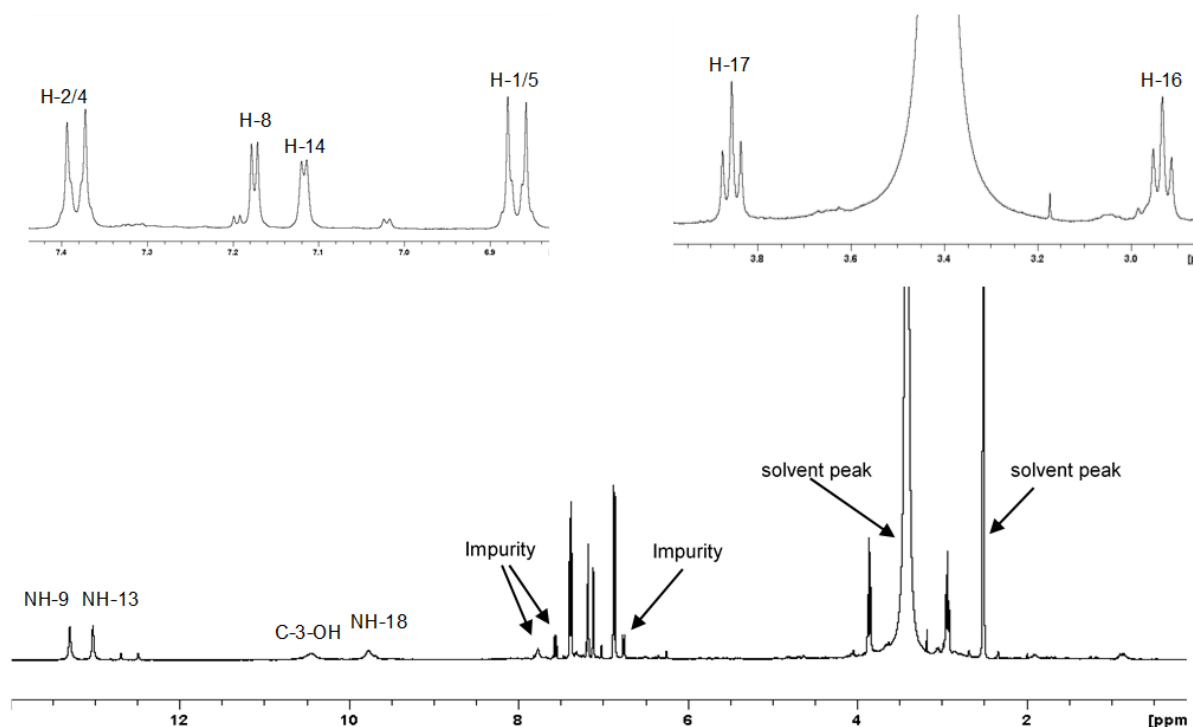


Figure 4.8. ^1H NMR spectrum of compound **4.6** (400 MHz, DMSO-d_6).

HSQC NMR data, complemented by ^{13}C DEPT-135 data, showed the methylene protons to be residing on carbons at $\delta 18.2$ and 45.6 , while the aromatic protons were shown to be attached to carbons at $\delta 116.5$ (C-1/5), 129.8 (C-2/4), 125.4 (C-8) and 123.7 (C-14), verifying that the molecule has ten quaternary carbons. The methylene protons at $\delta 2.93$ and 3.85 were attached to carbons at 18.2 (C-16) and 45.2 (C-17), respectively.

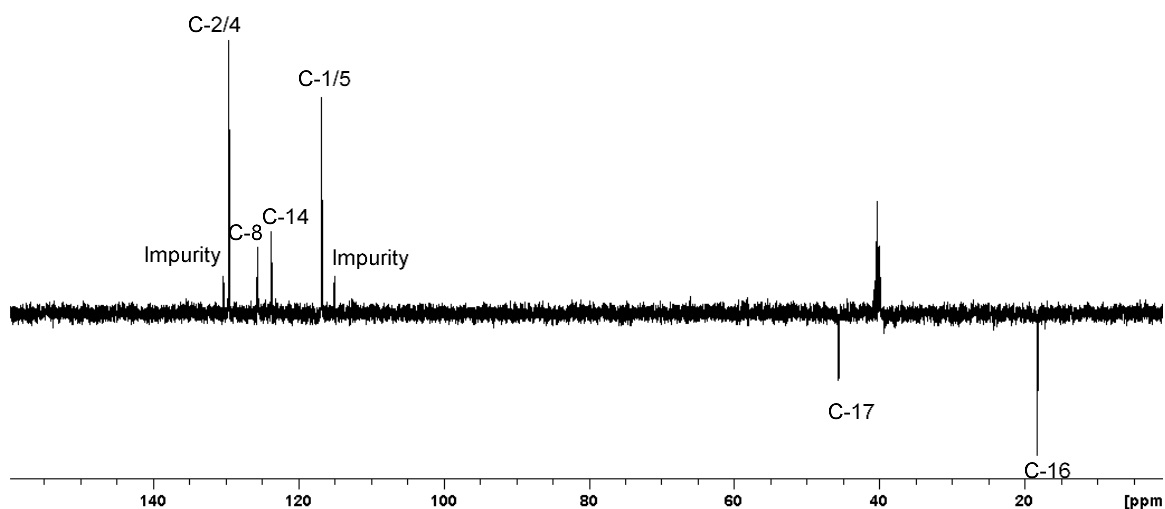


Figure 4.9. ^{13}C DEPT 135 of compound **4.6** (400 MHz, DMSO-d_6)

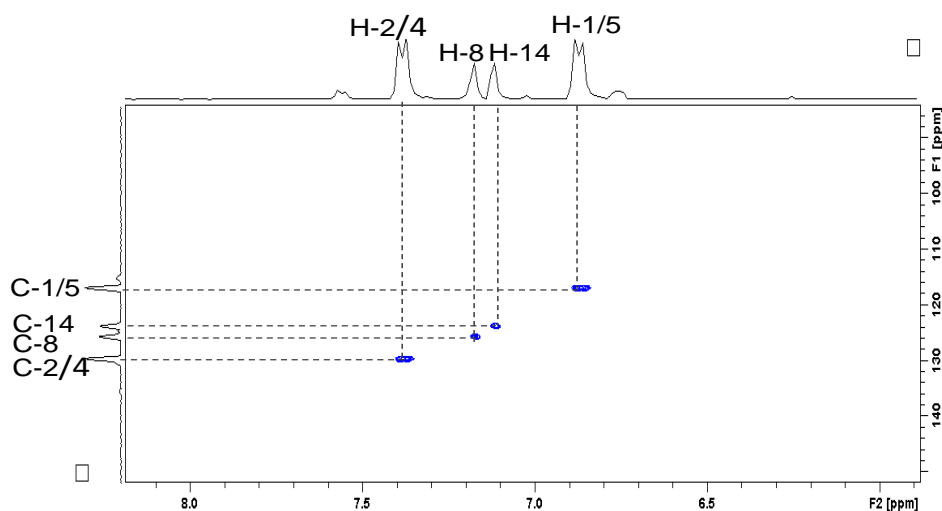


Figure 4.10. A section of the HSQC spectrum showing aromatic hydrogens correlations to corresponding carbons.

The long range ^1H - ^{13}C HMBC correlation of H-1 to C-6 and C-5 confirmed the attachment of a six membered ring to the pyrrole ring on the eastern side of the molecule, and the attachment at C-7 was supported by the correlation of H-8 to C-1/5, and C-6. H-16 displayed correlations to C-15 and C-17, while H-17 displayed correlations to C-15, C-16 and C-19. A long range correlation of H-14 to C-21 was observed, suggesting a closed ring system. H-14 also displayed correlations to C-12 and C-21.

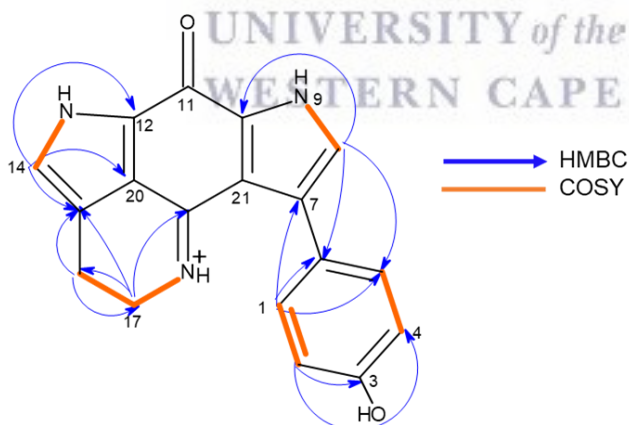


Figure 4.11. COSY and HMBC correlations of compound **4.6**.

Tsitsikammamine A was isolated as a dark red powder, LR-ESIMS m/z of 304.02 calculated for $\text{C}_{18}\text{H}_{14}\text{N}_3\text{O}_2$. ^1H and ^{13}C NMR data (400/100 MHz, $\text{DMSO}-d_6$) see table 4.2.

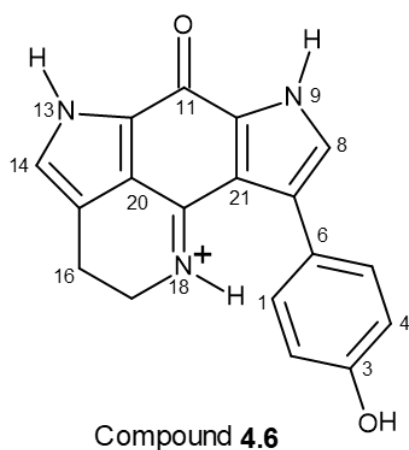


Table 4.2. NMR data for compound **4.6**, (400 MHz, DMSO- d_6)

Position	δC	δH (mult., J, Hz)	COSY	HMBC
1	116.5	6.87 (d, $J=8.4$)	H-2/4	C-5, C-3, C-7
2	129.8	7.38 (d, $J=8.4$)	H-1/5	C-4, C3
3	157.1	-		
4	129.8	7.38 (d, $J=8.4$)	H-1/5	C-2, C3
5	116.5	6.87 (d, $J=8.4$)	H-2/4	C-1, C-3, C-7
6	127.9	-		
7	123.0	-		
8	125.4	7.17 (d, $J=2.7$)	H-9	C-1, C-6, C-10
NH-9		13.29 (brs)	NH-8	
10	134.9	-		
11	168.5	-		
12	128.4	-		
NH-13		13.02 (brs)	H-14	
14	123.4	7.12 (d, $J=2.3$)	NH-13/H-16	C-15, C-12
15	119.3	-		
16	18.2	2.93 (t, $J=7.8$)	H-14/H17	C-15, C-17
17	45.5	3.85 (t, $J=7.8$)	H-16/NH-18	C-15, C-16, C-19
NH-18		9.76 (brs)	H-17	
19	157.0	-		
20	124.6	-		
21	121.6	-		
OH		10.44 (brs)		

Tsitsikammamine A N-18 Oxime (compound 4.7)

LR-ESIMS for **4.7** displayed a molecular ion peak at m/z 322.07 consistent with the calculated molecular weight of $C_{18}H_{14}O_3N_3$. The 1H NMR spectrum of **4.7** in DMSO- d_6) looked similar to that of **4.6** displaying three singlets allocated to C-3-OH, NH-9 and NH-13 with an additional broad singlet at δ 7.76 allocated to N-18-OH. It also showed a significant chemical shift of H-17 signal from δ 3.85 to 3.04. A notable difference in the ^{13}C NMR spectrum was an upfield chemical shift for C17 from δ 45.5 to 39.4, and downfield chemical shift for C-16 from δ 18.2 to 24.2. Another significant chemical shift was observed in the downfield shift of C-19 from δ

157.0 to 181.4. The COSY spectrum for **4.6** showed a close correlation of N-18-OH with H-17. These changes in the NMR spectra of **4.6** and **4.7** together with the molecular mass difference of 16 amu (equivalent to one oxygen atom) was enough to conclude that **4.7** has an extra oxygen atom attached at position N-18 of the molecule.

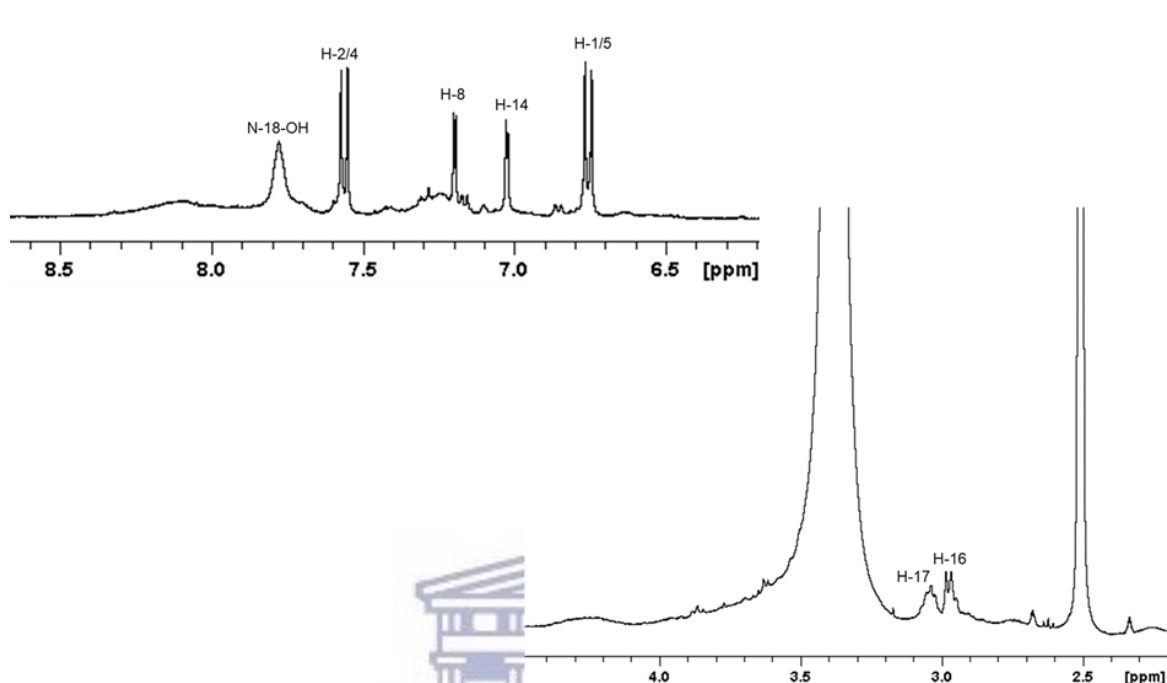
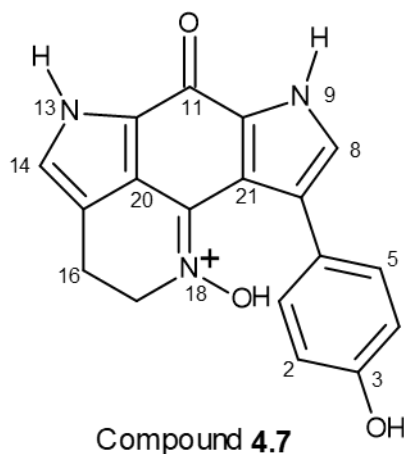


Figure 4.12. A section of ^1H NMR of compound **4.7**.

Table 4.3. NMR data for compound **4.7**, (400 MHz, DMSO- d_6)

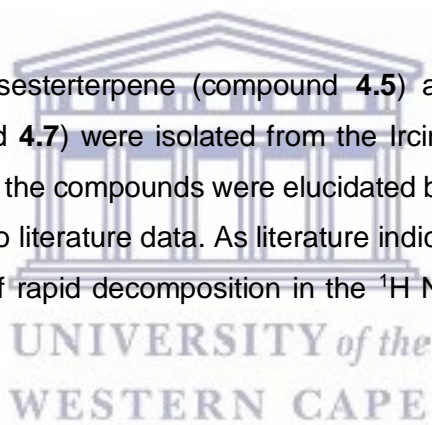
Position	δC	δH (mult., J, Hz)	COSY	HMBC
1	115.0	6.6.75 (d, $J=8.4$)	H-2/4	C-5, C-3, C-7
2	130.2	7.56 (d, $J=8.4$)	H-1/5	C-4, C3
3	157.0	-		
4	130.2	7.56 (d, $J=8.4$)	H-1/5	C-2, C3
5	115.0	6.75 (d, $J=8.4$)	H-2/4	C-1, C-3, C-7
6	127.4	-		
7	122.2	-		
8	124.6	7.19 (d, $J=2.7$)	H-9	C-1, C-6, C-10
NH-9		12.69 (brs)	NH-8	
10	133.3	-		
11	168.5	-		
12	129.6	-		
NH-13		12.48 (brs)	H-14	
14	132.2	7.02 (d, $J=2.3$)	NH-13/H-16	C-15, C-12
15	119.8	-		
16	24.1	2.98 (t, $J=7.8$)	H-14/H17	C-15, C-17
17	39.4	3.05 (t, $J=7.8$)	H-16/NH-18	C-15, C-16, C-19
N18-OH		7.77 (brs)	H-17	
19	181.4	-		
20	124.4	-		
21	125.2	-		
OH		9.47 (brs)		

Tsitsikammamine A N-18 Oxime was isolated as a bright red powder, LR-ESIMS m/z of 322.07 calculated for $C_{18}H_{14}N_3O_3$. The 1H and ^{13}C NMR data (400/100 MHz, $DMSO-d_6$) are listed in table 4.3.



4.3 Conclusion

In summary, a linear furanosesterterpene (compound **4.5**) and two pyrroloiminoquinone alkaloids (compounds **4.6** and **4.7**) were isolated from the *Ircinia* and *Latrunculi* sponges, respectively. The structures of the compounds were elucidated by detailed analysis of 1D and 2D NMR data with reference to literature data. As literature indicated, compound **4.5** is highly unstable and showed signs of rapid decomposition in the 1H NMR spectra after only a few days following isolation.



4.4 Experimental

General

Solid phase extraction of *Ircinia* and *Latrunculid* sponges were performed on Supelco Dianion® HP20SS (USA), silica gel 60 (0.040-0.063mm) from Merck KGaA (Germany) and Waters Sep-Paks® C₁₈ 10g respectively. Normal phase TLC was performed on Silica gel 60 F254 aluminium sheets purchased from Merck KGaA (Germany) and visualised under UV light at 254 and 365nm. Separation of furanosesterterpenes was carried using Whatman 10µm silica (2) semi-preparative column 50cm, while pyrroloiminoquinone separation was done on Luna 10u C₁₈ (2) 100A column 250 x 10mm. All high performance liquid chromatography procedures were carried out with Agilent technologies equipped with ultra violet and refractive index detectors. NMR samples were prepared using deuterated solvents and NMR experiments were obtained from Avance Bruker 400MHz spectrometer. Chemical shifts are referenced to deuterated solvent peaks (CDCl₃ δ_H 7.26, δ_C 77.23; DMSO-d₆ δ_H 2.50, δ_C 39.43) and reported in ppm.

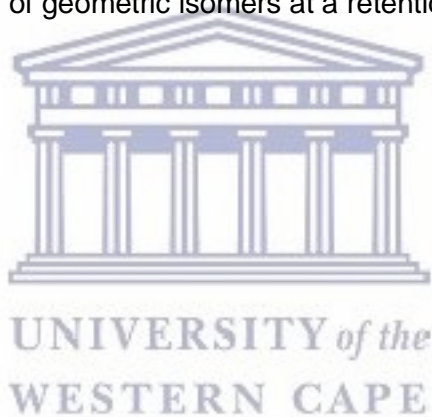
Invertebrate material

The *Ircinia* sponge was collected from Grootbank (Plettenberg bay), South Africa by SCUBA at the depth of 17 m and given a code TS2713. The morphology of the sponge used in this study fitted the description given by Su et al., (2011) as “globular and massive. Remarkably elastic, very tough, and extremely hard when dry. Difficult to cut or tear. The specimen has medium to very coarse sand embedded in the base and sparsely distributed in the endoderm. Cortex black, golden-brown internally”. The *Latrunculid* sponge was collected from St Francis bay in 2016 and given a code TS3392. All sponge samples were stored at -20°C until processed. Voucher specimen are kept at Marine Biodiscovery laboratory at University of the Western Cape.

Isolation and extraction

Frozen sample of *Latrunculid* sponge was sequentially extracted with CH₃OH and CH₃OH:CH₂Cl₂ (1:1) and the extract was dried under reduced pressure. The resulting crude extract was partitioned using modified Kupchan method to give three fractions: chloroform, hexane and MeOH. Aqueous MeOH fraction was further separated on C₁₈ Sep-Pak® using gradient elution system of CH₃OH:H₂O:TFA (0:100:0.05, 20:80:0.05, 40:60:0.05, 60:40:0.05, 80:20:0.05, 100:0:0.05) and CH₂Cl₂ 100% to obtain 7 fractions. CH₃OH:H₂O:TFA (40:60:0.05) fraction was repeatedly subjected to C₁₈ reversed phase HPLC, eluted with ACN:H₂O:TFA (25:75:0.05) at elution rate of 3ml/min to give compounds **4.6** (6.2mg) and **4.7** (3.4mg).

A frozen specimen of *Ircinia* sponge was thawed at room temperature prior to exhaustive extraction with 400 ml of CH₃OH, followed by CH₃OH:CH₂Cl₂ (1:1). Each solvent was allowed to extract metabolites overnight, at room temperature, away from direct light and the extracts were combined and dried under reduced pressure. The resultant extract was subjected to a solid phase extraction with Dianson HP20ss using a stepwise gradient elution with CH₃OH - H₂O (0:100, 10:90, 20:80, 60:40, 20:80, 100:0), CH₃OH -EtOAc (50:50) and EtOAc 100%. Thin layer chromatography of all the 9 fractions was developed using different mobile phases consisting of ethyl acetate and hexane to establish a solvent mixture that affords better separation. CH₃OH -EtOAc 50:50 fraction was further separated on silica gel 60 (0.040 - 0.063 mm) and eluted with hexane-EtOAc (7:3) resulting in collection of 18 fractions which were later grouped based on their TLC similarities resulting into 7 fractions: 8A (1-2), 8B (3-4), 8C (5-8), 8D (9-10), 8E (11-14), 8F (15-17) and 8G (EtOAc wash). Fraction 8B was injected into semi-preparative HPLC (Agilent technologies phenomenon silica gel 10um column 50mm), and eluted with hexane-EtOAc (7:3) at a rate of 3 mL/min elution over 20 minutes and compound **4.5** was collected as a mixture of geometric isomers at a retention time of 14.50 minutes.



4.5 References

- Antunes, E.M. PhD thesis; Pyrroloiminiquinone metabolites from South African Latrunculid sponges. Rhodes University. **2004**. 46-48.
- Antunes, E.M.; Beukes, D.R.; Kelly, M.; Samaai, T. Barrows, L.R.; Marshall, K.M.; Sincich, C.; Davies-Coleman, M.T. Cytotoxic Pyrroloiminoquinones from Four new Species of South African Latrunculid sponge. *Journal of Natural Products* **2004**, 67(8): 1268-1276.
- Barrow, C.J.; Blunt, J.W.; Munro, M.H.G. Autooxidation studies on marine sesterterpene tetronic acid, variabilin. *Journal of Natural Products* **1989**, 52(2), 346-359.
- Barrow, C.J.; Blunt, J.W.; Munro, M.H.G.; Perry, N.B., Variabilin and related compounds from a sponge of the genus *Sarcotragus*. *Journal Natural Products* **1988**, 51(2), 275-281.
- Boury-Esnault, N.; van Soest, R.; *Ircinia* Nardo, 1833. In: Van Soest, R.W.M; Boury-Esnault, N.; Hooper, J.N.A.; Rützler, K.; de Voogd, N.J.; Alvarez de Glasby, B.; Hajdu, E.; Pisera, A.B.; Manconi, R.; Schoenberg, C.; Klautau, M.; Picton, B.; Kelly, M.; Vacelet, J.; Dohrmann, M.; Díaz, M.-C.; Cárdenas, P.; Carballo, J. L. (2016). World Porifera database. Accessed at <http://www.marinespecies.org/porifera/porifera.php?p=taxdetails&id=131751> on 2016-11-22.
- Choi, K.; Hong, J.; Lee, C.O.; Kim, D.K.; Sim, C.J.; Im, K.S. Cytotoxic Furanosesterterpenes from a Marine Sponge *Psammocinia* sp. *Journal Natural Products* **2004**, 67, 1186-1189.
- Davis-Coleman, M.T.; Beukes, D.R. Ten years of marine natural products research at Rhodes University. *South African Journal of Science* **2004**, 100, 539 - 544.
- Ford, J.; Capon, R.J. Discorhabdin R: A New Antibacterial Pyrroloiminoquinone from Two Latrunculiid Marine Sponges, *Latrunculia* sp. and *Negombata* sp. *Journal Natural Products* 2000; 63(11): 1527-1528.
- Hardoim, C.C.P.; Costa, R. Microbial Communities and Bioactive Compounds in Marine Sponges of the Family Irciniidae—A Review. *Marine Drugs*. **2014**, 12(10), 5089-5182.
- Höller, U.; and König, G.M.; Wright, A. D. Two New Sesterterpene Tetronic Acids from the Marine Sponge *Ircinia oros*. *Journal Natural Products* **1997**, 60(8), 832-835.
- Hooper, G.J.; Davis-Coleman, M.T.; Kelly-Borges, M.; Coetzee, P.S. ew alkaloids from a South African Latrunculid sponge. *Tetrahedron letters* **1996**, 37(39), 7135-7138.
- Hu, J-F.; Fan, H.; Xiong, J.; Wu, S-B. Discorhabdins and Pyrroloiminoquinone-Related Alkaloids. *ChemicalReviews* **2011**, 111, 5465–5491.

Keyzers, R.A.; Samaai, T.; Davies-Coleman, M.T. Novel Pyrroloiminoquinone Ribosides from South African Latrunculid sponge *Strongylodesma aliwaliensis*. *Tetrahedron Letters* **2004**, *45*(51), 9415-9418.

Mehbub, M.F.; Perkins, M.M.V.; Zhang, W.; Franco, C.M.M. New marine natural products from sponges (Porifera) of the order Dictyoceratida (2001-2012); a promising source for drug discovery, exploration and future prospects. *Biotechnology Advances* **2016**, *34*, 473-491.

Muller, R.H.; Mader, K.; Gohla, S. Solid lipid nanoparticles (SLN) for controlled drug delivery – a review of the state of the art. *European Journal of Pharmaceutics and Biopharmaceutics* **2000**, *50*(1), 161-177.

Pooja, D.; Kulhari, H.; Kuncha, M.; Rachamalla, S.S.; Adams, D.J.; Bansal, V.; Sistla R. Improving Efficacy, Oral Bioavailability, and Delivery of Paclitaxel Using Protein-Grafted Solid Lipid Nanoparticles. *Molecular Pharmaceutics* **2016**, *13*, 3903–3912.

Shenderova, A.; Burke, T.G.; Schwendeman S.P. Stabilization of 10-hydroxycamptothecin in poly(lactide-co-glycolide) microsphere delivery vehicles. *Pharmaceutical Research* **1997**, *14*(10), 1406-1414.

Su, H-J.; Tseng, S-W.; Lu, M-C.; Liu, L-L.; Chou, Y.; Sung P-J. Cytotoxic C₂₁ and C₂₂ terpenoid-derived metabolites from the sponge *Ircinia* sp. *Journal of Natural Products* **2011**, *74*, 2005-2009.

Utkina, N.K.; Makarchenko, A.E.; Denisenko, V.A.; Dmitrenko, P.S.; Zyzzyanone A, a Novel pyrrol[3,2-f]indole Alkaloid from the Australian Sponge *Zyzzya fuliginosa*. *Tetrahedron Letters* **2004**; *45*(40), 7491-7494.

Watkins, R.; Wu, L.; Zhang, C.; Davis, R.M.; Xu, B. Natural product-based nanomedicine: recent advances and issues. *International Journal of Nanomedicine* **2015**, *10*, 6055-6074.

**Cytotoxicity of furanosesterterpenes and pyrroloiminoquinone alkaloids
and improvement of activity by incorporation into solid lipid
nanoparticles.**

5.1 Introduction

Cancer is a major health burden worldwide and one of the leading causes of death [Siegel et al., 2017]. Among women, breast cancer is the most diagnosed type of cancer globally [Harbeck and Gnant, 2017]. It accounts for 25% of all diagnosed cancers and 20% malignancy related mortalities reported in African women [Vanderpuye et al., 2017]. In males on the other hand, most common malignancy diagnosed is prostate cancer, with the highest incidence rate reported among men of African descent [Babb et al., 2014]. It is further estimated that the burden of cancer will increase in low- and middle-income countries' populations due to adaptation to western lifestyles and longer life spans [Ferlay et al., 2014]. Due to the high prevalence of breast and prostate cancer, we found it relevant to explore the cytotoxicity of our isolated compounds against breast cancer and prostate cancer cell lines.

Literature points out that Latrunculid sponges have often produced potent cytotoxic pyrroloiminoquinone alkaloid metabolites [Davis-Coleman and Beukes, 2004; Davis-Coleman, 2010]. A study done by Antunes et al. (2004), tested many of these compounds, including the discorhabdins, tsitsikammamines and makaluvamines and revealed that most of these compounds possess potent cytotoxic properties against Human Colon Tumour (HCT-116) at low micromolar concentrations. Other studies carried out on pyrroloiminoquinone alkaloids have reported on the potent cytotoxic properties of these compounds against oesophageal cancer and breast cancer cell lines [Shinkre et al., 2007; Keyzers et al., 2005].

Furanosesterterpenes have been studied for their cytotoxicity against several human cancer cell lines such as A549 (lung cancer cells), SK-OV-3 (ovarian cancer cells), SK-MEL-2 (skin cancer cells), XF498 (Central Nervous System cancer cells) and HCT15 (colon cancer cells) and showing moderate cytotoxic behaviour [Choi et al., 2004; Liu et al., 2003]. Rifai et al. (2005) revealed that fasciculation, isolated from *Ircinia variabilis* had a comparable cytotoxicity to that of doxorubicin against MCF-7 cells and superior activity against NCI-H460 (lung) and SF-268 (CNS) cancer cell lines. However, it has been reported that furanosesterterpenes bearing tetronic acid and furan moieties are known to be unstable and decompose readily in the presence of light and air into a mixture of more polar compounds. These were confirmed to be up to 10 times less active than variabilin [Barrow et al., 1989]. This suggests that in order to obtain more accurate results in the biological assays that assess the cytotoxicity of these

compounds, it is crucial to protect them from degradation and this could be done by incorporating them into nanoparticles.

Solid lipid nanoparticles (SLNP) are colloidal carriers and they were introduced in 1991 as a substitute to traditional carriers such as emulsions, liposomes and polymeric nanoparticles [Muller et al., 2000]. They are spherical bodies made of a solid lipid core surrounded by phospholipids (figure 5.1), ranging in diameter from 50 to 1000 nm [Watkins et al., 2015]. Solid lipid nanoparticles provide protection for sensitive molecules from unfavourable environmental factors such as moisture, light and pH. A study done by Shenderova et al. (1997), showed that lipid nanoparticles were able to prevent hydrolysis of 10-hydroxycamptothecin to its carboxylate isoform which is more abundant at physiologic pH of 7.4. In addition, solid lipid nanoparticles have been used for the delivery of poorly water soluble anticancer natural product derived drugs such as paclitaxel and camptothecin [Pooja et al., 2016].

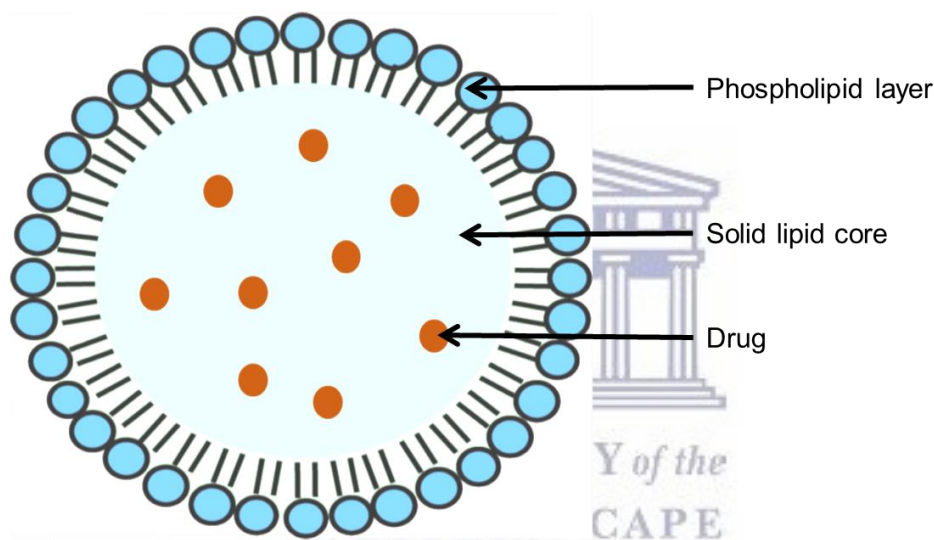


Figure 5.1. Structure of a solid lipid nanoparticle.

After isolation of furanosesterterpenes and pyrroloiminoquinone alkaloids from an *Ircinia* sp. and a *Latrunculi* sponge, respectively, (discussed in the previous chapter), and published evidence on cytotoxicity of these compounds, the cytotoxicity of compounds **4.5**, **4.6** and **4.7** against MCF-7, PC-3, U-87 and HEK-293 cells was studied. The method of cell death induced by compounds **4.5**, **4.6** and **4.7** on MCF-7 and PC-3 cells was evaluated. This chapter also discusses potential stabilisation and improvement of activity of compound **4.5** by encapsulation into SLNP.

5.2 Results and discussion

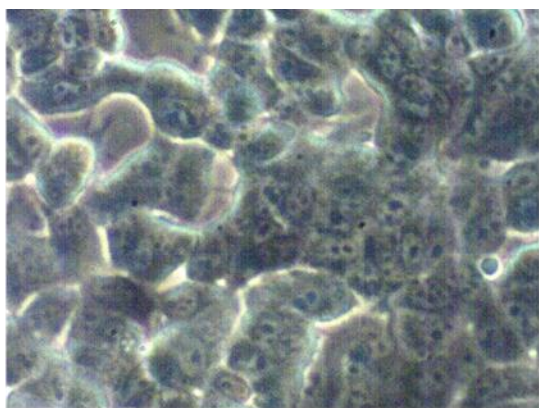
5.2.1 Cytotoxicity assay

MCF-7, PC-3, U-87 and HEK-293 were cultured to approximately 90% confluence prior to treatment with compound **4.5** and its solid lipid nanoparticles, compounds **4.6** and **4.7** at five

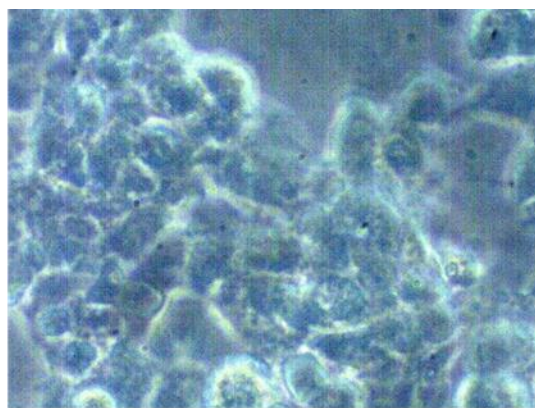
different concentrations. The cytotoxicity of the compounds was determined using a tetrazolium salt (WST-1) antiproliferation assay, while apoptotic assays was done using APOPercentage™ dye. Figures 5.2 and 5.3 shows morphological changes of cells after 24 hours of treatment with compounds 4.5, 4.6 and 4.7. Viability of the cells was calculated and figure 5.4 shows the dose response charts obtained for the compounds against treated cell lines.

The dose response chart for compound **4.5** (figure 5.4) shows moderate to no activity for PC-3 cells at low concentrations, with moderate activity at high concentrations (50 µg/ml). The compound displayed moderate activity against MCF-7 and U-87 cells at all concentrations and slightly higher activity against HEK-293 cells. At a concentration of 50 µg/ml, **4.5** displayed 100% cell proliferation of the HEK-293 cells. Compound **4.5** showed the highest activity against non-cancer cell line (HEK-293) with an IC₅₀ of 11.94 µg/ml- the lowest IC₅₀ for this compound against all tested cell lines.

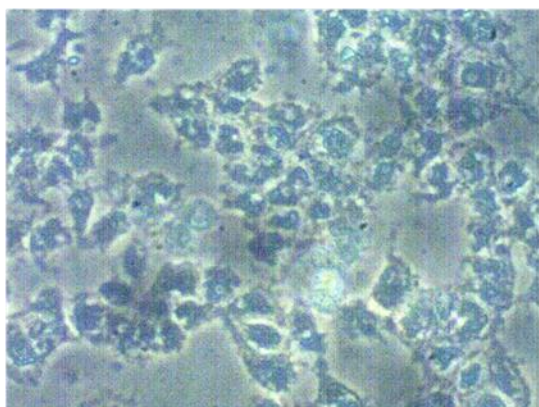
Compound **4.6** showed potent activity against the HEK-293, PC-3 and U-87 cells at low concentrations i.e. below 6.25 µg/ml, with an IC₅₀ 3.215 µg/ml for the HEK-293, a non-cancer cell line. The HEK-293 cell line was the most susceptible of the tested cell lines to compound **4.6**, demonstrating a lack of selectivity of this compound for cancer cells. The viability of the MCF-7 cells remained high, above 50%, even at high concentrations at 50 and 25 µg/ml of compound **4.6**, however, the cell viability dropped significantly when treated with compound **4.7** at the same concentrations. Compound **4.7** displayed potent activity against all four cell lines at concentrations of 50 µg/ml, showing a cell viability of 25% and 6% for the MCF-7 and PC-3 cell lines, respectively, and 100% cells proliferation inhibition for HEK-293 and U-87 cells. Cell viability of PC-3 cells remained unaffected by compound **4.7** at low doses of 3.125 and 6.25 µg/ml, however, as the concentration increased, cell viability decreased significantly. HEK-293 and U-87 were the most affected by compound **4.7**; about 50% of the cells were inhibited by compound **4.7** at 6.25 µg/ml.



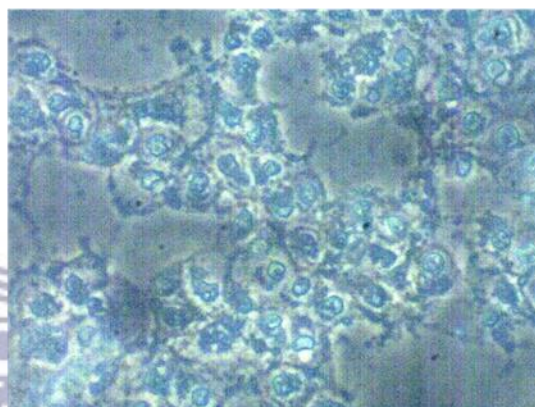
(a)



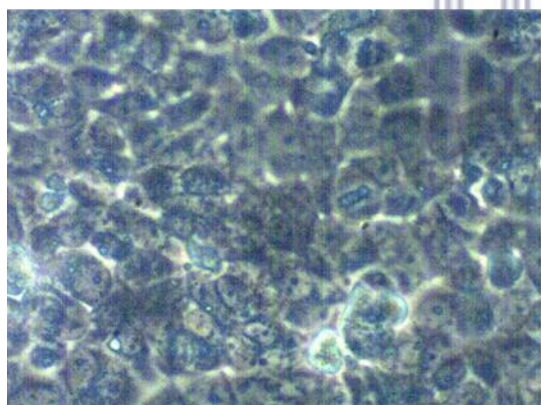
(b)



(c)



(d)



(e)

Figure 5.2. Morphological changes in MCF-7 cells after treatment with compounds **4.5**, **4.6** and **4.7**. MCF-7 cells were treated for 24 hours with 100 μ M of compound **4.5** (**c**), 100 μ M of compound **4.6** (**d**) and 9.7 μ M of compound **4.7** (**e**). Cells in (**a**) was left untreated, while cells in (**b**) represent the positive control i.e. cells treated with 60 μ M ceramide. The cells were observed at 20X magnification using an inverted (Nikon) light microscope.

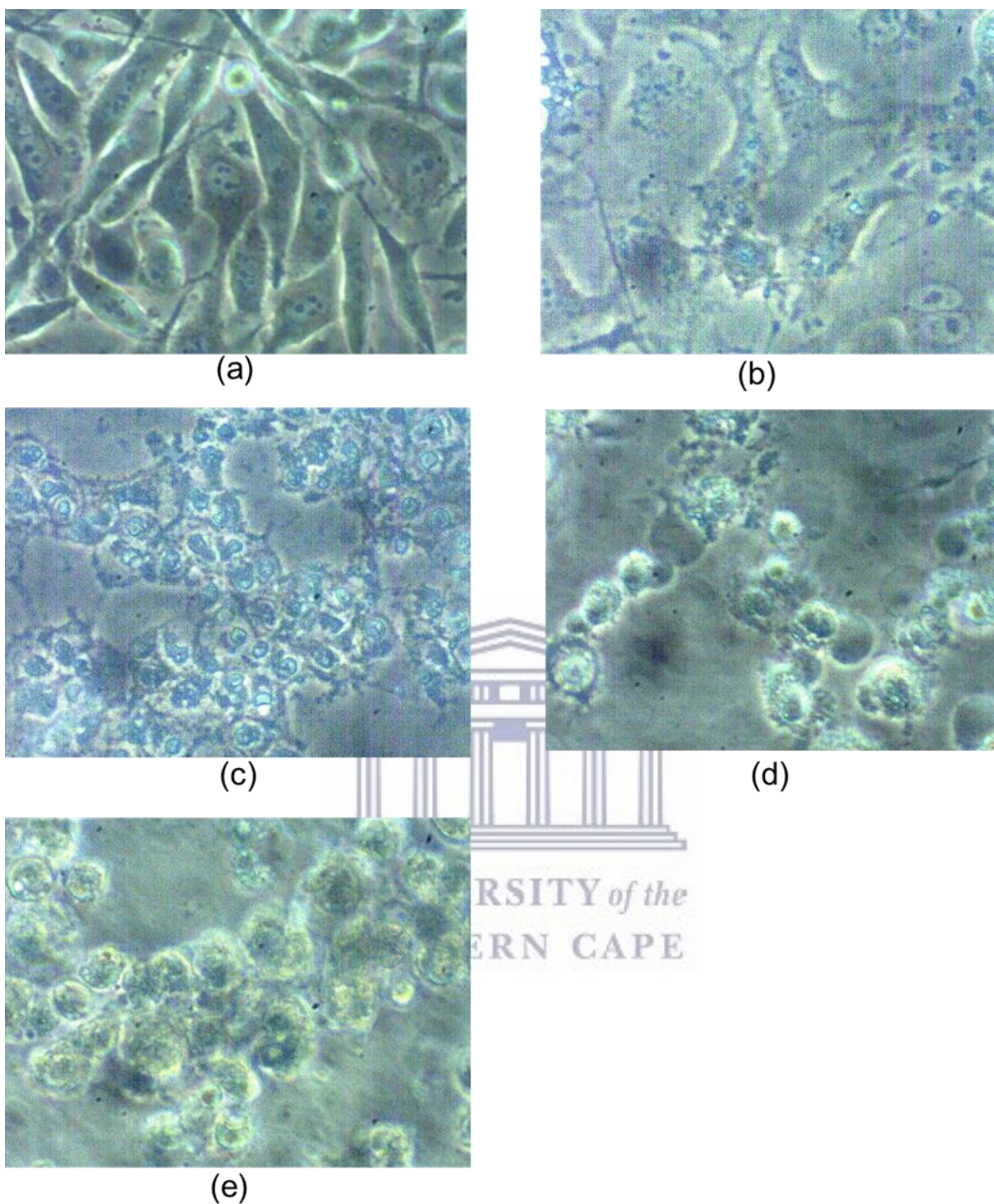


Figure 5.3. Morphological changes in PC-3 cells after treatment with compounds **4.5**, **4.6** and **4.7**. MCF-7 cells were treated for 24 hours with 100μM of compound **4.5** (c), 100μM of compound **4.6** (d) and 9.7μM of compound **4.7** (e). Cells in (a) were left untreated, while cells in (b) represent the positive control i.e. cells treated with 60 μM ceramide. The cells were observed at 20X magnification using an inverted (Nikon) light microscope.

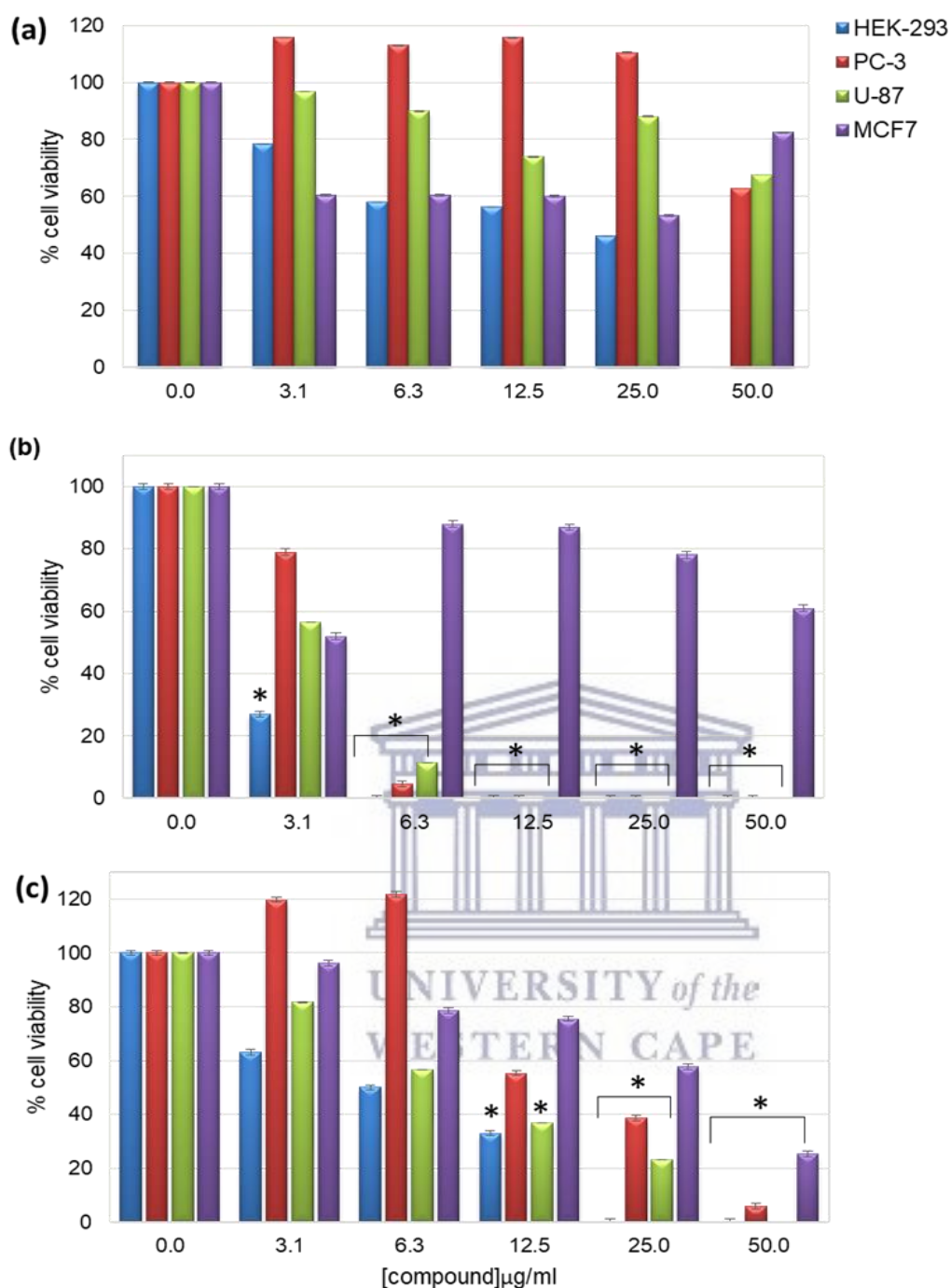


Figure 5.4. The viability of HEK-293, PC-3, U-87 and MCF-7 cells after treatment with compounds **4.5**, **4.6** and **4.7**. The cells were treated for 24 hours with increasing concentrations of compounds compound **4.5** (a), compound **4.6** (b) and compound **4.7** (c) and the viability of the cells was assed using the WST-1 assay.

*: Statistical significance ($p < 0.05$) of compounds **4.5**, **4.6** and **4.7** compared to untreated cells.

A summary of the cytotoxicity of all the three compounds is presented in table 5.1 below shows compound **4.6** to be the most active, while compound **4.5** was the least active of the three.

Table 5.1. IC₅₀ (μM) values for compounds **4.5**, **4.6** and **4.7** in PC-3, HEK-293, U-87 and MCF-7 cells

Cell line	Compound 4.5	Compound 4.6	Compound 4.7
PC-3	>100	1.3	5.6
HEK-293	30	0.5	1.7
U-87	>100	1.1	2.6
MCF-7	>100	>100	9.7

5.2.2 Solid lipid nanoparticles

Compound **4.5** displayed changes in NMR data within a week of isolation (figure 5.5) which was attributed to its known instability in presence of air and light and to improve its stability, compound **4.5** was encapsulated into SLNP for more accurate cytotoxicity assay. Compound **4.5**-SLNP were synthesised by homogenisation of stearic acid, poloxamer and compound **4.5**. Incorporation of compound **4.5** into solid lipid nanoparticles was confirmed by extracting the nanoparticles with chloroform and analysing with ¹H NMR spectroscopy (figure 5.6). Nanoparticles with an average size of 267 ± 0.7 nm with a zeta potential of 29.2 mV were formed. The ¹H NMR spectrum displayed signals for the furan moiety of compound **4.5**, confirming incorporation of the compound **4.5** into the nanoparticles figure 5.6.

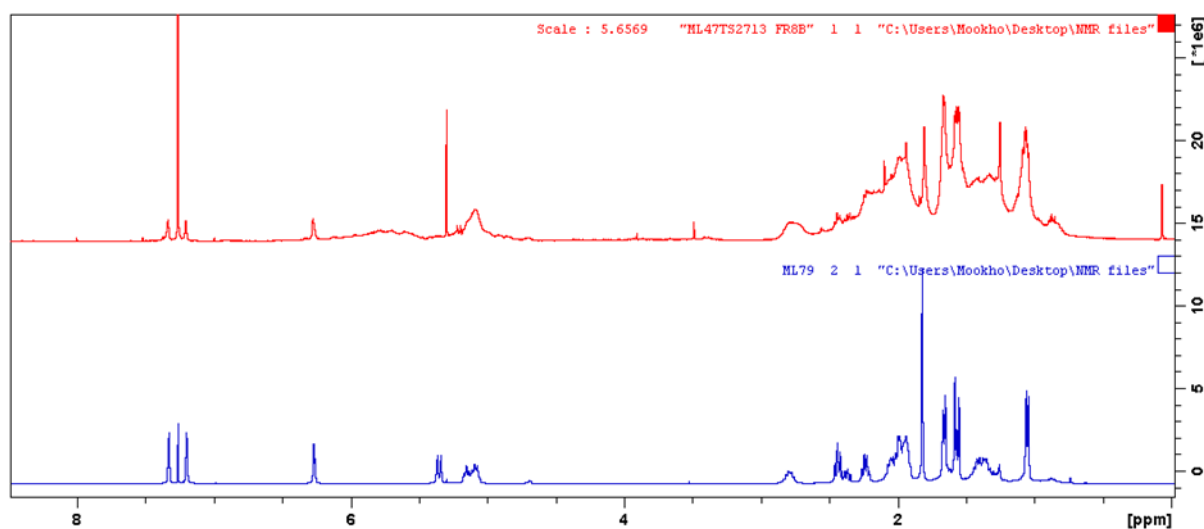


Figure 5.5. Changes in the ¹H NMR spectrum of compound **4.5** over time. The ¹H NMR spectrum (400 MHz, CDCl₃) of compound **4.5** was taken within 24 hours of isolation (blue) and after a week of isolation (red).

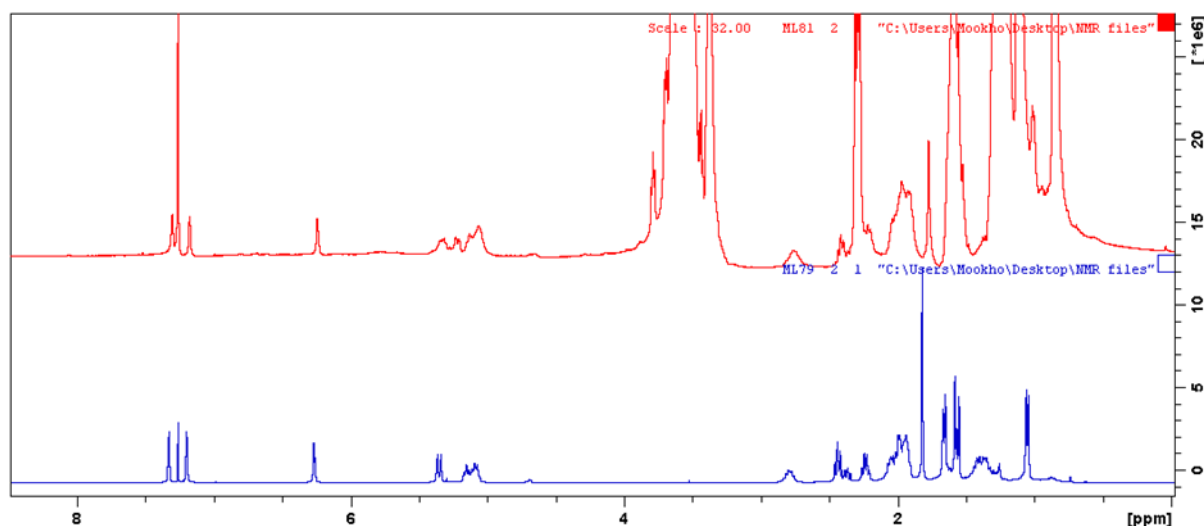


Figure 5.6. ^1H NMR spectrum of compound **4.5** (blue) and compound **4.5-SLNP** (red) (400 MHz, CDCl_3).

5.2.3 Solid lipid nanoparticles: Improved cytotoxicity of compound **4.5**.

The cytotoxic activity of compound **4.5** encapsulated in the solid lipid nanoparticles was also evaluated and compared with compound alone. Incorporation of compound **4.5** into solid lipid nanoparticles (**4.5-SLNP**) resulted in a remarkable improvement of activity (figure 5.7). PC-3 cells were unaffected by compound **4.5** except at high concentrations (50 $\mu\text{m}/\text{ml}$), however, after incorporation into SLNP, the cell viability dropped significantly. Compound **4.5-SLNP** displayed significant ($p < 0.05$) improvement in cytotoxicity for PC-3 cells at concentrations of 12.5, 25 and 50 $\mu\text{m}/\text{ml}$, while for MCF-7 a significant change was observed at concentrations of 25 and 50 $\mu\text{m}/\text{ml}$ suggesting that encapsulating compound **4.5** into SLNP has potential positive effect to the compound's cytotoxic effects.

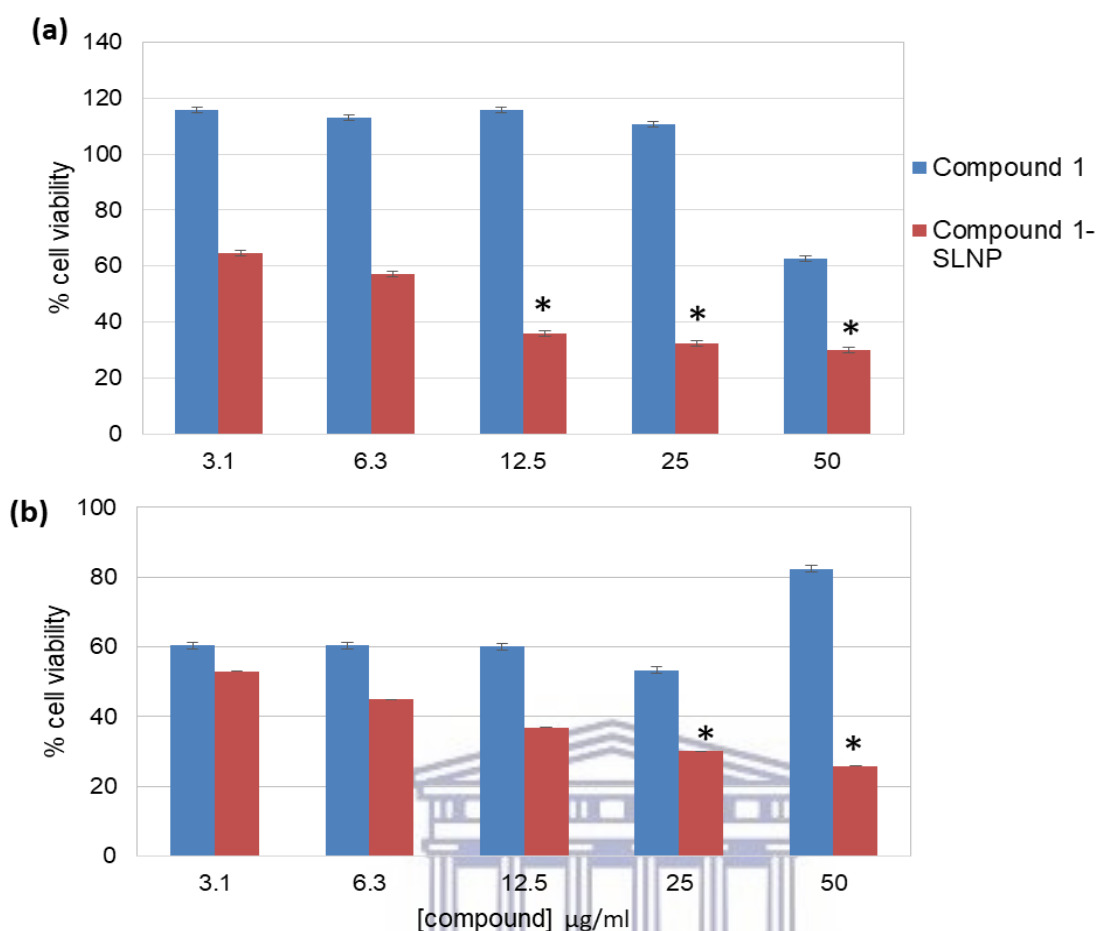


Figure 5.7. Comparative analysis of toxicity of compound **4.5** and compound **4.5**-SLNP. PC-3 (a) and MCF-7 (b) cells were treated for 24 hours with increasing concentrations of compound **4.5** and compound **4.5**-SLNP and the viability of the cells was assessed using the WST-1 assay. *: Statistical significance ($p < 0.05$) of compounds **4.5**, and compounds **4.5**-SLNP compared to untreated cells.

Table 5.2. IC_{50} (μM) values for compounds **4.5** and compound **4.5**-SLNP in PC-3 and MCF-7 cells.

Cell line	Compound 4.5	Compound 4.5-SLNP
PC-3	>100	17.0
MCF-7	>100	94.2

5.2.4 APOPercentage™ assay

Following the cytotoxic evaluation for compounds **4.5**, **4.6** and **4.7** against MCF-7, U-87, PC-3 and HEK-293 cells, it was evident that the compounds possessed anticancer activity, therefore the method of cell death induced by these compounds to the cells using APOPercentage™ dye was evaluated. For this assay, MCF-7 cells, which showed the most

resistance to the compounds, and PC-3, which showed a diverse response to different compounds, were selected. All cells were treated for 24 hours with compounds **4.5**, **4.6** and **4.7** at concentrations equivalent to their IC₅₀. Positive control cells were treated with ceramide, while negative control cells were left untreated. To determine induction of apoptosis, the cells were stained with APOPercentage™ dye and the staining quantified using flow cytometry. Cells were also viewed under a light microscope for morphological changes. Cells undergoing apoptosis possess certain characteristics such as shrinking and condensation of the nuclear chromatin, as well as lyses of nucleus [Saraste and Pulkki, 2000, Majno and Joris, 1995]. It was evident from the morphological changes observed for both MCF-7 and PC-3 cells that compounds **4.5**, **4.6** and **4.7** induced apoptosis as the cells appeared to have shrunk (figure 5.6 and 5.7). Flow cytometry quantification results showed that more than 80% of both MCF-7 and PC-3 cells treated with compounds **4.5** and **4.6** had undergone apoptosis, surpassing ceramide, the positive control which induced apoptosis in 58% and 75% of PC-3 and MCF-7 cells, respectively (figure 5.8). The results also show that Compound **4.5** induced significant apoptosis to MCF-7 cells, more so than it did to PC-3 cells, where only 26% of PC-3 cells treated with compound **4.5** were apoptotic compared to 75% observed with MCF-7 cells.

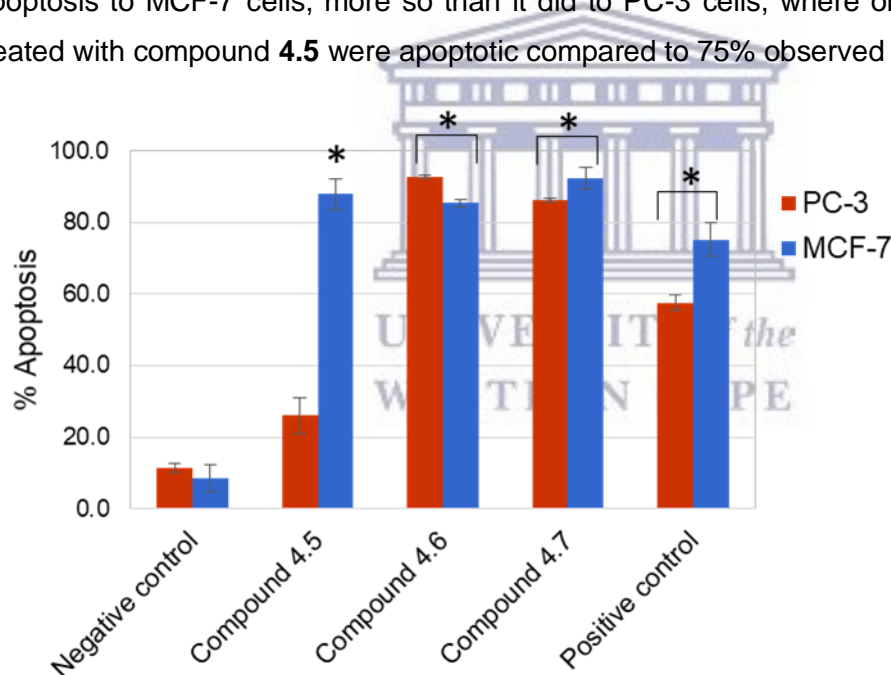


Figure 5.8. Percentage of apoptotic PC-3 and MCF-7 cells induced by compounds **4.5**, **4.6** and **4.7** and ceramide after treating for 24 hours. PC-3 cells were treated with compounds **4.5** (100μM), **4.6** (1.3μM), **4.7** (5.6μM) and ceramide (60μM). MCF-7 cells were treated with compounds **4.5** (100μM), **4.6** (100μM), **4.7** (97μM) and ceramide (60μM). Negative control cells were left untreated. Apoptosis was assessed using the APOPercentage™ dye. *: Statistical significance (p<0.05) of compounds **4.5**, **4.6**, **4.7** and ceramide compared to untreated cells

5.3 Conclusion

This chapter reports on the biological activity of furanosesterterpenes (compound **4.5**), compound **4.5**-SLNP and pyrroloiminoquinones (compounds **4.5** and **4.6**) and their effect on activity. Compound **4.5** was moderately cytotoxic to HEK-293, MCF-7, PC-3 and U-87 cells, while incorporation of compound **4.5** into SLNPs further increased its activity against MCF-7 and PC-3 cell. Pyrroloiminoquinones demonstrated potent cytotoxicity against HEK293, PC-3 and U-87 and moderate activity against MCF-7 cells. Both furanosesterterpenes and pyrroloiminoquinones exhibited their cytotoxicity by induction of apoptosis in the MCF-7 and PC-3 cells. The study investigated the method of cell death induced by compounds **4.5 – 4.7**, however, going further, it would be interesting to evaluate their mechanism of apoptosis.



5.4 Experimental procedures

5.4.1 Synthesis of solid lipid nanoparticles (SLNPs) incorporating compound **4.5**

Stearic acid (50 mg) was melted and heated to 75 °C and variabilin (25 mg) was added while stirring to form a stearic acid-variabilin complex at a ratio of 2:1. Separately, poloxamer 188 (25 mg) in water was heated to 75 °C to achieve a final poloxamer content dispersion of 5% w/v. The stearic acid-variabilin complex was added to poloxamer 188 and the mixture was stirred at 1000 rpm at 80 °C for five minutes followed by homogenisation at 10000 rpm with T25 digital Untra-Turrax® (IKA Work, Inc) homogeniser for five minutes and sonication at 50% with Vibra cell™ VCX 130 sonicator for one minute. The resultant mixture was rapidly cooled to room temperature in ice an ice bath and particle size and zeta potential were measured using Marvern Zetasizer Nano ZS for the **4.5**-SLNPs. NMR data was recorded on a Bruker Avance spectrometer at 400 MHz and processed using TopSpin 3.2 software.

5.4.2 Cytotoxicity assays

WST-1 (Roche, Germany) antiproliferation assay was carried out as outlined in chapter 3. For the determination of IC₅₀, cells were treated with different concentrations (50 µg/ml, 25 µg/ml, 12.5 µg/ml, 6.25 µg/ml and 3.125 µg/ml) of compounds **4.5**, **4.6** and **4.7** prepared by serial dilutions from stock solutions of 10mg/ml. Cells were treated for 24 hours with compounds **4.5** – **4.7** (as well as **4.5**-SLNPs) and cell viabilities calculated was for each concentration and a dose response chart was generated.

5.4.3 APOPercentage™ assay

APOPercentage™ assay was carried out as outline in Sibuyi N thesis with modifications (Sibuyi, 2015) Cells were seeded in 12-well plates at a density of 2 x 10⁵ cells/ml and incubated for 24 hours in a humidified CO₂ incubator at 37 °C after which the culture media was replaced with fresh media containing compounds **4.5**, **4.6** and **4.7** at the concentrations a concentration equivalent to their IC₅₀ obtained from the cytotoxicity assay above and incubated for another 24 hours. At the end of 24 hours, culture media containing floating cells from each well was transferred to labelled centrifuge tubes and adherent cells were obtained by gentle trypsinization and added to the corresponding centrifuge tubes and centrifuged at 3000 rpm for 5 minutes using 5412 R centrifuge. The supernatant was gently removed, and the pellet resuspended in 250 µl of APOPercentage™ dye (diluted 1:160 in culture medium) and incubated at 37 °C for thirty minutes. After thirty minutes of incubation, 4 ml on PBS was added to each tube and the tubes were centrifuged for another 5 minutes at 3000 rpm. The supernatant was discarded, and the pellet resuspended in 300 µl of PBS. Cells were then

analysed for apoptosis using Accuri B flow cytometer (BD Sciences), and data was processed with BD Accuri™ 6 (BD Sciences)



5.5 References

- Babb, C.; Urban, M.; Keilkowski, D.; Kellet, P. Prostate cancer in South Africa: Pathology based national cancer registry data (1996-2006) and mortality rates (1997-2007). *Prostate cancer* **2014**, *2014*, 319252.
- Bharali, D.J.; Siddiqui, I.A.; Adhami, V.M.; Chamcheu, C.J.; Aldahmash, A.M.; Mukhtar, H.; Mousa, S. Nanoparticle delivery of natural products in the prevention and treatment of cancers: current status and future prospects. *Cancers* **2011**, *3*, 4025-4045.
- Choi, K.; Hong, J.; Lee, C.O.; Kim, D.K.; Sim, C.J.; Im, K.S. Cytotoxic Furanosesterterpenes from a Marine Sponge *Psammocinia* sp. *Journal of Natural Products* **2004**, *67*, 1186-1189.
- Davis-Coleman, M.T. Natural Products Research in South Africa: End of an Era on Land or the Beginning of an Endless Opportunity in the Sea? *South African Journal of Chemistry* **2010**, *63*, 105–113.
- Davis-Coleman, M.T.; Beukes, D.R. Ten years of marine natural products research at Rhodes University. *South African Journal of Science* **2004**, *100*, 539 - 544.
- Ferlay, J.; Soerjomataram, I.; Dikshit, R.; Eser, S.; Mathers, C.; Rebelo, M.; Parkin, D.M.; Forman, D.; Bray, F. Cancer incidence and mortality worldwide: Sources, methods and major patterns in GLOBOCAN 2012. *International Journal of Cancer* **2014**, *136*, 359-386.
- Harbeck, N.; Gnant, M. Breast cancer. *Lancet* **2017**, *389*, 1134-1150.
- Keyzers, R.A.; Arendse, C.E.; Hendricks, D.T.; Samaai, T.; Davis-Coleman, M.T.; Makaluvic Acids from the South African Latrunculid sponge *Strongylodesma aliwaliensis*. *Journal of Natural Products* **2005**, *68*, 506-510.
- Liu, Y.; Mansoor, T.; Hong, J.; Lee, C-O.; Sim, C.J.; Im, K.S.; Kim, N.D.; Jung, J.H. New cytotoxic sesterterpenoids and norsesterterpenoids from two sponges of the genus *Sarcotragus*. *Journal of Natural Products* **2003**, *66*, 1451-1456.
- Majno, G.; Joris, I. Apoptosis, oncosis and necrosis. An overview of cell death. *American Journal of Pathology* **1995**, *146*(1), 3-5.
- Rifai, S.; Fassouane, A.; Pinho, P.M.; Kijjoa, A.; Nazareth, N.; Nascimento M.S.J. Herz, W. Cytotoxicity and inhibition of lymphocyte proliferation of fasciculatin, a kinear furanosesterterpene isolated from *Ircinia variabilis* collected from the Atlantic coast of Morocco. *Marine Drugs* **2005**, *3*(1), 15-21.
- Saraste, A.; Pulkki, K. Morphologic and biochemical hallmarks of apoptosis, *Cardiovascular Research* **2000**, *45*(3), 528–537.
- Shenderova, A.; Burke, T.G.; Schwendeman, S.P. Stabilization of 10 hydroxycamptothecin in Poly(lactide-co-glycolide) microsphere delivery vehicles. *Pharmaceutical research* **1997**, *14*(10), 1406-1414.

Shinkre, B.A.; Raisch, K.P.; Fan, L.; Velu, S.E. Analogs of the marine alkaloid makaluvamines: Synthesis, topoisomerase II inhibition, and anticancer activity. *Bioorganic and Medicinal Chemistry* **2007**, *17*, 2890–2893.

Sibuyi, N.R.S. PhD thesis; Development of a receptor targeted nanotherapy using a proapoptotic peptide. University of the Western Cape. **2015**, 92.

Siegel, R.L.; Miller, K.D.; Fedewa, S.A.; Ahnen, D.J.; Meester R.G.S.; Barzi, A.; Jemal, A. Cancer statistics. *CA: A Cancer Journal for Clinicians* **2017**, *67*, 7-30.

Vanderpuye, V.; Grover, S.; Hammad, N.; Prabhaker P.; Simonds, H.; Olopade, F.; Stefan, D.C. An update on the management of breast cancer in Africa. *Infectious Agents and Cancer* **2017**, *12*, 13.



General Conclusion and Recommendations

This study explored fourteen marine sponges collected in South Africa, through different separation techniques. Through prefractionation, a library of seventy fractions for the sponge samples was prepared. Liquid-liquid partitioning of the extracts was able to eliminate inorganic salts and nuisance compounds, however, this method may also have resulted in loss of some interesting non-polar compounds. A functionalised silica gel column chromatography was therefore used and found to be effective in separating metabolites, enabling easy biological and chemical profiling (chapter 3), which was then used to prioritize samples for further studies.

Priority sponges, following chemical and biological profiling, resulted in the isolation of a known sesterterpene (7E,12Z,20Z,18S-variabilin) and two pyrroloiminoquinone alkaloids (tsitsikammamine A and tsitsikammamine A N-18 Oxime) from *Ircinia* and *Latrunculid* sp. sponges respectively, as discussed in chapter 4.

Evaluation of the three compounds against selected cells lines, as discussed in chapter 5, displayed potent cytotoxicity for the pyrroloiminoquinones, while moderate activities were shown for the sesterterpenes. The instability of variabilin, isolated from *Ircinia* sponge, was a concern for determining precise biological assay outcomes, hence the compound was incorporated into solid lipid nanoparticles. This in turn resulted in an improved bioactivity for the compound. Solid lipid nanoparticles thus can serve as an important tool in improving stability and biological activities for natural compounds. Although incorporation of variabilin into SLNP improved activity of the compound, more studies have to be done to determine the other properties such as shape and stability at different environments.

With the results obtained from the flow cytometry assay, all the three compounds were shown to induce apoptosis to MCF-7 and PC-3 cell lines, however, the test does not describe the mechanism of action. To explore the mechanism of action of these compounds, additional assays are required which describe apoptotic pathways affected by the compounds.

Supplementary data

Chapter 3

Table S3.1. Cell viability of MCF-7, SKOV-3 and HEK-293.

Sample	MCF-7					SKOV-3					HEK-293				
	Fraction 1	Fraction 2	Fraction 3	Fraction 4	Fraction 5	Fraction 1	Fraction 2	Fraction 3	Fraction 4	Fraction 5	Fraction 1	Fraction 2	Fraction 3	Fraction 4	Fraction 5
TS2707	0	27	44	0	0	0	6	29	0	0	38	19	53	20	1
TS2710	12	44	29	12	0	9	41	38	34	0	56	35	42	62	50
TS2712	29	39	0	17	34	17	34	31	25	13	39	59	79	52	44
TS2713	20	38	35	27	28	28	49	33	43	36	28	40	46	44	31
TS2714	61	73	72	66	53	24	86	100	49	40	0	55	38	50	32
TS2715	54	77	81	62	92	22	89	99	79	98	28	100	100	38	100
TS2716	60	39	48	69	66	25	35	42	48	24	34	27	31	96	37
SAF96-003	0	52	32	32	0	0	72	84	29	3	11	0	26	28	6
SAF96-026	0	27	33	0	0	9	25	42	16	10	13	22	49	20	27
SAF96-053	0	20	7	0	0	0	3	20	0	2	7	23	30	24	38
SAF96-096	5	60	55	5	0	0	56	59	54	20	46	67	34	20	18
SAF96-082	0	67	57	48	23	0	0	0	98	64	21	33	24	38	28
SAF96-108	29	85	63	33	14	58	49	0	12	0	41	84	57	26	20
SAF96-114	4	37	44	83	84	46	81	46	4	0	22	50	34	30	37

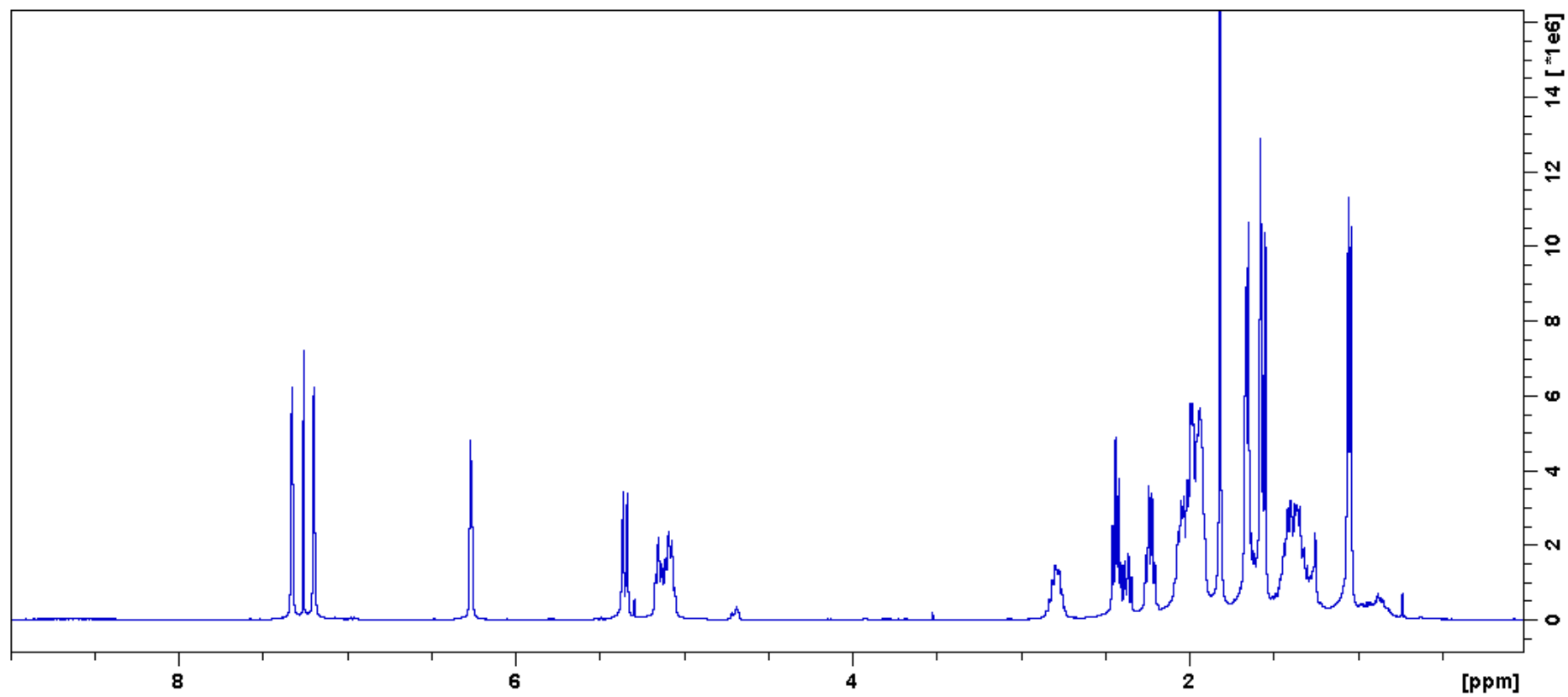


Figure S4.1 ^1H NMR spectrum of compound **4.5** (400MHz, CDCl_3)

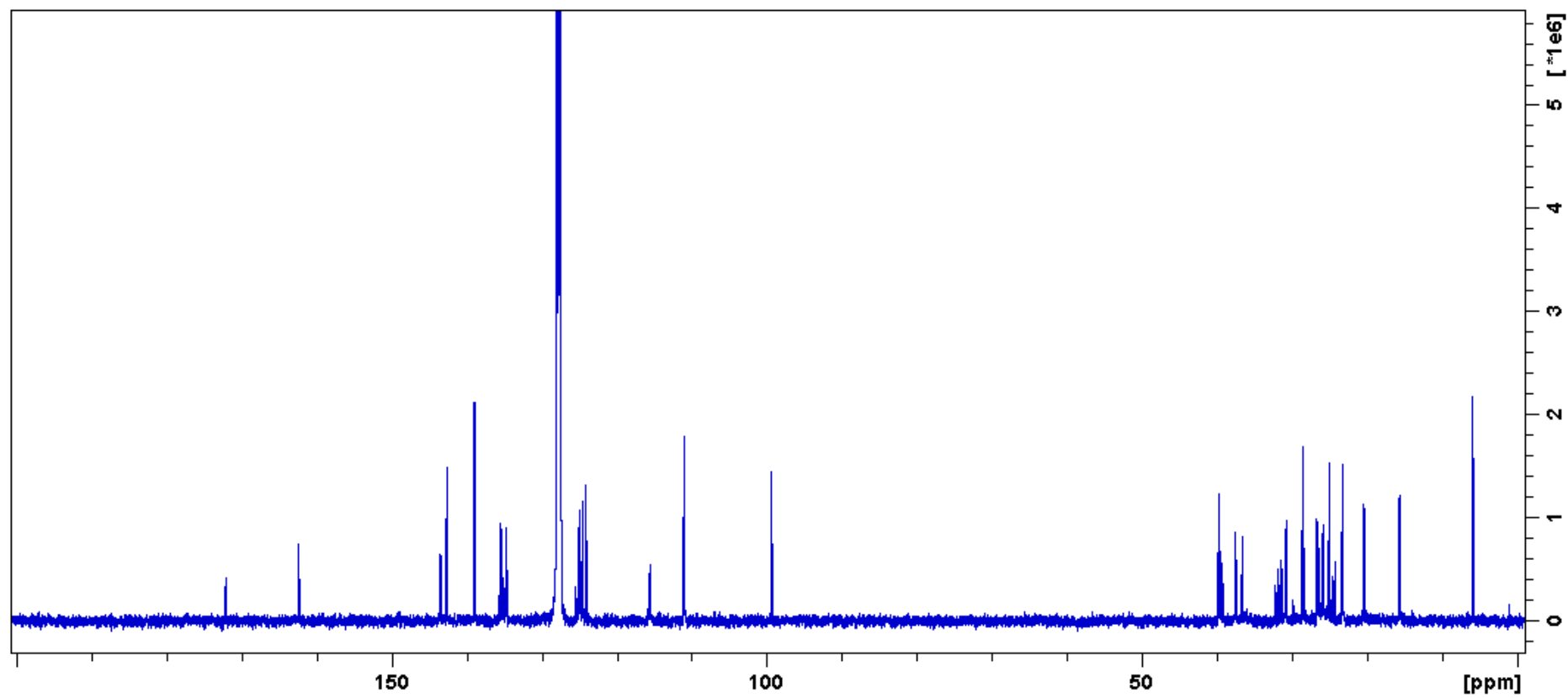


Figure S4.2 ^{13}C NMR spectrum of compound **4.5** (100MHz, CDCl_3)

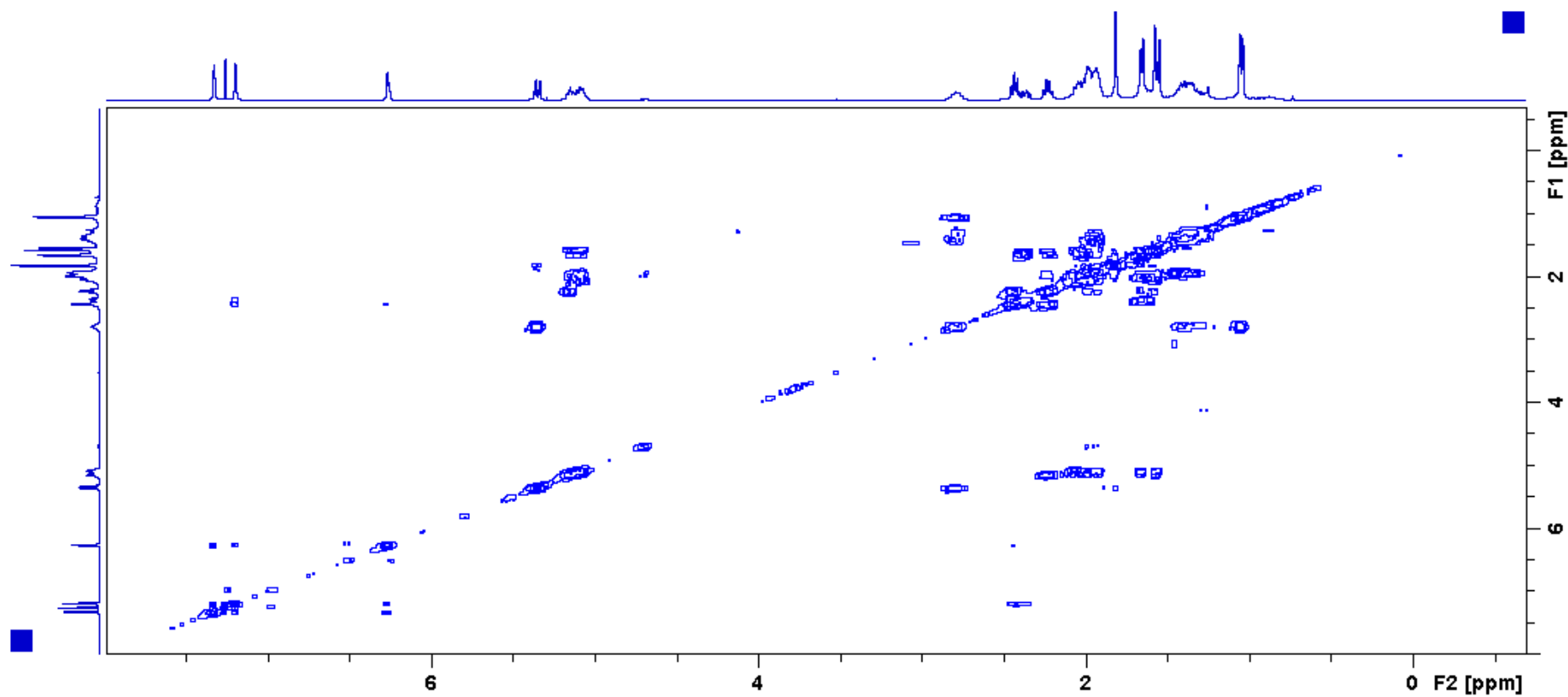


Figure S4.3 COSY spectrum of compound **4.5**

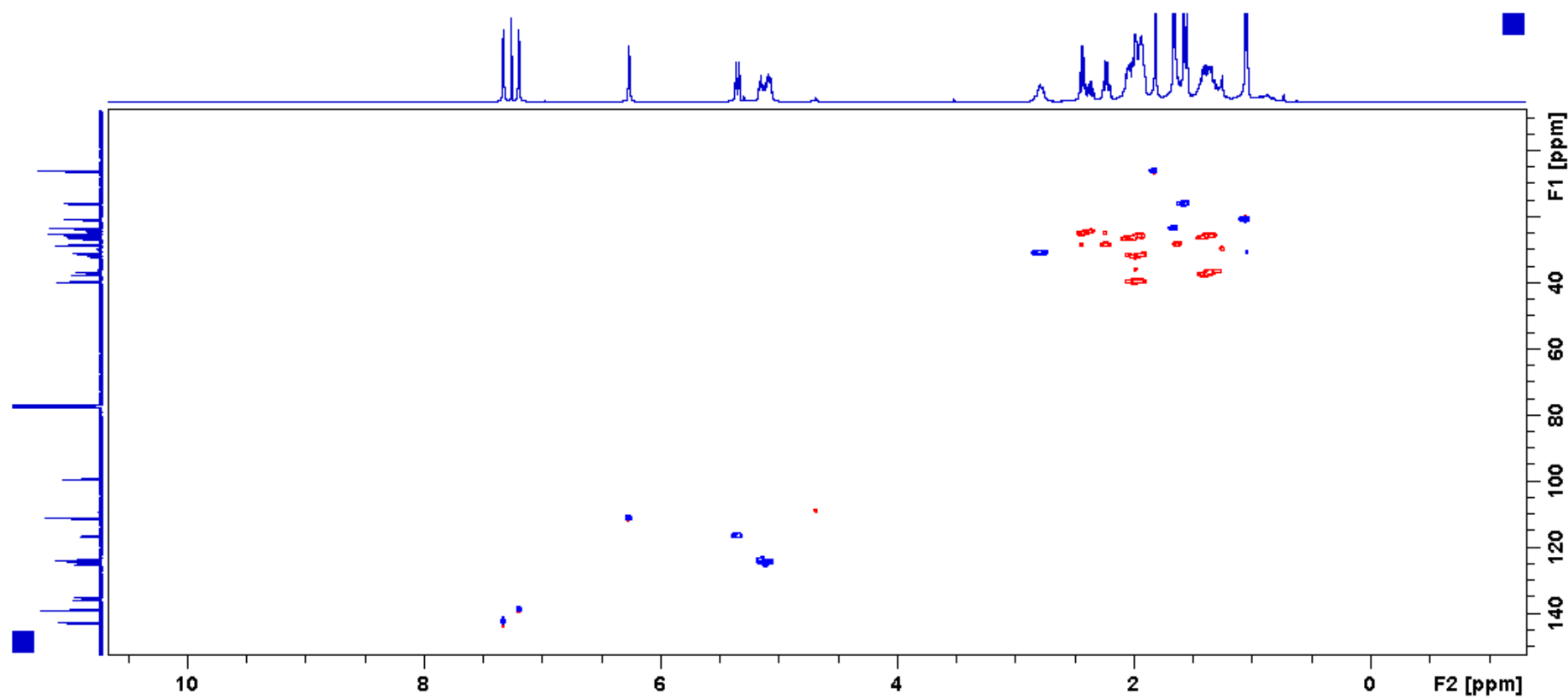


Figure S4.4 HSQC spectrum of compound 4.5

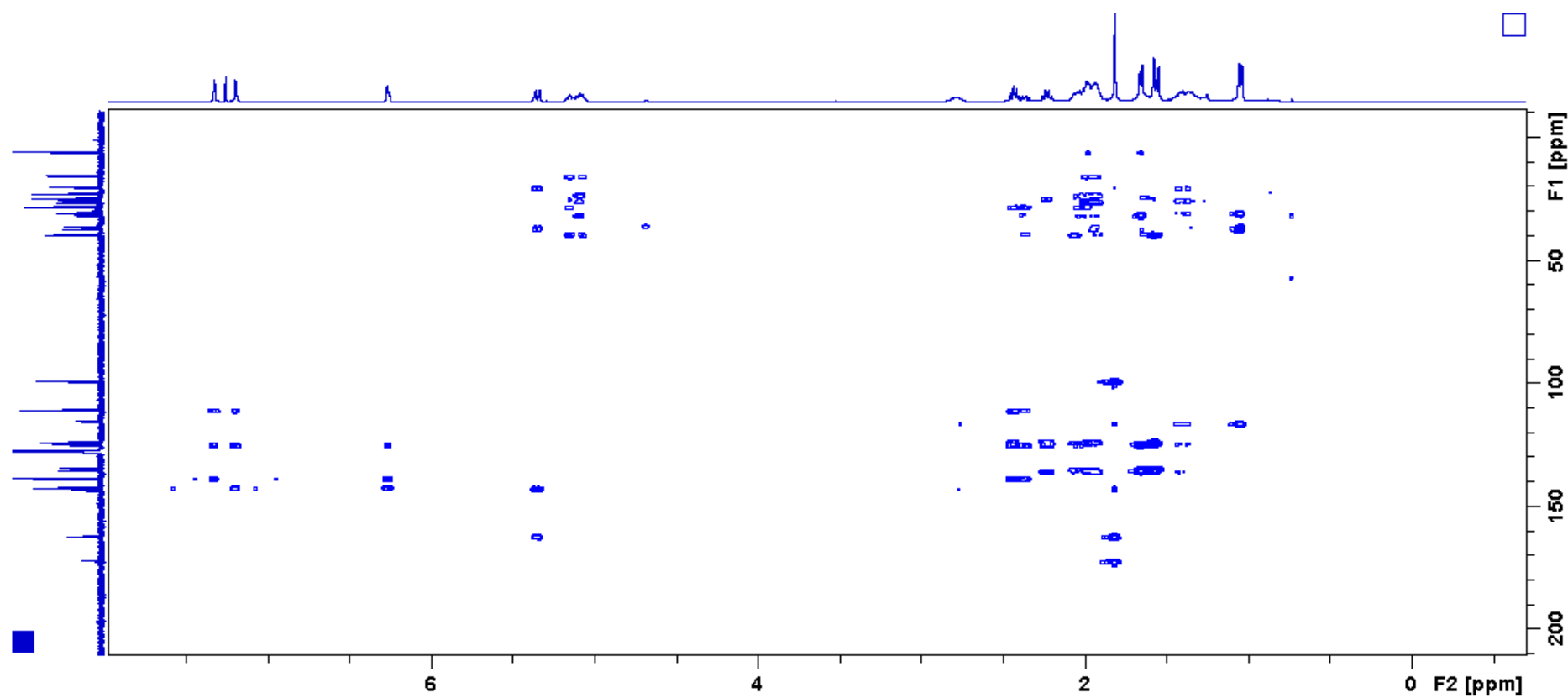


Figure S4.4 HMBC spectrum of compound 4.5

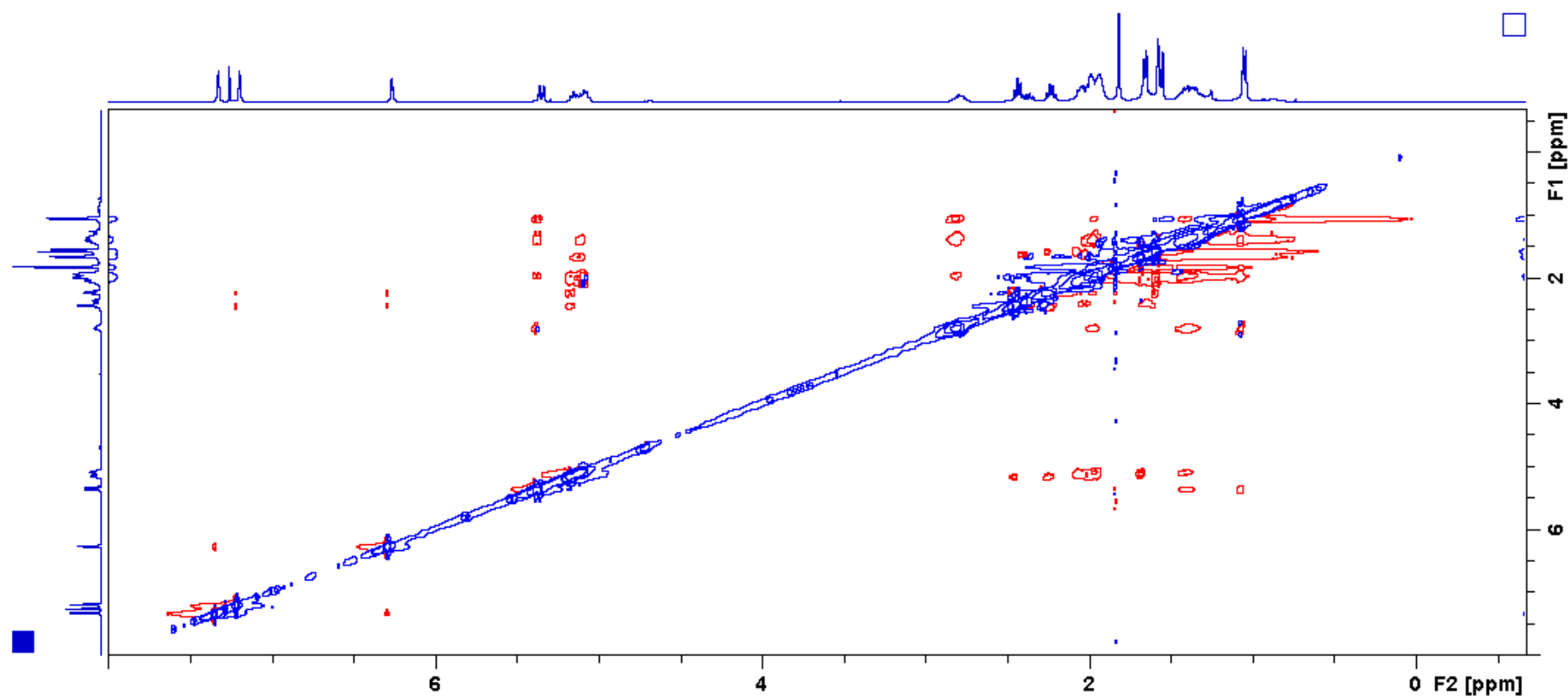


Figure S4.5 NOESY spectrum of compound 4.5

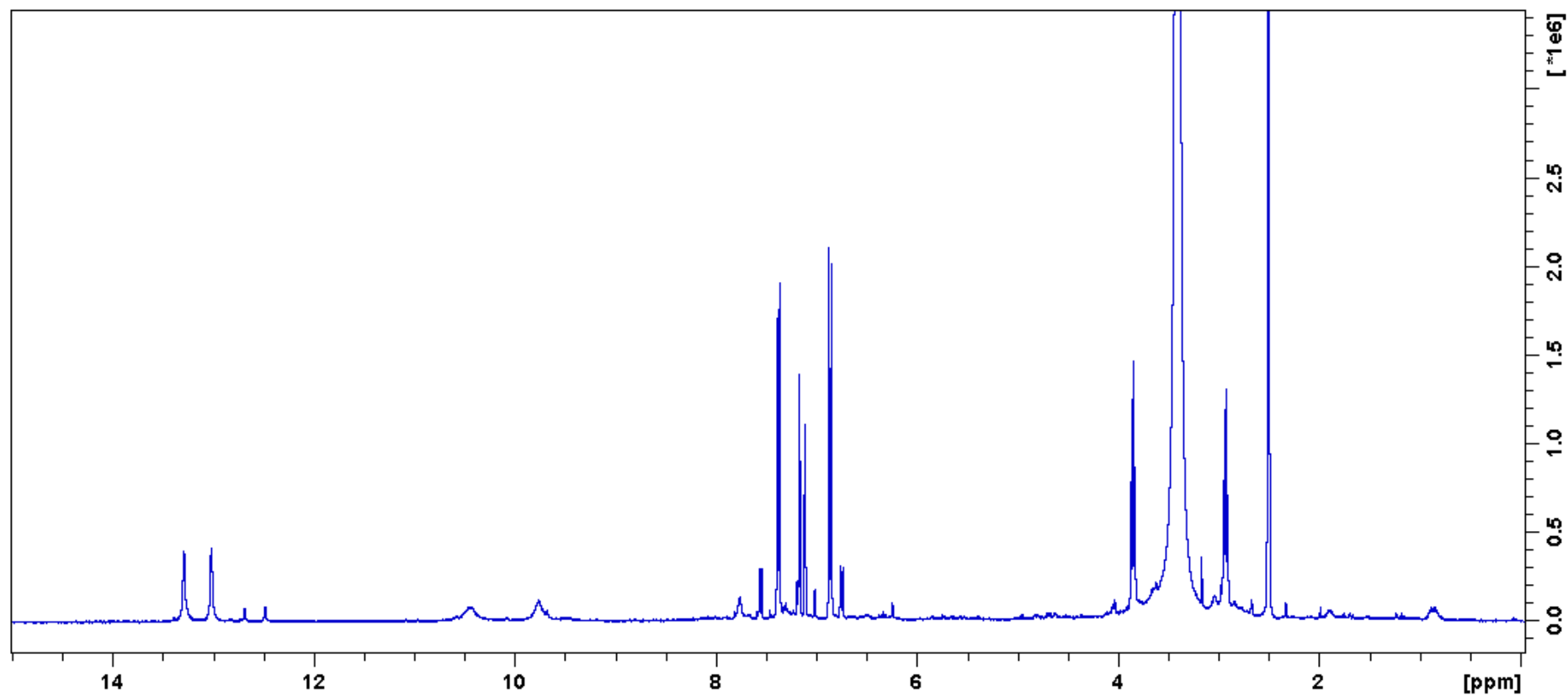


Figure S4.6 ^1H NMR spectrum of compound **4.6** (400MHz, *DMSO-d*₆)

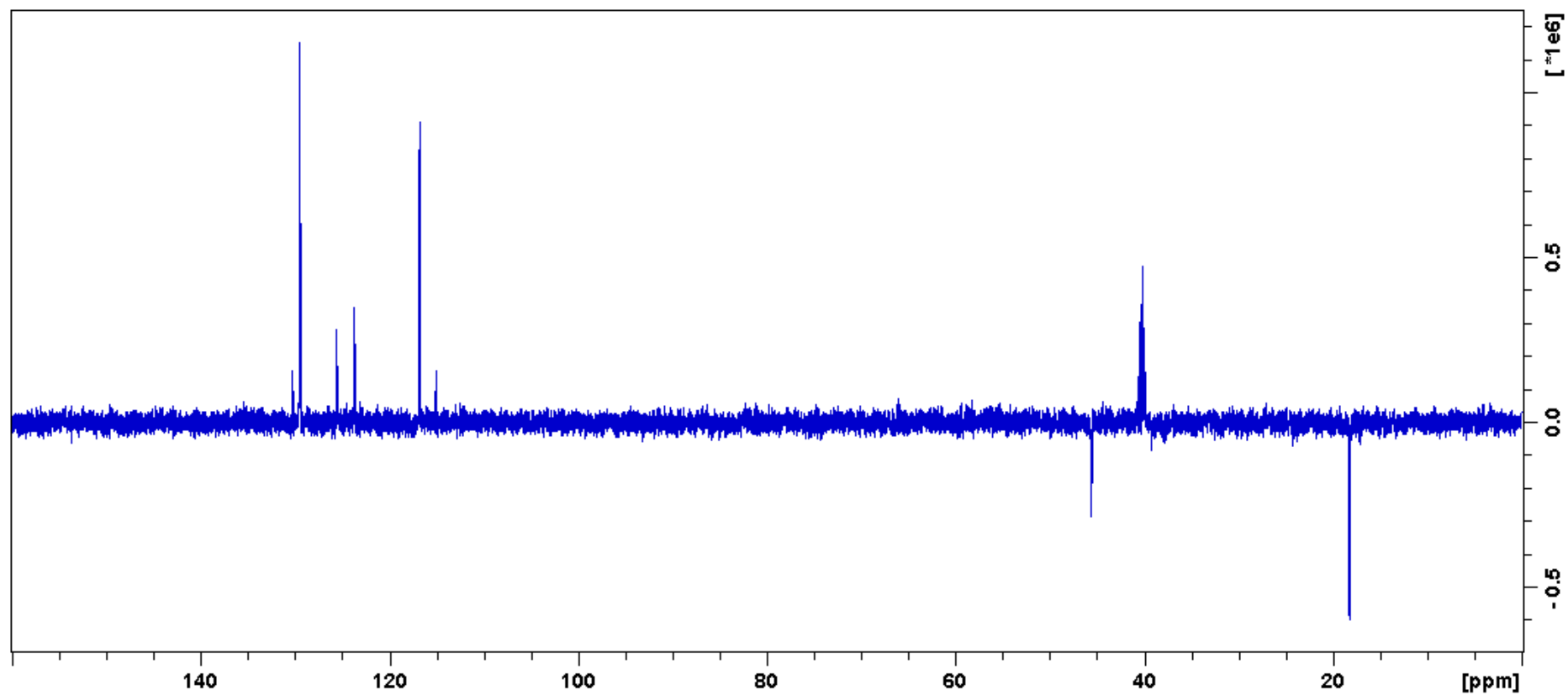


Figure S4.6 ^{13}C DEPT 135 of compound **4.6** (400MHz, $\text{DMSO}-d_6$)

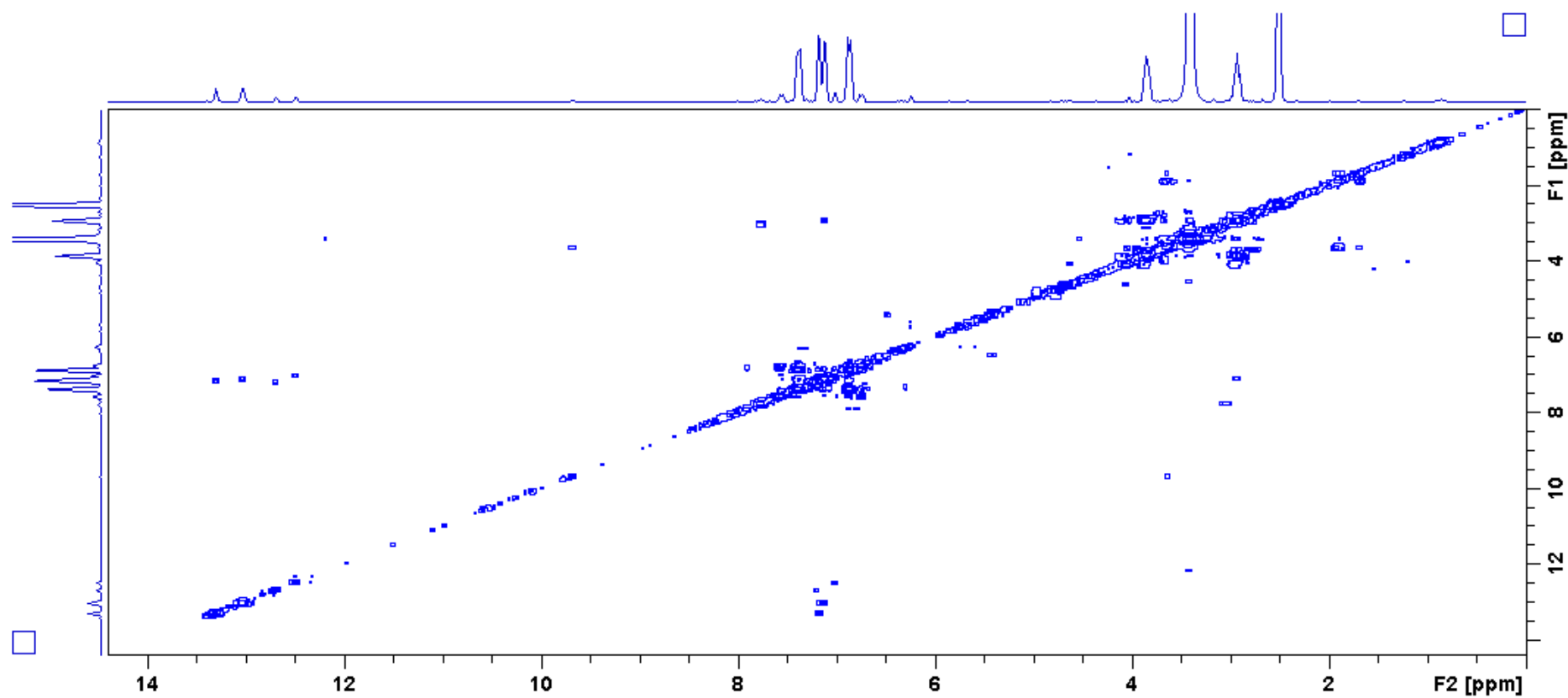


Figure S4.7 COSY spectrum of compound 4.6

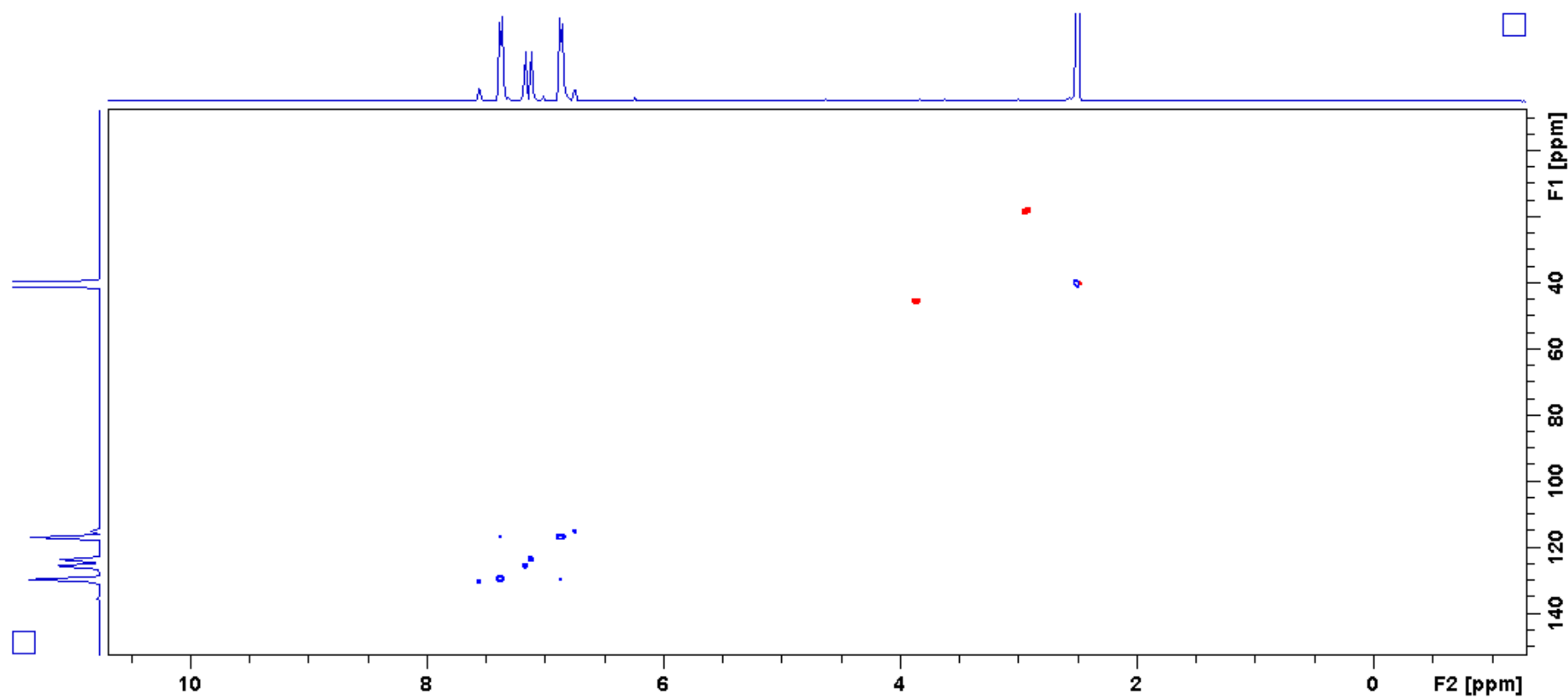


Figure S4.8 HSQC spectrum of compound 4.6

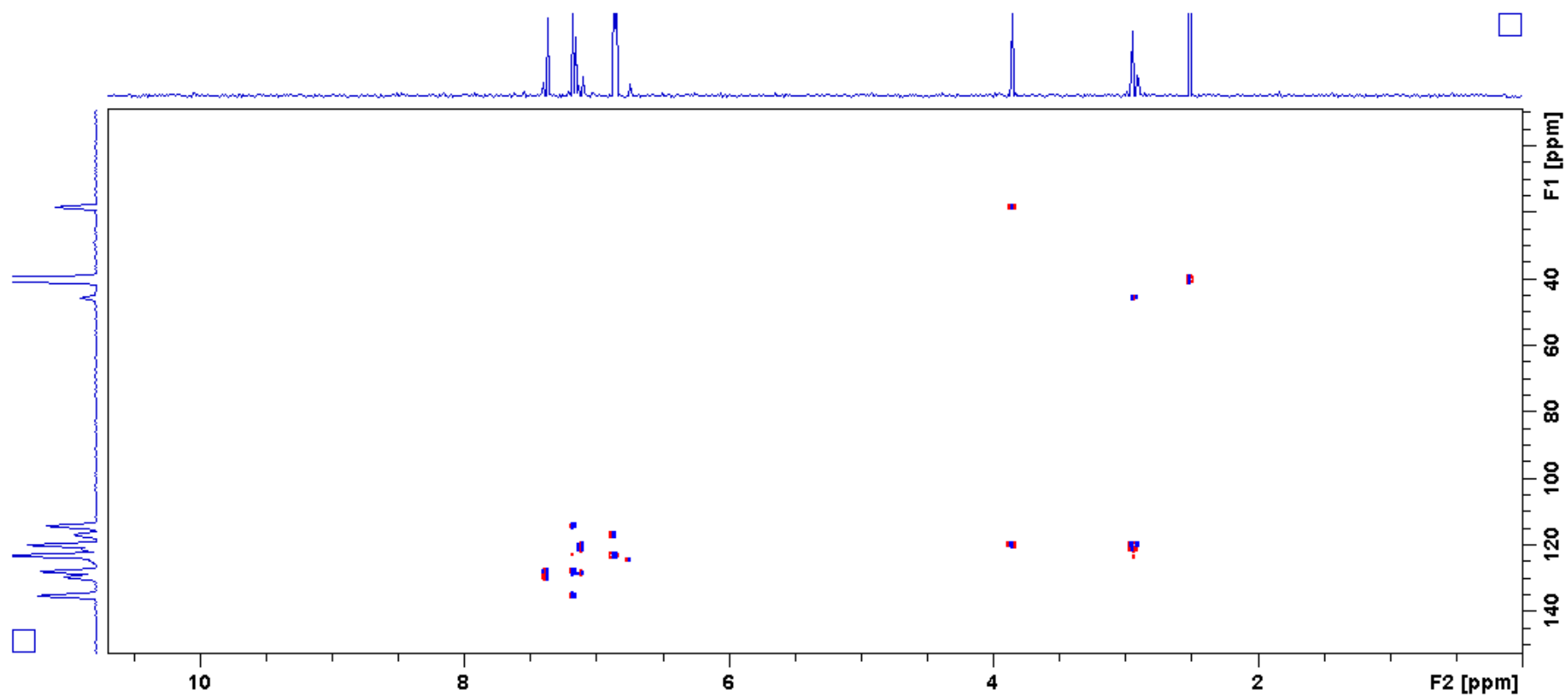


Figure S4.9 HMBC spectrum of compound 4.6

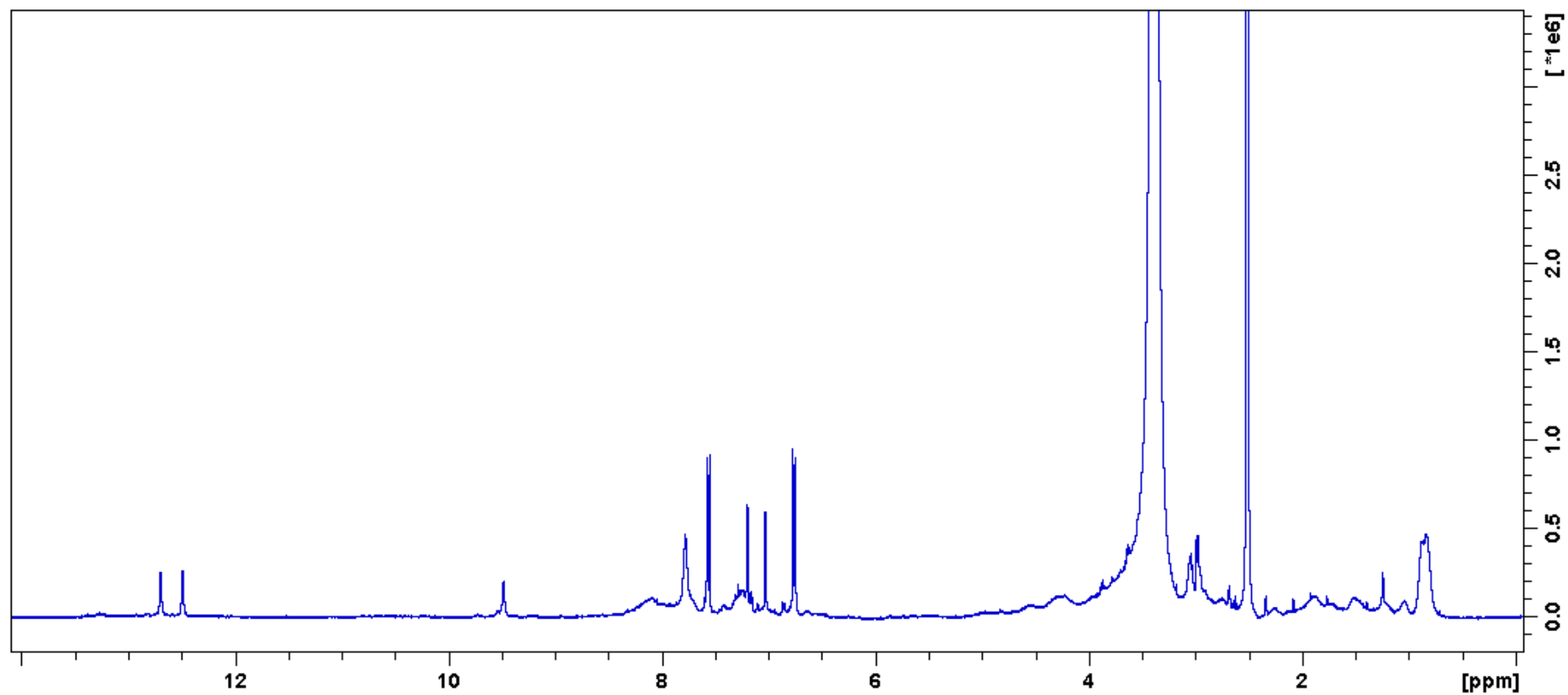


Figure S4.10 ^1H NMR spectrum of compound **4.7** (400MHz, $\text{DMSO-}d_6$)

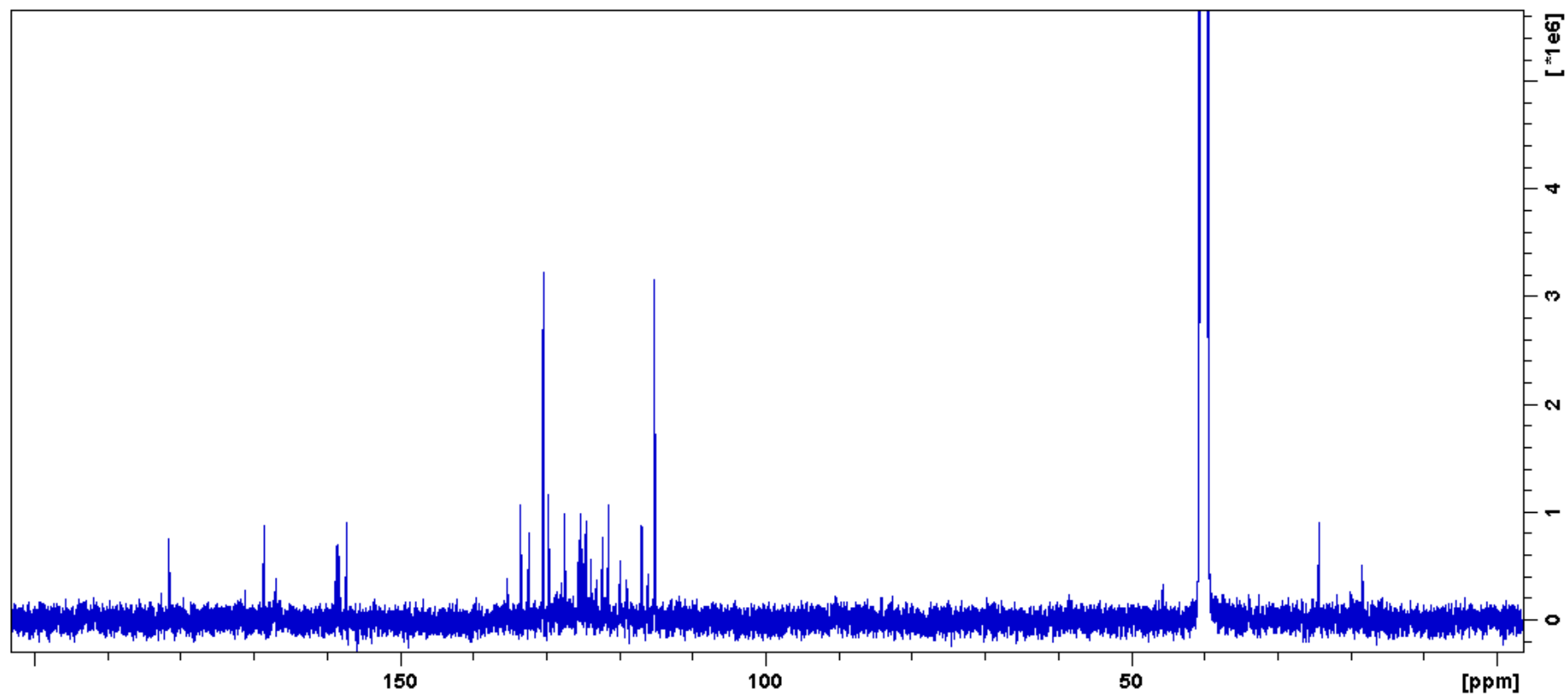


Figure S4.11 ^{13}C NMR spectrum of compound 4.7 (100MHz, DMSO- d_6)



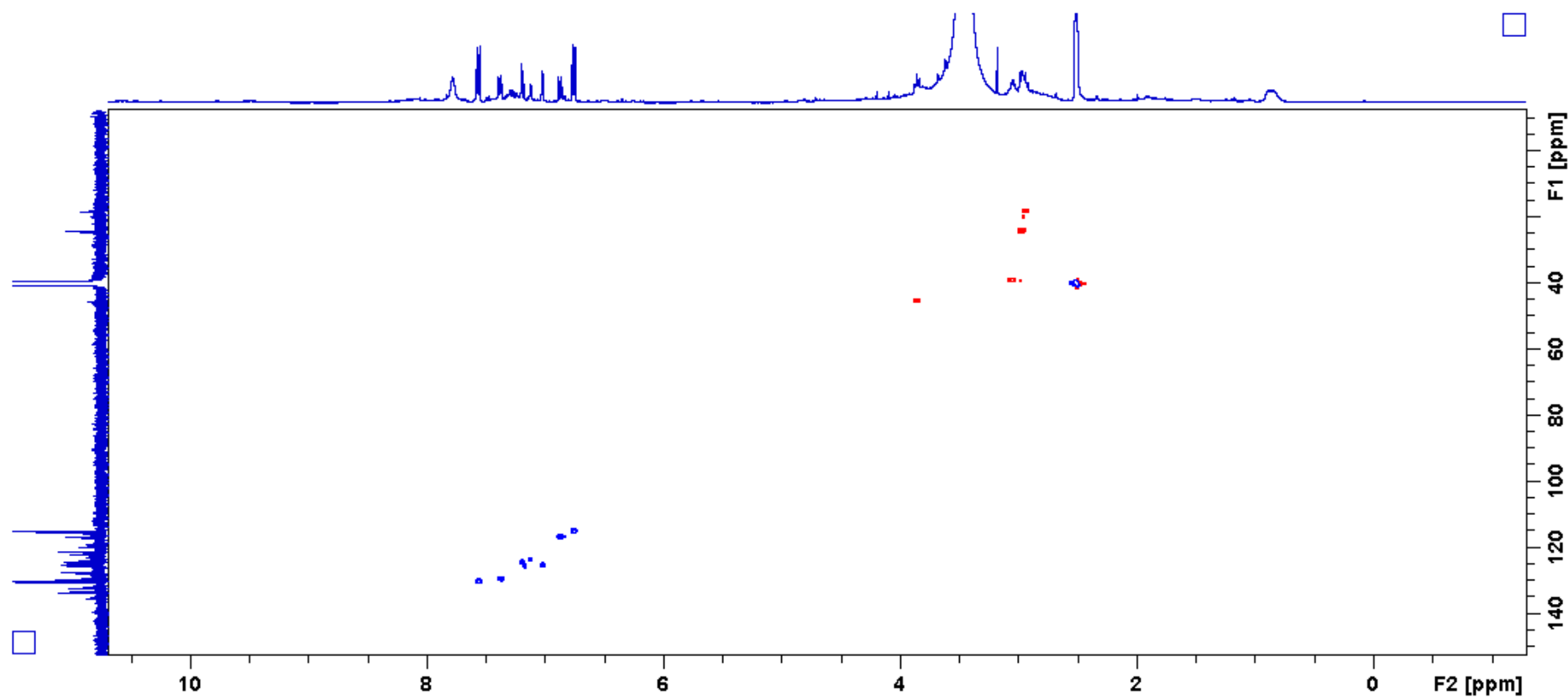


Figure S4.12 HSQC spectrum of compound 4.7

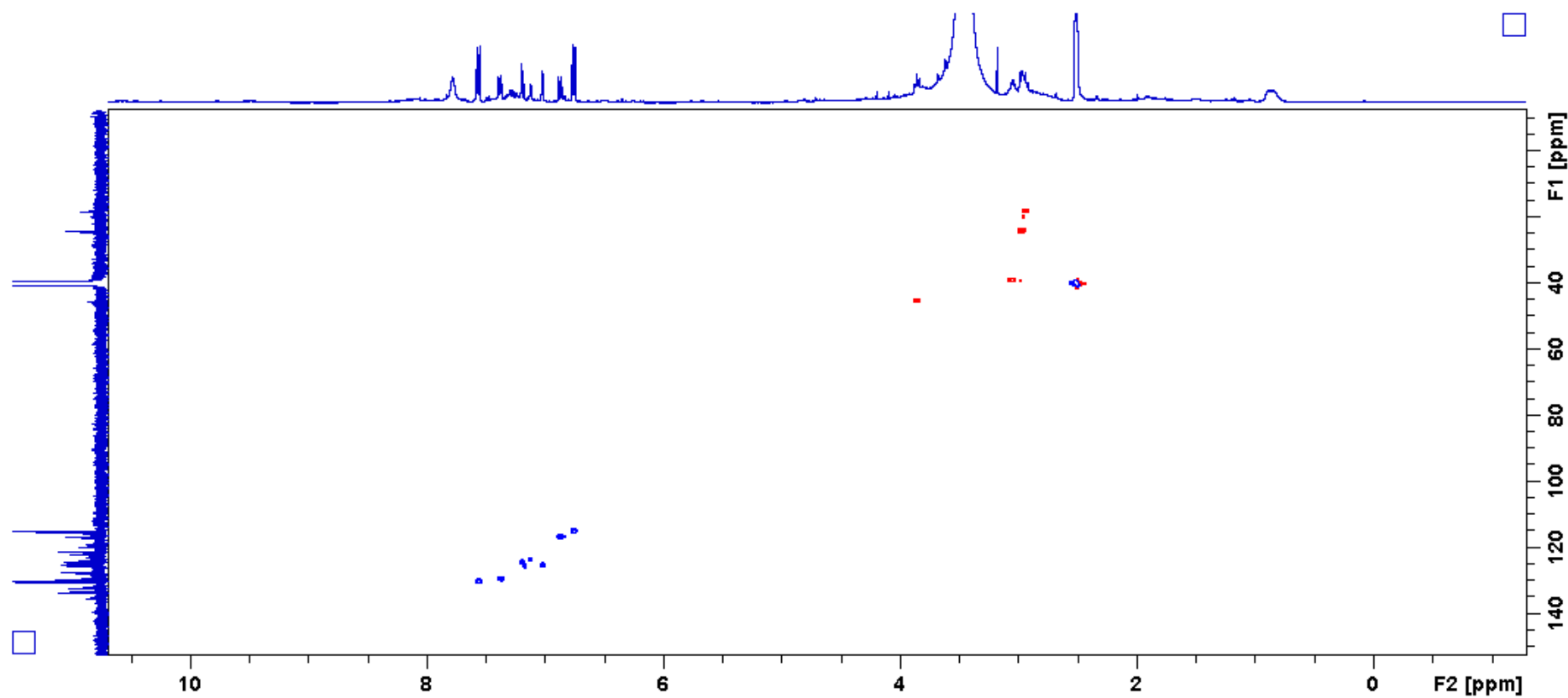


Figure S4.13 HMBC spectrum of compound 4.7